

Dissertation zur Erlangung des Doktorgrades
der Fakultät für Chemie und Pharmazie
der Ludwig-Maximilians-Universität München

**Genetic analysis of *Drosophila* adult
muscle type specification**

Cornelia Schönbauer

aus

Waidhofen an der Thaya, Österreich

2013

Erklärung

Diese Dissertation wurde im Sinne von § 7 der Promotionsordnung vom 28. November 2011 von Herrn Prof. Dr. Matthias Mann betreut .

Eidesstattliche Versicherung

Diese Dissertation wurde eigenständig und ohne unerlaubte Hilfe erarbeitet.

München, am 25.04.2013

Cornelia Schönbauer

Dissertation eingereicht am 25.04.2013

1. Gutachter Prof. Dr. Matthias Mann
2. Gutachter Prof. Dr. Klaus Förstemann

Mündliche Prüfung am 07.06.2013

Table of contents

Table of contents	1
1. List of publications	3
2. Summary	4
3. Acknowledgements	6
4. Introduction	8
4.1 <i>Drosophila</i> adult muscle system	9
4.1.1 Adult muscle pattern	9
4.1.2 Basic muscle architecture: myofibrils and sarcomeres.....	11
4.1.3 Adult muscle types: fibrillar and tubular muscles.....	12
4.2 <i>Drosophila</i> adult muscle development	16
4.2.1 Origin and diversification of adult muscle progenitors.....	16
4.2.2 Adult muscle fiber formation.....	23
4.2.3 Adult muscle attachment site formation	28
4.2.4 Adult myofibrillogenesis and sarcomere formation.....	30
4.3 Transgenic RNAi in <i>Drosophila</i>	32
5. Aim of the thesis	36
6. Summary of publications	37
6.1 Summary of publication I.....	37
6.2 Summary of publication II	39
6.3 Summary of publication III.....	40
6.4 Summary of publication IV	41
7. Conclusion and outlook	43
7.1 Regulation of IFM-specific <i>Salm</i> expression	43
7.2 Downstream targets of <i>salm</i>	44
7.3 Spalt and the evolution of fibrillar flight muscles	45
8. References	48
9. Supplements	62

1. List of publications

This thesis is based on the following publications:

- I. Langer CC*, Ejsmont RK*, **Schönbauer C***, Schnorrer F, Tomancak P.
In vivo RNAi rescue in *Drosophila melanogaster* with genomic transgenes from *Drosophila pseudoobscura*.
PLoS One. 2010 Jan 28;5(1):e8928.

* These authors contributed equally to this work.
- II. Jährling N, Becker K, **Schönbauer C**, Schnorrer F, Dodt HU.
Three-dimensional reconstruction and segmentation of intact *Drosophila* by ultramicroscopy.
Front Syst Neurosci. 2010 Feb 8;4:1.
- III. Schnorrer F, **Schönbauer C**, Langer CC, Dietzl G, Novatchkova M, Schernhuber K, Fellner M, Azaryan A, Radolf M, Stark A, Keleman K, Dickson BJ.
Systematic genetic analysis of muscle morphogenesis and function in *Drosophila*.
Nature. 2010 Mar 11;464(7286):287-91.
- IV. **Schönbauer C**, Distler J, Jährling N, Radolf M, Dodt HU, Frasch M, Schnorrer F.
Spalt mediates an evolutionarily conserved switch to fibrillar muscle fate in insects.
Nature. 2011 Nov 16;479(7373):406-9

2. Summary

Muscles of all higher animals comprise different muscle types adapted to perform distinct functions in the body. These express different sets of genes controlled by distinct combinations of transcriptional programs and extracellular signals, and thus differ in their myofibrillar organization and contractile properties. Despite major progress in our understanding of myogenesis, the genetic pathways controlling the formation and function of different muscle types are still largely uncharacterized.

Flying insects possess specialized flight muscles enabling wing oscillations with frequencies of up to 1000 Hz together with high power outputs of 80 W per kg muscle. To achieve these parameters, flight muscles contain stretch-activated myofibrils with a unique fibrillar organization, whereas all other, more slowly contracting muscles, such as leg muscles, display a tubular morphology.

To delineate the genetic regulation of muscle development and function, and, in particular, muscle type specification, we performed a genome-wide RNA interference (RNAi) screen in *Drosophila*, in which we systematically inactivate genes exclusively in muscle tissue. We uncovered more than 2000 genes with putative roles in muscles, many of which we were able to assign to specific functions in muscle, myofibril or sarcomere organization by phenotypic characterization. Muscle-specific knockdown of 315 genes resulted in viable, but completely flightless animals, indicating a specific function of those genes in fibrillar flight muscles.

Detailed morphological analysis of these 315 genes revealed a striking phenotype upon knockdown of the zinc finger transcription factor *spalt major (salm)*: the fibrillar flight muscles are switched to tubular muscles, whereas tubular leg muscles are wild type, demonstrating that *salm* is a key determinant of fibrillar muscle fate. We could show that the transcription factor *vestigial (vg)* acts upstream of *salm* to induce its expression specifically in fibrillar flight muscles. Importantly, *salm* is not only required but also sufficient to induce the fibrillar muscle fate upon ectopic expression in other muscle types. Microarray analysis, comparing mRNA expression from adult wild-type flight and leg muscles to *salm* knockdown flight muscles, indicates that *salm* instructs most features of fibrillar muscles by regulating both gene

expression as well as alternative splicing. Remarkably, we could show that *spalt*'s function in programming stretch-activated fibrillar muscles is conserved in insect species separated by 280 million years of evolution. Interestingly, in mouse two of the four *spalt-like* (*sall*) genes are expressed in heart, a stretch-activated muscle, sharing some features with insect fibrillar flight muscles. Since heart abnormalities observed in patients suffering from the Towns-Brocks syndrome are caused by a mutation in SALL1, it is possible that Spalt's function to determine a fibrillar, stretch-modulated muscle type is conserved to vertebrates.

3. Acknowledgements

This work would not have been possible without the help, advice and support of many people and here I would like to express my sincere gratitude to all of them.

I am particularly thankful to my supervisor and mentor Frank Schnorrer for introducing me to the exciting field of science, excellent supervision and giving me constant support and encouragement throughout my Diploma and PhD studies.

Moreover, I would like to thank Matthias Mann for being my doctor father and member of my thesis advisory committee, his interest in my project, and valuable discussions and advices.

I am also very grateful to Reinhard Fässler not only for supporting the “fly group” by generously providing lab space and sharing technical equipment but also for stimulating scientific discussions during department seminars.

I am greatly thankful to Barry Dickson for being a member of my thesis advisory committee, his support, valuable advices and useful input to my project. Similarly, I would like to thank Takashi Suzuki for being a member of my thesis advisory committee and his input to my project.

Great thanks to Nina Jährling, Hans-Ulrich Dodt, Martin Radolf, Radoslaw Ejsmont, Pavel Tomancak, Jutta Distler and Manfred Frasch for successful collaborations and to Alexis Lalouette for experimental help and advice.

I am especially thankful to all the former and present members of the Schnorrer lab for all their help, advice and invaluable input to my project, and, of course, also for the fun and nice chats during our numerous coffee and ice cream breaks or in the fly room making even flipping an (almost) enjoyable activity.

Also, I would like thank all the members of my examination board for their time and dedication to review my thesis: Matthias Mann (first referee), Klaus Förstemann (second referee), Reinhard Fässler, Babara Conradt, Christian Wahl-Schott and Karl-Peter Hopfner.

Finally, I am deeply grateful to my friends and family, especially to my parents, for their understanding, patience, constant moral support and encouragement whenever I needed their help.

4. Introduction

Not only the admirable achievements of the world's top athletes during the Olympic Games but also every step we make, every breath we take, and every bite we chew, all these apparently simple, but nonetheless essential tasks we perform every day, depend on the orchestrated contractions of different muscles in our body. Our body muscles comprise various distinct muscle types such as the slow- and fast-twitch skeletal muscles, as well as a rhythmically beating muscle, the heart. All of these muscles are adapted to perform different functions in the body ranging from sustained, low intensity work (e.g. maintaining posture), rapid and powerful movements (like jumping or kicking), to life-long continuous contractions (such as pumping of blood by the heart), and, hence, differ in their molecular composition and contractile properties (Schiaffino and Reggiani, 1996).

This striking diversity is first established during embryogenesis by specification of muscle type identity through intrinsic transcriptional regulatory mechanisms (Baxendale et al., 2004; Hofsten et al., 2008; Niro et al., 2010; Braun and Gautel, 2011) and can be modified later, during postnatal life, by neuronal activity and hormonal factors, mainly, by reactivating the embryonic developmental programs (Schiaffino et al., 2007). Despite major progress in understanding the basics of muscle progenitor origin, specification and differentiation (Vincent and Buckingham, 2010; Braun and Gautel, 2011), a comprehensive delineation of the genetic pathways controlling myogenesis and, in particular, the generation of different muscle types is still missing.

The *Drosophila* adult muscles offer an excellent model to systematically study myoblast diversification and muscle type differentiation. First, the basic muscle cell structure and events of myogenesis, including muscle progenitor specification, fusion, attachment to tendon cells, and assembly of the contractile apparatus are conserved from insects to mammals (Baylies et al., 1998; Schnorrer and Dickson, 2004; Hartenstein, 2006). Furthermore, similar to vertebrate skeletal muscles and in contrast to the single cell larval muscles, they consist of several muscle fibers that are bundled together to form one contractile unit (Bate, 1993; Dutta and VijayRaghavan, 2006).

Second, the *Drosophila* adult muscles comprise different muscle types with characteristic myofibrillar composition and contractile properties, which can be easily

identified based on their distinct fiber morphology (Tiegs, 1955; Dutta and VijayRaghavan, 2006).

Finally, with the recent development of genome-wide, transgenic RNAi libraries in *Drosophila* (Dietzl et al., 2007; Matsumoto et al., 2007; Ni et al., 2009) it is now possible to conditionally inactivate gene function even in such complex tissues as syncytial muscles in a systematic manner. Thus, we set out to define the genetic regulatory programs determining muscle identity in *Drosophila* by performing a genome-wide muscle-specific RNAi screen.

4.1 *Drosophila* adult muscle system

4.1.1 Adult muscle pattern

The most prominent adult muscles are the flight muscles in the thorax (Miller, 1950; Fig. 1). They can be classified in two functionally distinct groups: the direct flight muscles (DFMs; Fig. 1B), directly attaching to the wing, and the indirect flight muscles (IFMs; Fig. 1A), connecting to the thoracic exoskeleton. The small DFMs are needed for steering by controlling the position of the wing blades during flight, whereas the much larger IFMs generate the power for flight, and move the wings by deforming the thorax (Josephson, 2006). The IFMs are composed of two antagonistic sets of muscles: the dorso-longitudinal muscles (DLM), consisting of six fibers per hemithorax, and three groups of dorsal-ventral muscles: DVM I (three fibers), DVM II (two fibers) and DVM III (two fibers). Contraction of DLMs causes a downward movement of the wings (i. e. they act as depressors), whereas contraction of DVMs results in upward movement of wings (i.e. they act as elevators) (Fernandes et al., 1991; Dutta and VijayRaghavan, 2006). Another large thoracic muscle is the tergal depressor of trochanter (TDT) or jump muscle, which spans from the dorsal notum (the cuticular plate at the back of the fly) to the second pair of legs, and is essential for the escape response and the initiation of flight (Jaramillo et al., 2009; Fig. 1B).

The fly musculature needed for locomotion is located in the legs and consists of numerous small, multi-fiber muscles, which are organized into a stereotyped pattern along the proximal-distal axis (Miller, 1950; Soler et al., 2004; Fig. 1A). In the abdomen the muscles of each hemisegment are classified into dorsal, lateral and

ventral muscles each consisting of a defined number of fibers (Miller, 1950; Bate et al., 1991; Currie and Bate, 1991; Fig. 1A).

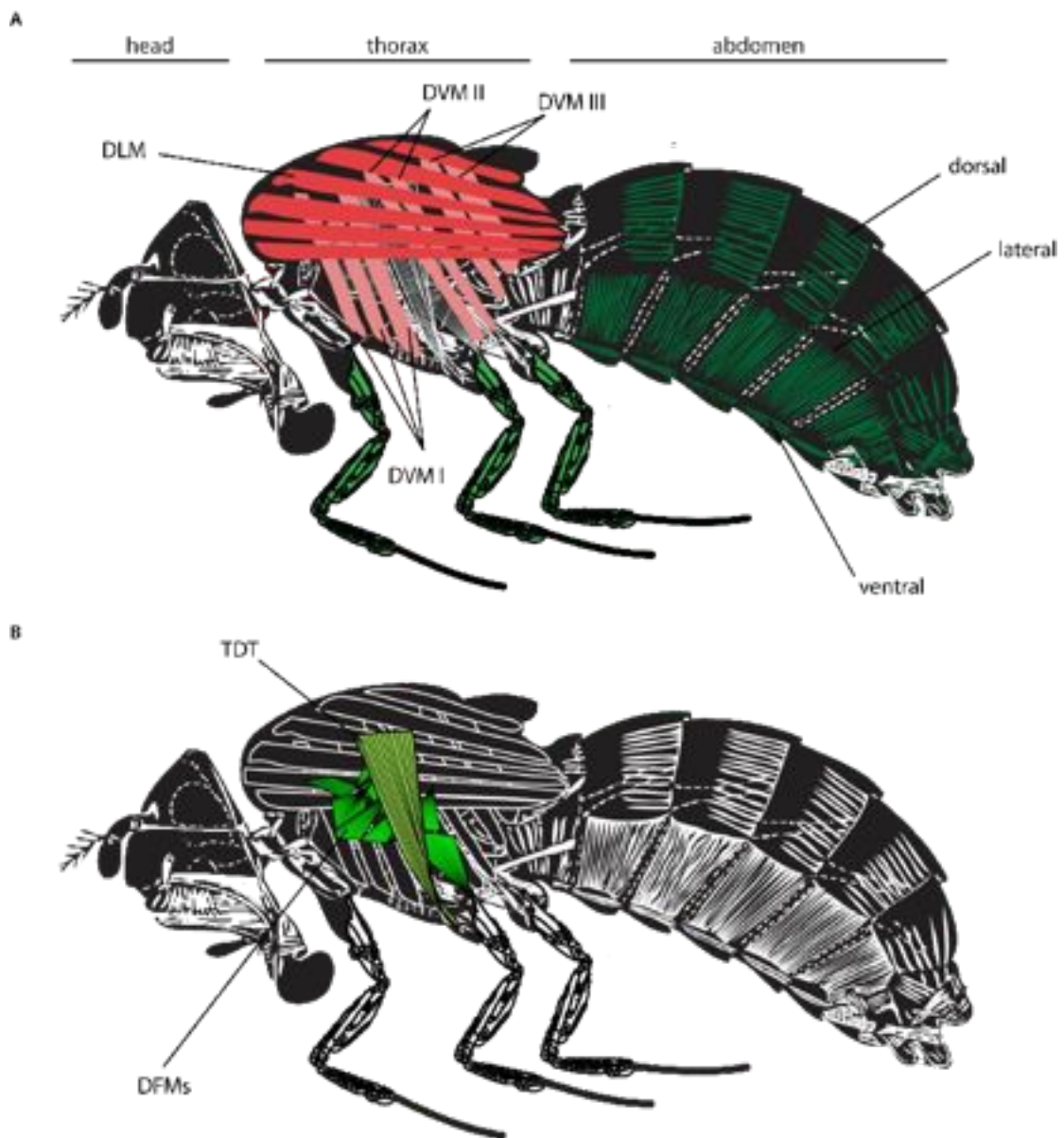


Fig. 1 | Adult *Drosophila* muscles

Sagittal view of *Drosophila* adult muscles in thorax, leg and abdomen. (A) The indirect flight muscles (IFMs) in the thorax comprise two antagonistic muscle sets: the dorso-longitudinal muscles (DLMs; dark red) and the three groups of dorso-ventral muscles (DVMs; light red). Leg muscles are shown in light green. Abdominal muscles (dark green) consist of dorsal, lateral and ventral muscles. (B) Laterally located thoracic muscles. Jump muscle or tergal depressor of trochanter (TDT) is depicted in light green and the various small direct flight muscles (DFMs) in bright green. Anterior is to the left, dorsal up.

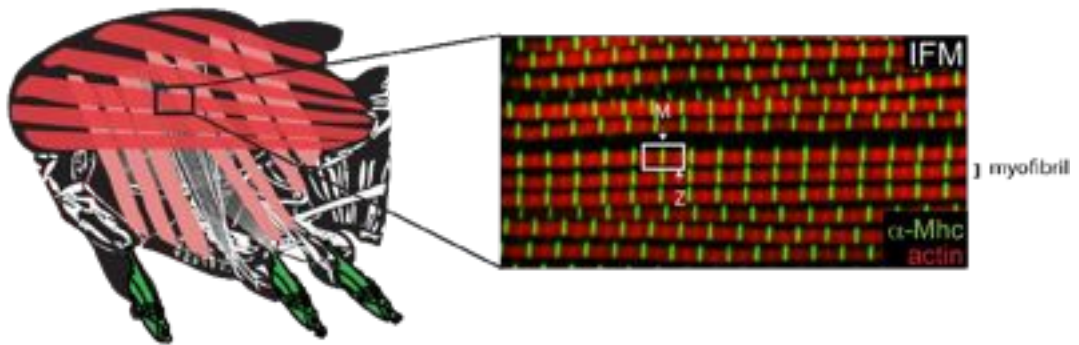
4.1.2 Basic muscle architecture: myofibrils and sarcomeres

Like skeletal muscles, *Drosophila* adult muscles are composed of several large, multinucleated cells called muscle fibers because of their elongated shape. Their actin and myosin filaments are assembled into highly ordered, contractile elements, the myofibrils, filling up most of their cytoplasm (Fig. 2A). Each myofibril consists of a series of repeating small contractile units, the sarcomeres, representing the structural basis for contraction (Hanson and Huxley, 1953; Huxley and Niedergerke, 1954).

Sarcomeres are precisely ordered assemblies of partially overlapping thin actin and thick myosin filaments with almost crystalline regularity. The thick filaments are anchored to the M line in the center of the sarcomeres, whereas the thin filaments are cross-linked at the Z-disc at each sarcomere end and project towards the middle, where they overlap with the thick filaments (Fig. 2B).

In addition to myosin and actin, myofibrils contain various other structural proteins that are associated with the actin and/or myosin filaments to maintain their precise lattice arrangement, to control their ordered assembly, and to modify their contractile properties (Clark et al., 2002).

A



B

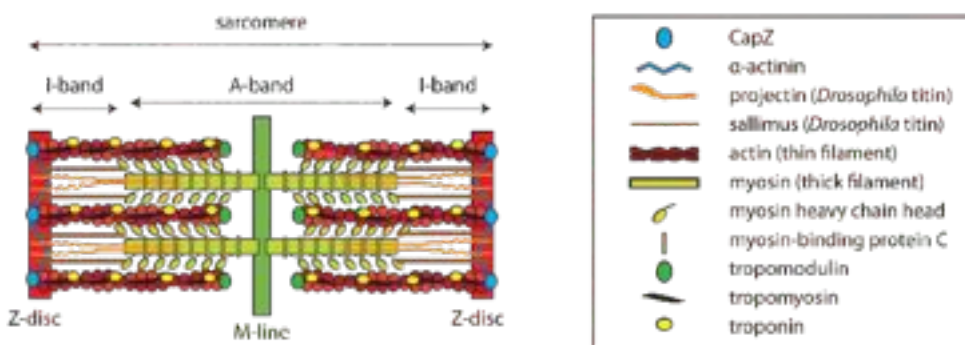


Fig. 2 | Myofibrils and sarcomeres

(A) Each muscle fiber is composed of elongated contractile bundles, the myofibrils, which are arranged in parallel and have a striated pattern. White box marks the smallest contractile unit of muscles, the sarcomere. M line is labeled with myosin heavy chain antibody (green) and actin (red) accumulates at Z line. (B) Scheme of a sarcomere. Thin actin filaments (red) are cross-linked at Z-disc defining the ends of a sarcomere. Thick myosin filaments (light green) are anchored at M-line (green). Actin filaments overlap with myosin filaments in A-bands, marking the whole length of myosin filaments. I-bands are zones of non-overlap only containing actin. Various accessory proteins and their location within the sarcomere are indicated.

4.1.3 Adult muscle types: fibrillar and tubular muscles

Distinct morphology of fibrillar and tubular muscles

Based on their distinct morphology the *Drosophila* adult muscles (and flying insect muscles in general) can be classified into two main muscle types: the fibrillar and the tubular muscles. The fibrillar morphology is unique to IFMs. All other adult muscles, including leg, jump and abdominal body wall muscles, are tubular (Snodgrass, 1935; Tiegs, 1955).

Fibrillar muscles are termed as such, because they are composed of large, easily dissociable myofibrils, which are not laterally connected. Their nuclei are distributed throughout the muscle cell localizing inline with the myofibrils (Fig. 3B and C). In tubular muscles, by contrast, myofibrils are small in diameter, held in register to each other by lateral connections, and are organized into hollow, tube-like structures. Noticeably, the nuclei are located in the center of these tubes (Fig. 3D and E).

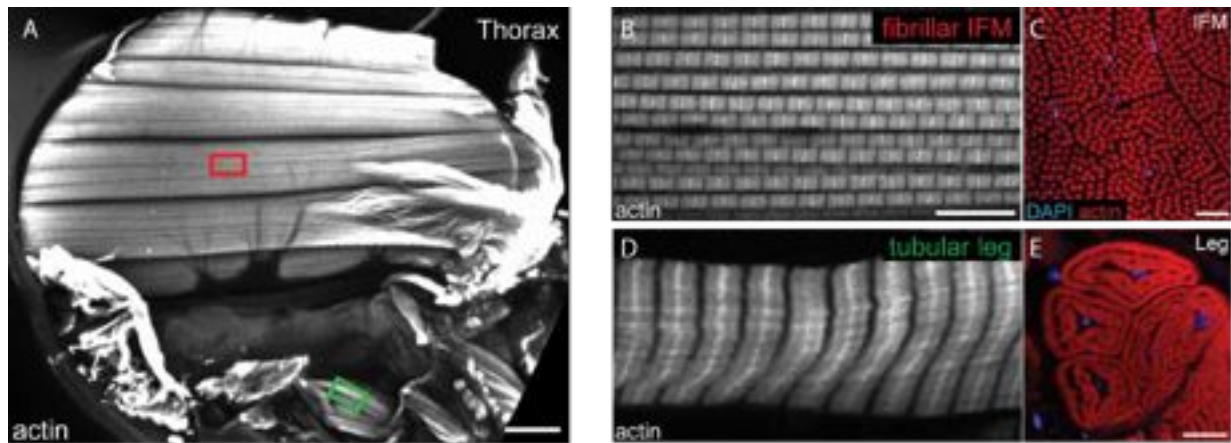


Fig. 3 | Fibrillar and tubular muscles

(A) Hemi-thorax stained with phalloidin visualizing actin. Red and green boxes indicate the approximate views in B and D. (B-C) Fibrillar indirect flight muscles (IFMs). (B) Sagittal cut showing large, non-aligned, individual myofibrils. (C) Cross-section of IFMs. Note, in fibrillar IFMs nuclei localize in between the myofibrils. (D-E) Tubular leg muscles. (D) Sagittal cut showing thin laterally connected myofibrils (E) Cross-section of leg muscles revealing the tubular myofibril arrangement with centrally positioned nuclei. Myofibrils are labeled in red and nuclei are labeled with DAPI in blue in C and E. Scales are 100 μm in A and 10 μm in B to E. In A anterior is left and dorsal up.

Fibrillar IFMs are fast contracting muscles specialized for flight

The huge evolutionary success of insects (measured in terms of abundance and species diversity) can largely be attributed to their small size and their acquisition of flight. However, smaller body size for flying animals means having to achieve higher wing beat frequencies; otherwise they would not be capable to offset gravity. The fibrillar IFMs have evolved to adapt to these special requirements and possess the remarkable ability to generate high power at high frequencies (Dickinson, 2006).

How can fibrillar muscles achieve this? All fibrillar IFMs are asynchronous muscles, as their contraction frequencies are not synchronized with action potential firing of their motor neurons (Josephson et al., 2000; Josephson, 2006). Unlike in

more slowly contracting, synchronous muscles, in which each contraction is induced by a rise in Ca^{2+} that is released from the sarcoplasmic reticulum (SR) in response to a motor neuron spike, the contractions in fibrillar IFMs are regulated mechanically by stretch. In the thorax the two antagonistic IFM units, the DLMs and DVMs, are arranged perpendicularly to each other (Fig. 1). Therefore, contraction of DVMs not only moves the wings upwards but, simultaneously, also stretches and thus activates the DLMs; they in turn contract to move the wings down again and stretch the DVMs, thereby propagating a self-sustaining circle, which results in the fast oscillatory movement of the cuticular thorax and attached wings with frequencies as high as 1000 Hz in tiny midges.

Some synchronous muscles can also contract at high frequencies of up to 100 Hz (e.g. those moving rattles of rattlesnakes) (Schaeffer et al., 1996). These muscles usually contain enormous amounts of SR, because they need to quickly reuptake Ca^{2+} into the SR by active transport, before the next contraction can be initiated (Schaeffer et al., 1996). However, this increase in SR comes at the expense of contractile filaments and mitochondria, creating a trade-off between deactivation speed and power output in fast contracting synchronous muscles. The stretch-activated, fibrillar IFMs, by contrast, contain only sparse and scattered SR, and instead their muscles are densely packed with large myofibrils and mitochondria, making them both fast contracting and powerful muscles (Pringle, 1981).

Distinct protein and protein-isoform composition of tubular and fibrillar muscles

Although tubular and fibrillar muscles share the organization of their contractile filaments into sarcomeres, they display a great heterogeneity in molecular composition, which is directly related to their distinctive morphologies and contractile properties.

They express, for example, distinct actin genes generating proteins with slightly different amino acid sequences (Fyrberg et al., 1983). In addition, their myosin molecules exist in various muscle-type-specific isoforms produced by alternative splicing of their transcripts (Falkenthal et al., 1987; Hastings and Emerson, 1991; Bernstein and Milligan, 1997; Swank et al., 2001; 2002). Finally, fibrillar and tubular muscles contain a wealth of accessory proteins or protein-isoforms specific to each type (Karlik and Fyrberg, 1986; Ayme-Southgate et al., 1989; Barbas et al., 1991;

Maroto et al., 1996; Domingo et al., 1998; Reedy et al., 2000; Qiu et al., 2003; 2005; reviewed in Marden, 2006), contributing to their distinct contractile properties.

Importantly, both muscle-type-specific gene expression and splicing are essential for proper muscle function. Especially, the highly ordered fibrillar IFMs are extremely sensitive to changes in their protein composition, such as switching of actin isoforms only differing in a few amino acids (Barbas et al., 1993; Fyrberg et al., 1998; Brault et al., 1999; Reedy et al., 2000; Agianian et al., 2004; Nongthomba et al., 2007).

The heterogeneity of vertebrate muscles (i.e. cardiac and skeletal) and skeletal muscle fiber types (fast- and slow-twitch), is similarly, attained either by differential exon splicing or by muscle-type-specific gene expression of actin, myosin and various accessory proteins (Schiaffino and Reggiani, 1996). To date, however, the molecular mechanisms by which alternative splicing and gene expression are coordinated to generate distinct muscle types during muscle differentiation are still largely unclear.

Fibrillar muscles are similar to vertebrate cardiac muscles, whereas tubular muscles resemble vertebrate skeletal muscles

Noteworthy, stretch-activation is not only required for the function of fibrillar insect flight muscles, but it is also important for the physiology of vertebrate cardiac muscles (Vemuri et al., 1999; Davis et al., 2001; Campbell, 2006; Shiels and White, 2008). As in fibrillar IFMs, stretch of cardiac myocytes, which happens when the heart fills with blood, increases their contraction strength during the next systole, when the blood is ejected from the ventricles. This phenomenon is referred to as “Frank-Starling mechanism”, applies to all vertebrate cardiac muscles, and, as in fibrillar insect flight muscles, constitutes an intrinsic property of cardiac myofibrils (Steiger, 1971; 1977; Stelzer et al., 2006).

Like fibrillar IFMs, cardiac muscles contain only little SR, largely depend on aerobic metabolism (therefore they have many, large mitochondria) and possess branched myofibrils that are not as linearly arranged as in skeletal muscles (Kossmann and Fawcett, 1961). The tubular muscles, by contrast, are more similar to vertebrate skeletal muscles: both are synchronous, depend on Ca^{2+} cycling and not mechanical stretch for their activation, contain a well-developed, extensive SR and

their myofibrils are laterally connected (Wang and Ramirez-Mitchell, 1983; Tonino et al., 2010).

4.2 *Drosophila* adult muscle development

Like many insects *Drosophila* undergoes metamorphosis meaning that in the course of a fly's life cycle most tissues, including muscles, are developed twice - once in the embryo, when the segmentally repeated pattern of larval muscles is set up, and a second time in the pupa, when all larval muscles are dissolved and the adult muscles are built *de novo* from adult muscle progenitor cells (AMPs) (Roy and VijayRaghavan, 1999). The AMPs are specified within the somatic mesoderm in the embryo together with the progenitors of larval muscles (Baylies et al., 1998).

4.2.1 Origin and diversification of adult muscle progenitors

Mesoderm specification

All the *Drosophila* muscles, including somatic, visceral and cardiac muscles, are of mesodermal origin (Bate, 1993). The specification of the mesoderm primordium starts right after cellularization of the embryo. At the blastoderm stage *dorsal (dl)* (Roth et al., 1989), the key determinant of dorsal-ventral axis formation, induces expression of the bHLH transcription factor *twist (twi)* (Thisse et al., 1991) in the ventral most cells of the embryo. During gastrulation the *twi* expressing cells first invaginate ventrally, then lose their epithelial character, divide and migrate dorso-laterally along the inner surface of the ectoderm to form the single cell layer of mesoderm (Leptin and Grunewald, 1990).

Mesoderm patterning

Initially, the mesoderm is a uniform cell layer. All mesodermal cells are characterized by expression of *twi* and its direct targets *snail (sna)* (Ray et al., 1991), *heartless (htl)* (Shishido et al., 1993), *tinman (tin)* (Bodmer et al., 1990; Bodmer, 1993) and *Myocyte enhancer factor 2 (Mef2)* (Lilly et al., 1994; Nguyen et al., 1994; Lilly et al., 1995; Taylor et al., 1995).

Soon after the invagination of *twi* expressing cells, however, the uniform field of mesoderm cells in each segment is rapidly subdivided into several distinct units,

from which the progenitors of visceral muscles, the fat body, somatic muscles and the heart are generated (Borkowski et al., 1995; Azpiazu et al., 1996). This segmental patterning is mediated by the inductive activity of the signaling molecules Wingless (Wg, the *Drosophila* Wnt), Hedgehog (Hh) and Decapentaplegic (Dpp, TGF β in vertebrates), which are secreted from the overlying ectoderm. Dpp patterns the mesoderm into dorsal and ventral sectors by maintaining high levels of *tin* in dorsal cells and repressing ventrally expressed genes like *pox meso* (*pxm*) (Staehling-Hampton et al., 1994; Frasch, 1995). The patterning along the anterior-posterior axis is mediated by the activity of the segment polarity genes *even-skipped* (*eve*) and *sloppy-paired* (*slp*), which are induced by ectodermal Hh and Wg signaling, respectively (Riechmann et al., 1997). The anterior *eve* domain, characterized by low levels of *twi* expression, gives rise to progenitors of fat body and visceral muscles, whereas cells of the posterior *slp* domain, expressing high levels of *twi*, constitute the progenitors of somatic and cardiac muscles (Baylies and Bate, 1996 and Fig. 4).

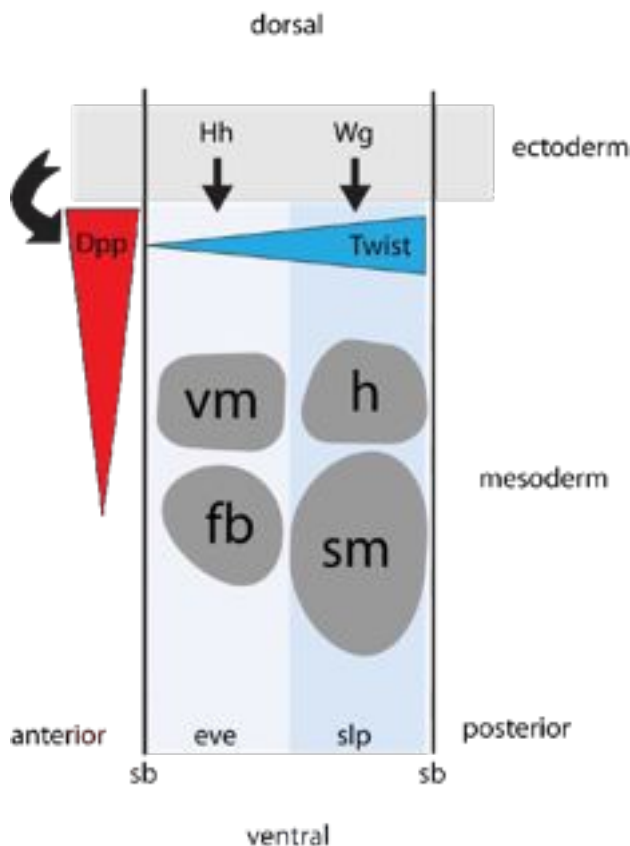


Fig. 4 | Mesoderm segmentation

In each segment the uniform mesoderm cell layer is subdivided into distinct fields of visceral muscle (vm), heart (h), fat body (fb) and somatic muscle (sm) progenitor cells by the activity of ectodermal signals. A Dpp gradient organizes mesoderm along the dorsal-ventral axis and along the anterior-posterior axis the mesoderm is subdivided by a *twist* (*twi*) gradient between low *twi* expressing *even-skipped* (*eve*) and high *twi* expressing *sloppy-paired* (*slp*) domains. *eve* and *slp* are segment polarity genes, the expression of which was initially induced by ectodermal Hh and Wg signals, respectively.

(sb = segment border) (Modified from Riechmann et al., 1996)

Common origin of embryonic and adult muscle progenitors

Both the adult muscle progenitors (AMPs) and the founder myoblasts of embryonic muscles originate from the high *twi* expressing mesodermal cells in the embryo (reviewed in Baylies et al., 1998; Schnorrer and Dickson, 2004; Dutta and VijayRaghavan, 2006).

In the abdominal segments the specification of myogenic progenitors is initiated at embryonic stage 10, when Wg induces the expression of the proneural gene *lethal of scute (l'sc)* in clusters of cells within the somatic mesoderm (Fig. 5). Subsequently, *l'sc* expression is progressively restricted to one or two cells only by Notch/Delta mediated lateral inhibition (Carmena et al., 1995; Martín-Bermudo et al., 1995). These *l'sc* expressing cells are the muscle progenitor cells, whereas all the remaining cells are fusion competent cells (FCMs) (Fig. 5).

By late stage 11 the progenitor cells undergo one further asymmetric division into two daughter cells, one of which is a muscle founder cell, while the other can either be a second founder cell or an AMP (Ruiz-Gómez and Bate, 1997; Carmena et al., 1998). Each founder cell seeds the formation of a single muscle by fusing with a defined number of FCMs and expresses a unique set of identity genes, determining the specific properties (position, size, attachment sites and innervation pattern) of the individual larval muscles (Baylies et al., 1998; Bataillé et al., 2010). Thus, founders specify muscle identity, whereas FCMs are solely needed for muscle growth.

AMPs are also generated in thoracic segments in the embryo. However, this process has not yet been investigated in detail. Presumably, the mechanisms are akin to the generation of AMPs in the abdomen.

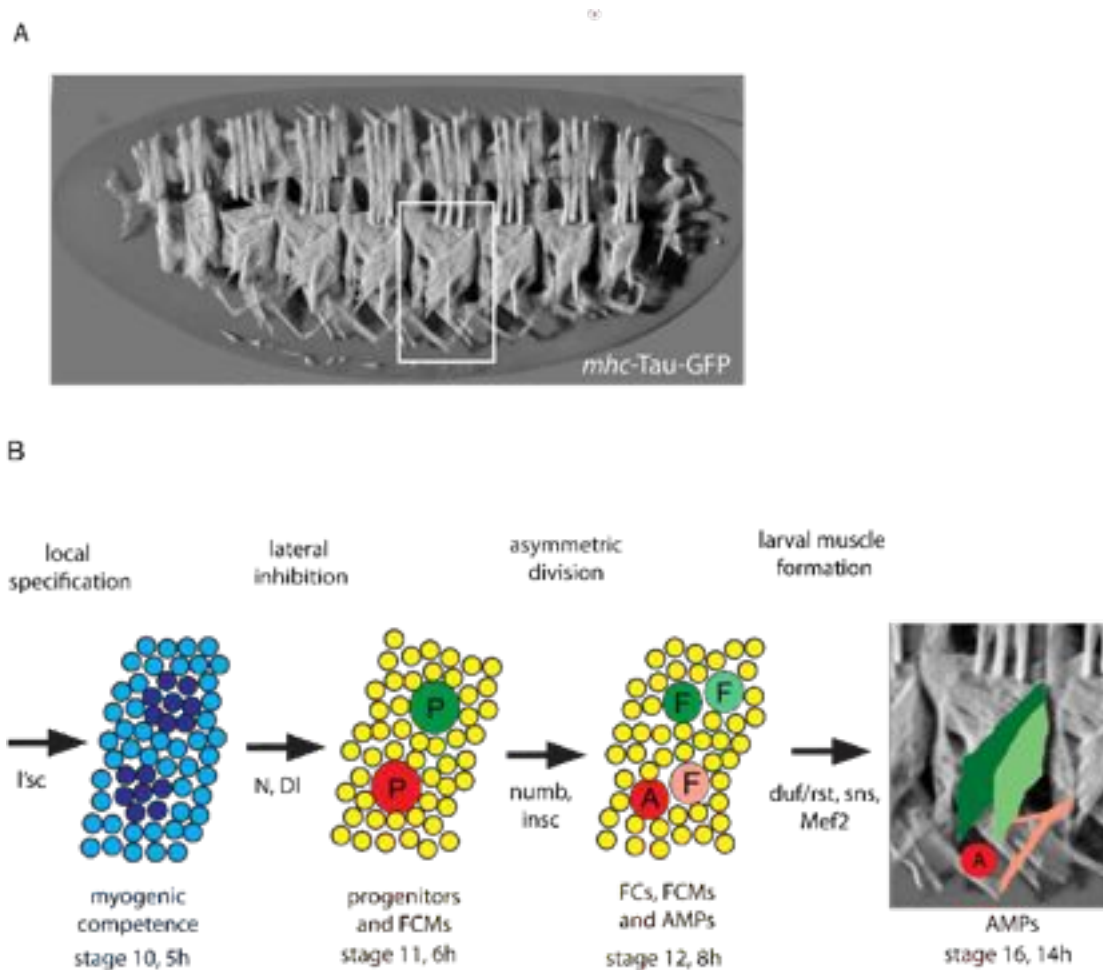


Fig. 5 | Specification of adult muscle progenitors

(A) Dorso-lateral view of muscle pattern of a stage 17 embryo visualized with *mhc-Tau-GFP*. Anterior is left, dorsal is up. Box marks ventral muscles shown in B. (B) Scheme showing steps involved in adult muscle precursor (AMP) specification in the embryo. Progenitor cells (P) marked by high *lethal of scute* (*l'sc*) expression (dark blue) are singled out from a pool of equivalent cells (light blue) by lateral inhibition. They divide asymmetrically to generate either a pair of founders (F) or a founder cell and an AMP (A, red). Founders differentiate and fuse with fusion competent cells (FCMs, yellow) to form larval muscles, whereas AMPs stay quiescent and reside at defined sites within the abdominal hemisegments. (B is adapted from Schnorrer and Dickson, 2004).

Quiescent adult muscle progenitor cells reside at defined sites in embryo

While founders and FCMs fuse and differentiate to larval muscles, the AMPs continue to express high levels of *twi*, maintain active Notch signaling, and delay their differentiation until the onset of adult muscle formation (Bate et al., 1991; Figeac et al., 2010; 2011). This is achieved, at least in part, by repressing the differentiation-promoting activity of *Mef2* by the Notch target *Hole in muscles* (*Him*) (Liotta et al., 2007; Soler and Taylor, 2009; Figeac et al., 2010; 2011). At end of stage 13 the *twi* expressing AMPs will reside at defined sites in the embryo (Bate et al., 1991; Fig. 6)

In the thorax patches of AMPs localize in close proximity to the primordia of imaginal discs, which will generate future adult epidermal structures, such as wings and legs (Fig. 6A). In the abdomen the pattern is a much simpler one: in each abdominal segment there is a single ventral AMP, two lateral AMPs and three dorsal AMPs, two of which are located more dorso-laterally (Fig. 6B). All of the abdominal AMPs are closely associated with specific branches of peripheral nerves (Currie and Bate, 1991).

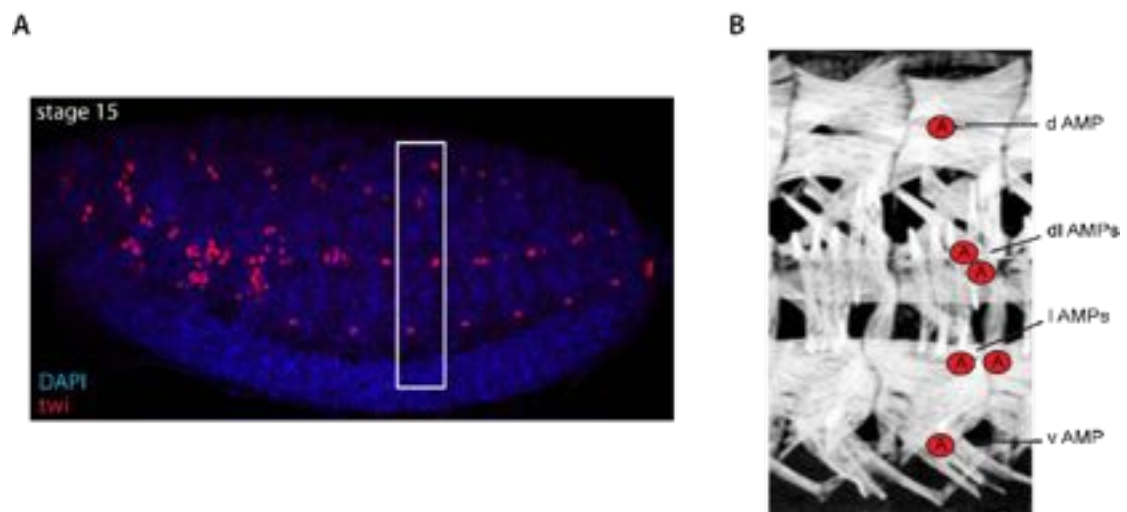


Fig. 6 | Localization of adult muscle progenitors in late embryo

(A) Lateral view of stage 15 embryo. Adult muscle progenitors (AMPs) are stained with anti-Twi (red). Note patches of AMPs in the thorax and single AMPs at defined positions in the abdomen. White box marks approximate view in B. Anterior is left, dorsal up. (B) Scheme illustrating positions of abdominal AMPs relative to larval muscles. In each segment there is a single dorsal (d), two dorso-lateral (dl), two lateral (l) and one ventral (v) AMP.

Fate of abdominal adult muscle progenitors

All adult abdominal muscles are generated from the six AMPs present in each abdominal segment of the embryo. These cells start to proliferate in the second larval instar to generate six clusters of cells per hemisegment. Importantly, the position of the AMPs in the embryo (dorsal, lateral or ventral) already reflects the position of the future adult muscles (dorsal, lateral or ventral). Ablation of AMPs during larval stages suggests that in the abdomen groups of AMPs are specified to generate specific adult muscle sets, each of which is composed of several muscle fibers (Broadie and Bate, 1991). To date, however, the molecular mechanisms mediating this fate restriction during early developmental stages are still unknown.

Diversification of thoracic adult muscle progenitors

Much more is known about the fate restriction of thoracic AMPs, in particular those forming the IFMs and DFMs. They similarly localize in an invariant pattern in the late embryo. In each of the thoracic hemisegments clusters of six to seven cells reside in close proximity to the primordia of the imaginal discs and, additionally, a few cells localize close to nerves (Bate et al., 1991).

Like their abdominal counterparts they start to proliferate from mid second larval instar stages onwards to generate pools of progenitors, which are associated with the imaginal discs throughout the larval stages and therefore are also called adepithelial cells (Poodry and Schneiderman, 1970; Reed et al., 1975).

Mosaic analysis and ablation studies revealed that both IFMs and DFMs are generated by the AMPs associated with the wing imaginal disc, whereas the leg muscles are formed by AMPs attached to leg discs. AMPs on the mesothoracic leg disc will not only form leg muscles of the second thoracic segment but also contribute to the generation of the jump muscle (Lawrence, 1982; Broadie and Bate, 1991).

The wing-disc-associated AMPs, forming the functionally distinct IFMs or DFMs, are not a uniform population. In fact, they already become distinct soon after their generation in the late embryo, when ectodermal Wg induces expression of the transcription factor *vestigial* (*vg*) in only a subset of them. By the late larval stages, they are subdivided into distinct groups of cells that are characterized by the differential expression of the transcription factors *cut* (*ct*) and *vg*: one population expresses high levels of *vg* and low levels of *ct*, whereas the other lacks *vg* and is

marked by high *ct* expression (Fig. 7). The larger group of high *vg* expressing cells will generate the IFMs, while the high *ct* expressing AMPs will form the DFMs. In the larva the differential expression of *ct* and *vg* in AMPs is maintained by ectodermal Wg signaling and reinforced by mutual transcriptional repression of *vg* and *ct* (Sudarsan et al., 2001).

During pupal development the DFMs are further differentiated by expression of the transcription factor *apterous* (*ap*), which is downregulated in IFMs by *vg* (Ghazi et al., 2000; Bernard et al., 2003). Thus, in the thorax myoblast diversification into distinct groups of cells giving rise to different muscle types is already initiated at late embryonic stages and this subdivision involves both intrinsic transcriptional and extrinsic signaling mechanisms.

However, this early channeling of AMPs, to develop along distinct lineages, is not yet definite: when wing discs with marked AMPs are transplanted into the abdomen of a larval host, the wing-disc-associated AMPs can contribute to diverse adult muscles, suggesting that they can still adapt to changing environmental cues at late larval stages (Lawrence and Brower, 1982).

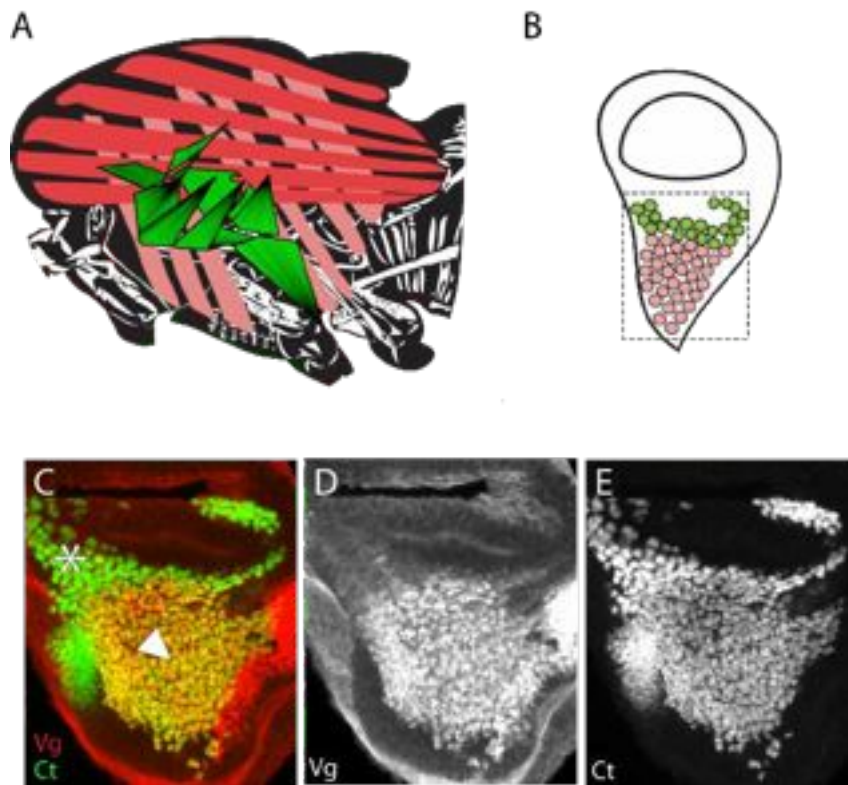


Fig. 7 | Adult myoblast diversification and the formation of indirect and direct flight muscles

(A) Scheme showing adult indirect flight muscles (IFMs, red) and direct flight muscles (DFMs, green) in the thorax. Anterior is left, dorsal up. (B) Scheme of L3 larval wing disc with associated adult myoblasts. Adult myoblasts giving rise to the future IFMs express high levels of *vestigial* (*vg*, red) and low levels of *cut* (*ct*, green), whereas DFM-forming myoblasts express no *vg*, but high levels of *ct*. Dashed box marks approximate view of region shown in C to D. (C-D) L3 wing discs stained with anti-Vg (in D and red in C) and anti-Ct (in E and green in C). White asterisk marks high Ct expressing DFM-forming myoblasts and white arrowhead labels IFM-forming myoblasts expressing high levels of Vg and low levels of Ct in C. L3 is 3rd larval instar.

4.2.2 Adult muscle fiber formation

During pupal development most of the larval muscles are histolyzed and replaced by newly formed adult muscles. In the first few hours after pupae formation (APF) AMPs continue to proliferate and migrate to sites, where adult muscles are generated in two distinct ways: they can either arise by *de novo* formation or AMPs use remodeled larval muscles as templates for fusion. This regeneration-like mode of formation is unique to DLMs, whereas all other adult muscles are generated *de novo*.

Adult founder cells determine fiber number and position

As larval muscle formation in the embryo, adult myogenesis is initiated by the selection of founder cells from pools of AMPs. For adult muscles, though, founder selection is not dependent on Notch-mediated lateral inhibition, but involves – at least in the abdomen – FGF signaling via *htl* (Dutta et al., 2004; 2005).

Both embryonic (Ruiz-Gómez et al., 2000) and adult founder cells (Dutta et al., 2004; 2005; Atreya and Fernandes, 2008; Jaramillo et al., 2009), are characterized by the expression of the immunoglobulin (Ig)-domain containing transmembrane protein *dumbfounded* (*duf*). In the embryo *duf* is exclusively expressed in founder cells (FCs), but not in fusion-competent cells (FCMs). It is required for the initial recognition and adhesion events during fusion and acts by attracting FCMs expressing the *duf* counter-receptor *sticks and stones* (*sns*) (Bour et al., 2000). The mutually exclusive expression of these receptors ensures that fusion only occurs between the two subtypes (FCs and FCMs), but not among themselves or any other cell type, thereby defining the number and position of muscles.

Similarly, the adult *duf* expressing founders seed the formation of the correct number of adult muscle fibers at the correct position. Founders have been identified for all adult muscles, and the localization and number of *duf* expressing cells in pupa prefigures the adult muscle pattern.

Founders for DVMs are selected at 6h APF, whereas founder selection for DFMs, leg, and abdominal muscles occurs later at about 24h APF, shortly before fusion is initiated. In the case of the DLMs, the larval templates serve as founders, which similarly start to express *duf* at 6h APF. Importantly, in the absence of templates, fusion and formation of multinucleated DLM fibers expressing differentiation markers still occurs, yet too many fibers are generated, suggesting that the remaining AMPs still have the capacity to respond to other cues to initiate fusion and differentiation (Farrell et al., 1996; Fernandes and Keshishian, 1996; Atreya and Fernandes, 2008). Thus, the main role of high *duf* expressing adult founders and templates is to regulate the formation of correct fiber number at the correct positions, but they are not required for fiber formation per se.

Formation of dorso-longitudinal muscles using larval templates

In the thorax histolysis is completed by 8h APF. By this time all the larval muscles of the thorax, but the three dorsally located larval oblique muscles (LOMs) have been dissolved. These muscles will serve as templates for DLM formation. As soon as wing discs start to evert at 5-6h APF, some of the associated AMPs leave the disc and migrate along the epidermis to sites, where templates are located.

Soon after, the LOMs lose their larval appearance: they disassemble their sarcomeres, become longer and thinner, and start to express high levels of *duf*. At 6-8h APF the AMPs start to fuse with the three templates, which induces their splitting into the six fibers comprising the DLMs (Fig. 8). The mechanisms regulating template splitting are still not understood. However, the interaction of fusing myoblasts with the templates is important, as splitting fails, when AMPs are ablated (Roy and VijayRaghavan, 1998). So far only a few genetic factors, including *erect wing (ewg)*, *twi* and its target *Mef2*, have been identified to be required for splitting. Mutants of these display a variable reduced number of DLM fibers in adults (DeSimone et al., 1996; Cripps et al., 1998). Similarly, both Notch loss and gain of function mutants have a splitting defect of DLMs (Anant et al., 1998).

After completion of splitting by about 14h APF, the adult myoblasts continue to fuse with the forming myofibers. As soon as fusion is completed by 30h APF, the myofibers compact (they become short and thick) and start to assemble their myofibrils and sarcomeres (Fig. 8). During the rest of pupal development muscles elongate and grow to their final size (Fernandes et al., 1991; Schönbauer et al., 2011).

De novo formation of other adult muscles

All other adult muscles form *de novo* without the use of templates. About the same time, by which the first adult myoblasts fuse with the larval templates, clusters of fusing myoblasts are detected around *duf* expressing founders at sites, where the future DVMs and the jump muscles are located. Just like DLMs, DVMs compact by 30h APF and initiate myofibril and sarcomere assembly (Fig. 8).

DFMs are generated by AMPs, which are associated with the wing disc together with the IFM-forming ones (Ghazi et al., 2000; Kozopas and Nusse, 2002 Fig. 7 and 8). When wing discs start to evert at 5-6h APF, the DFM progenitors, unlike IFM-forming AMPs, do not leave the discs, but remain attached with the everting disc

epithelium, where they localize to a region directly adjacent to the wing hinge primordium (Kozopas and Nusse, 2002). Subsequently, some DFM-forming AMPs migrate to additional sites located on the inner face of the ventral pleura, the epithelial structure giving rise to the future lateral parts of the thorax. Fusion is initiated by 24h APF and the final muscle pattern can be readily detected around 36h APF (Kozopas and Nusse, 2002).

Similarly, the formation of abdominal and leg muscles happens later than IFM formation. In the abdomen histolysis is not completed before 20h APF. In the first few hours of pupal formation abdominal AMPs proliferate and then, by 13h APF, start to migrate along nerves, with which they are associated, to the sites of muscle formation on the dorsal, lateral and ventral epidermis, where selection of founders takes place. Finally, fusion starts at 24h APF and by 40h APF the final muscle pattern is established (Currie and Bate, 1991).

In the leg fusion of AMPs with founders located closely to precursors of their epithelial attachment sites is initiated by 24h APF and completed by 40h, when myofibrillogenesis starts (Soler et al., 2004).

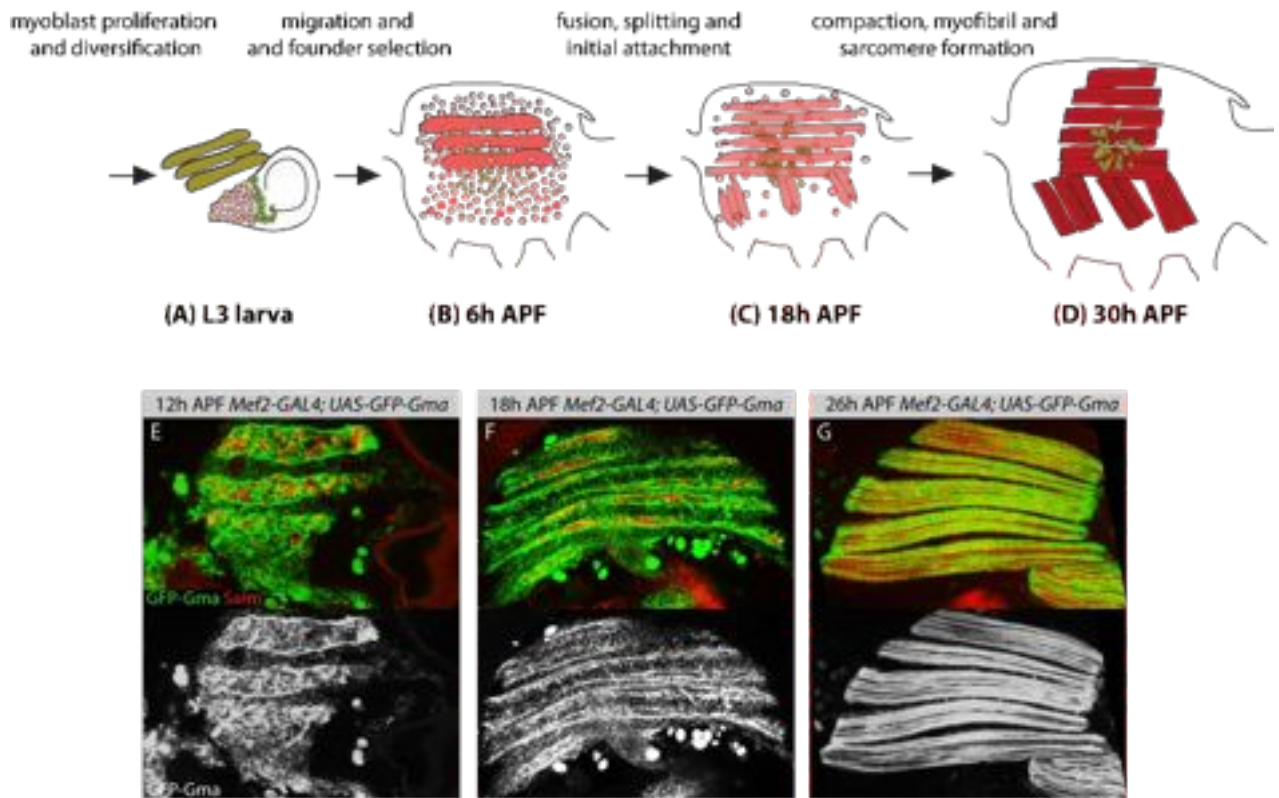


Fig. 8 | Adult muscle fiber development

(A-D) Scheme illustrating steps of adult muscle formation using indirect flight muscle (IFM) and direct flight muscles (DFM) formation as examples. (A) Adult myoblasts forming IFMs (light red) and DFMs (green) are associated with the wing imaginal discs and proliferate during larval stages. (B) At onset of pupa formation the myoblasts migrate to sites of muscle formation and start to fuse either with larval templates or with selected founders (dark red). Muscle formation using larval templates as scaffolds is unique mode of formation for dorso-longitudinal muscles (DLMs). All other adult muscles form *de novo*. (C) Fusion of myoblasts with templates induces their splitting into six fibers. Shortly after muscles form initial attachments with tendons. (D) At 30h APF muscles compact, become short and thick, and start to assembly their myofibrils and sarcomeres. Anterior is left, dorsal is up. APF: after puparium formation. L3: 3rd larval instar stage. (E-G) Confocal images of DLM development at (E) 12h APF before (F) at 16h APF after template splitting and (G) at 26h APF when muscles compact and assembly fibrillar actin structures. GFP-Gma labels actin of fusing myoblasts and forming myofibers in green, anti-Spalt major (Salm) stains nuclei of templates and forming myofibers in red.

4.2.3 Adult muscle attachment site formation

In *Drosophila* all muscles are anchored to the cuticle via specialized epidermal cells called tendons like their functional analogous in vertebrates that connect muscles to bones.

Specification of attachment sites at larval stages

As in the embryo the attachment sites of adult muscles are specified by the transcription factor *stripe* (*sr*) (Volk and VijayRaghavan, 1994; Lee et al., 1995; Fernandes et al., 1996; Frommer et al., 1996). The attachment sites for IFMs are already prefigured during larval stages: five discrete *sr* expressing domains on the larval wing discs correspond to the future attachment sites for DLMs and DVMs (Ghazi et al., 2003; Fig. 9). The transcription factor *apterous* (*ap*) and Notch signaling are required to induce the initial *sr* expression (Ghazi et al., 2000), which is further restricted to the final expression pattern by Wg signaling and the antagonizing transcription factors *pannier* (*pnr*) and *u-shaped* (*ush*) (Ghazi et al., 2003).

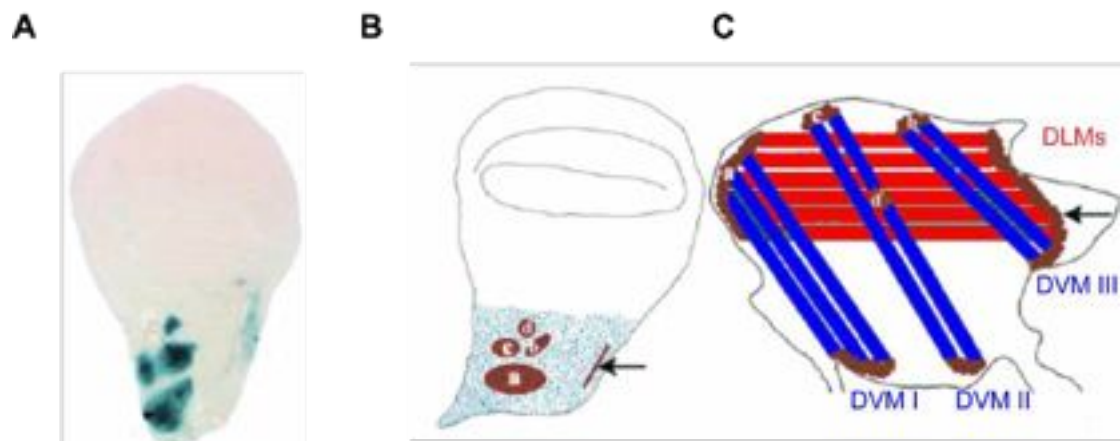


Fig. 9 | Attachment site specification

(A) Five domains of *sr* expressing cells prefiguring future attachment sites on larval wing disc. (B) Scheme of larval wing discs with five *sr* domains a-e and stripe (marked with arrow) in brown and (C) indirect flight muscles (IFMs) with attachment sites (brown). The medial domain (a) gives rise to anterior attachment sites of dorso-longitudinal muscles (DLMs, red). Domains a-d form attachment sites for dorso-ventral muscles (DVMs, blue) at their dorsal ends. All posterior DLM and ventral DVM attachments will be generated by the domain forming a stripe on wing disc (arrow). (modified from Ghazi et al., 2003).

Formation of force-resistant attachments during pupal stages

During pupal development the *sr* expressing domains first expand in size. At 16h APF, when splitting of the larval templates is completed, they send out long filopodia-like processes contacting the ends of the forming muscles, which similarly form short filopodia-like processes at their ends (Reedy and Beall, 1993b; Fernandes et al., 1996; Fig. 10).

As the epidermal-muscle contacts mature, they start to express the two major position specific (PS) integrin complexes PS1 (composed of alphaPS1 and the common betaPS subunit) and PS2 (comprising alphaPS2 together with betaPS) in a complementary fashion by 20h APF. PS1 is expressed in the tendon side of the attachments, while PS2 is expressed at the muscle ends (Brown, 1993; Fernandes et al., 1996). The myotendon junctions (MTJs) then further mature to generate force resistant attachments. At mature MTJs the myofibrils are anchored to the muscle membrane by modified terminal Z discs and the folded muscle cell membrane and the basal membrane of the tendons interdigitate extensively (Reedy and Beall, 1993b; Sandstrom and Restifo, 1999). Integrins and other linker proteins connect the cytoskeleton and membrane of tendons and muscles to a thick layer of extracellular matrix components deposited in between them (Brown, 2000). The force in tendon cells is transmitted from their basal (muscle) side to their apical (cuticle) side through bundles of microtubules (Reedy and Beall, 1993b). The proper differentiation of MTJs requires the function of *Broad complex (BR-C)*, a early response gene in the ecdysone cascade controlling metamorphosis (Karim et al., 1993), in tendon cells (Sandstrom et al., 1997; Sandstrom and Restifo, 1999).

In the embryo it has been shown that tendon cells do not only form epidermal attachment sites for muscles but also instruct the migration of the forming myotubes towards their correct insertion sites by providing guidance cues (Frommer et al., 1996; Vorbrüggen and Jäckle, 1997; Schnorrer and Dickson, 2004). However, if this is also true for adult myogenesis, has not been investigated so far.

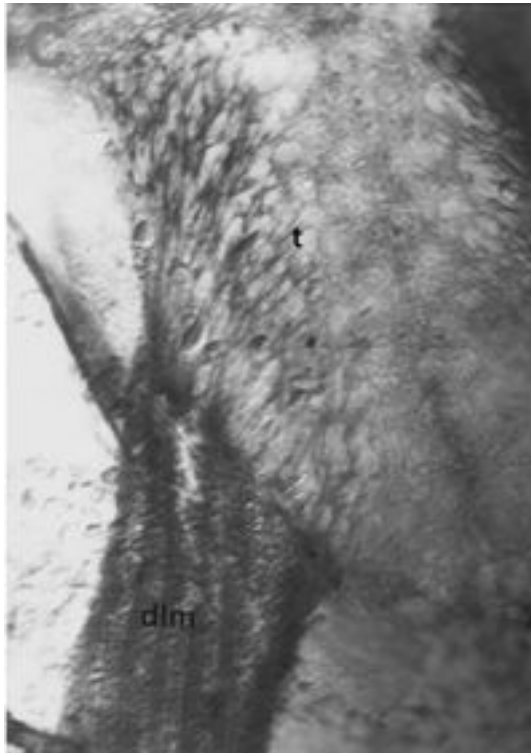


Fig. 10 | Filopodia-like extensions on muscles and tendons during attachment formation

Phase-contrast image of tendon cell extensions contacting dorso-longitudinal muscles (DLMs) at their growing ends similarly sending out filopodia-like extensions at 20h APF (dlm = dorso-longitudinal muscles, t = tendon cell). (From Fernandes et al., 1996).

4.2.4 Adult myofibrillogenesis and sarcomere formation

Our current knowledge about myofibril and sarcomere assembly and in particular its initiation is only scarce. Although numerous muscle proteins have been identified to be involved in the process, and many of these are also implicated in human muscle diseases (Clark et al., 2002), the mechanistic basis of the process still remains largely unknown (Gregorio et al., 1999; Gregorio and Antin, 2000; Sanger et al., 2005; Sparrow and Schöck, 2009).

Currently, there are several prevalent models attempting to explain how myofibril assembly occurs (Sanger et al., 2005). Most of these models are based on cell culture studies of skeletal and cardiac muscles and postulate the presence of non-muscle myosin II containing stress-fiber-like structures serving either as transitory templates (Holtzer et al., 1997; Sanger et al., 2005) or premyofibril precursor structures that gradually are transformed into mature myofibrils in which non-muscle myosin is replaced by muscle myosin II (Rhee et al., 1994; Dabiri et al., 1997; Sparrow and Schöck, 2009).

Myofibrillogenesis in *Drosophila* adult muscles has so far only been studied in forming IFMs (Reedy and Beall, 1993a). Reedy et al. performed a detailed ultrastructural characterization of forming IFMs with electron microscopy of fixed IFM samples at defined stages starting from 20h APF and ending with 110h APF (time of eclosion of adults at 22°C).

This study reveals, that in IFMs stress-fiber-like template structures can never be detected, but by 42h APF (roughly corresponding to 30h APF in Fig. 8 because of the lower temperature) thick myosin and thin actin filaments appear simultaneously as interdigitating arrays between evenly spaced Z bodies, the electron-dense precursors of Z discs still lacking the regular lattice arrangement.

Each of these tiny striated myofibrils forms within a sleeve of microtubules, which appear slightly before the first myofibrillar structures can be detected and will disassemble again during later stages. Interestingly, the microtubule network has similarly been reported to provide a dynamic scaffold essential for sarcomere assembly in mammalian heart muscle (Goldstein and Entman, 1979; Ehler and Gautel, 2008).

The newly generated myofibrillar structures are already attached to the muscle cell membrane at sites of muscle-tendon attachments before the first striated pattern can be observed, as are the bundles of microtubules surrounding them. These observations indicate, that force-resistant attachment may be a prerequisite for sarcomere assembly, which has also been suggested to be the case in cultured cardiomyocytes (Marino et al., 1987; Lin et al., 1989).

Initially, the sarcomeres of newly formed myofibrils are still small and as development proceeds they grow in length from 1,7 μm in newly formed myofibrils to 3,2 μm in adult myofibrils. In addition, myofibrils also become larger in width by lateral addition of myofilaments. Importantly, the increase in sarcomere length and width occurs simultaneously across the whole muscle, thus all sarcomeres have the same size at any given timepoint of IFM formation. Moreover, at no time during IFM development scattered myofilaments can be detected and also the number of initially formed sarcomeres remains constant during longitudinal muscle growth, indicating that in *Drosophila* IFMs, unlike to *C. elegans* and vertebrate striated muscles (Goldspink, 1968; Mackenzie et al., 1978), no addition of sarcomeres, which has been previously proposed to happen at myofibril ends with stress-fiber-like structures

(Goldspink, 1968; Williams and Goldspink, 1971; Dix and Eisenberg, 1990; Sanger et al., 2009; Russell et al., 2010), occurs.

Noteworthy, formation of stress-fiber-like structures and the generation of only loose not fully interdigitated assemblies of thick and thin filaments could be observed during the myofibril assembly of the tubular abdominal muscles. Furthermore, microtubule bundles around forming myofibrils are also absent in these muscles suggesting that different pathways may control myofibril assembly in *Drosophila* fibrillar and tubular muscles (Reedy and Beall, 1993a).

However, all these results are based on analysis of developmental snapshots of fixed samples at 2h time intervals making it possibly that short-lived steps involved myofibrillogenesis were missed.

4.3 Transgenic RNAi in *Drosophila*

RNA interference (RNAi) provides a widely applicable reverse genetic tool for rapid analysis of gene function enabling large-scale loss-of-function screens both *in vitro* and *in vivo* (Neumüller and Perrimon, 2011).

Classical forward genetic screens relying on random generation of mutations have proven to be very successful approaches for gene discovery, in particular when using *Drosophila* as a model (Nüsslein-Volhard and Wieschaus, 1980). However, this approach is limited by the inherent bias of mutagens and the challenge to map the genetic lesion responsible for the mutant phenotype. Moreover, many genes have multiple functions in different tissues and/or at different developmental timepoints, preventing their discovery in screens focusing on particular cell- and tissue-systems, especially when early lethality precludes the analysis of gene function at later developmental stages. With the generation of genome-wide, transgenic RNAi libraries in *Drosophila* it is now possible to systematically study tissue-specific gene function in a living multicellular organism (Dietzl et al., 2007).

***Drosophila* transgenic RNAi stock collections**

Currently, the most comprehensive *Drosophila* RNAi transgene collection is the Vienna *Drosophila* RNAi collection (VDRC) (Dietzl et al., 2007) comprising 22,270

transgenic RNAi lines targeting 12,088 genes covering 88 % of the annotated protein-coding *Drosophila* genome. Other available transgenic RNAi libraries are the National Institute of Genetics (NIG-FLY) collection (Matsumoto et al., 2007) targeting 6000, and the Transgenic RNAi Project (TRiP) collection (Ni et al., 2009) targeting 2034 of the total 13,929 annotated protein-coding genes in *Drosophila* (Perrimon et al., 2010).

Transgenic RNAi by using the UAS/GAL4 expression system

All these libraries are based on the same basic design principle that they use the binary *UAS/GAL4* expression system (Brand and Perrimon, 1993) to induce *in vivo* RNAi (Fig. 11A). In *Drosophila*, unlike to *C. elegans* for example (Timmons, 2003), RNAi is cell-autonomous and can be effectively triggered by the expression of a long dsRNA hairpin from a transgene containing 200-300 bp gene fragment cloned as inverted repeat (IR) behind the GAL4-responsive upstream activator sequence (*UAS*) (Roignant et al., 2003). Thus, directed expression of the *UAS-IR* transgenes by using the wealth of available GAL4-driver lines (Duffy, 2002) permits conditional gene inactivation in potentially any cell type at any stage during fly development.

Generation of second-generation libraries with the phi31 site-specific genome insertion method

The first generation of *UAS-IR* transgenes of the VDRC library were constructed by cloning the IRs generated by PCR into a modified pUAST transformation vector (Brand and Perrimon, 1993), pMF3 (Fig. 11B). Similarly, the transgenic NIG-FLY collection was constructed with a pUAST vector (Matsumoto et al., 2007; Perrimon et al., 2010). Since these RNAi lines were generated by random insertion in the genome using P-element mediated transformation (Rubin and Spradling, 1982), potential position effects can strongly influence transgene expression (Levis et al., 1985) and thus dampen RNAi efficiency or generate off-target effects (Dietzl et al., 2007; Perrimon et al., 2010). To overcome these limitations, several groups developed transformation vectors relying on the phiC31 site-specific integration method (Groth et al., 2004) enabling insertion of RNAi constructs at preselected sites tested for reliable and robust hairpin expression and high knockdown efficiency (Ni et al., 2008; 2009; Schnorrer et al., 2010). These transgenic lines are available from the VDRC and

TRIP transgenic RNAi resources, which have constructed a second generation of transgenic RNAi libraries using the phiC31 integrase system.

The strength of inducible transgenic RNAi

Transgenic RNAi provides a powerful alternative to classical forward genetic screens for the systematic study of gene function, especially when tissue-specific disruption of genes is required for functional analysis at later developmental stages. By combining the vast number of available GAL4 lines with various inducible GAL4 systems, RNAi can be further restricted to specific stages of fly development (McGuire et al., 2004) or expression of broadly expressing GAL4 lines can be refined to specific tissues or cell populations only (Potter et al., 2010; Yagi et al., 2010) allowing a spatial and temporal resolution of gene inactivation which is not or extremely difficult to achieve with other genetic methods. In fact, inducible RNAi provides the only genetic method available at the moment to systematically screen complex tissues composed of a diverse set of functionally specialized cell subtypes - such as neurons and muscles - in a feasible way (Dietzl et al., 2007).

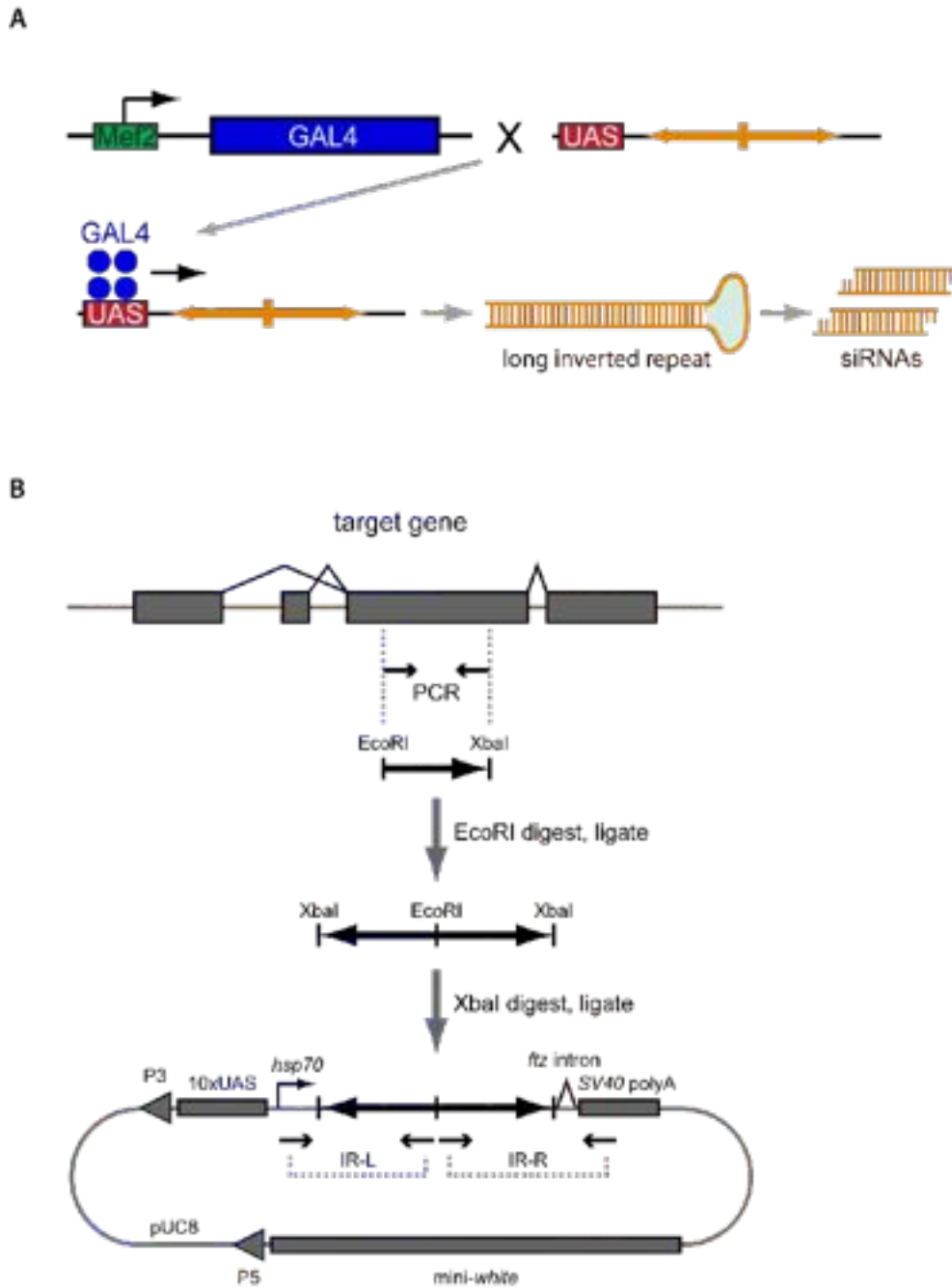


Fig. 11 | Transgenic inducible RNA interference

(A) Crossing of a driver fly line expressing the transcriptional activator GAL4 under the control of the muscle-specific *Mef2* promoter to a fly line harbouring a *UAS-IR* transgene induces expression of a long double-stranded hairpin RNA, which is processed to siRNAs triggering the muscle-specific knockdown of the targeted gene. (B) Cloning scheme for *UAS-IR* constructs. Inverted repeats were generated by PCR, ligated end-to-end and cloned into the pMF3 vector using indicated restriction sites which were introduced with PCR primers. pMF3 contains ten GAL4-responsive UAS elements, the basal *hsp70* promoter, the 150 bp second intron of *fushi tarazu* (*ftz*), the SV40 polyadenylation signal and the *mini-white* eye color selection marker gene. (Scheme adapted from Dietzl et al., 2007).

5. Aim of the thesis

Drosophila adult muscles consist of highly distinct muscle types, the fibrillar and tubular muscles, yet all of them are derived from AMPs that are specified within the somatic mesoderm. We wanted to address the question how muscle type diversity is established during adult myogenesis.

It has already been evident from previous studies that AMPs are subdivided into populations of cells expressing distinct markers and being biased to contribute to specific muscles only already at late embryonic and larval stages (Ghazi et al., 2000; Sudarsan et al., 2001; Maqbool et al., 2006; Fig. 7). However, the functions of these factors in establishing muscle diversity are still unclear and most likely additional, yet to be identified factors, are involved.

We performed a genome-wide muscle-specific RNAi screen (publication III) to systematically identify the underlying genetic mechanisms controlling myogenesis and in particular the specification of fibrillar and tubular adult muscles in *Drosophila*. In this screen we identified *spalt major (salm)* belonging to the conserved Spalt zinc finger transcription factor family (de Celis and Barrio, 2009) to be essential for IFM formation. The major goal of the thesis was to analyze the role of *salm* in *Drosophila* adult muscle type specification and to examine, how *salm* mediates the switch to fibrillar muscle fate (publication IV). Additionally, we also wanted to address, whether Spalt's function in establishing fibrillar muscle identity is evolutionarily conserved in flying insects.

6. Summary of publications

6.1 Summary of publication I

In vivo RNAi rescue in *Drosophila melanogaster* with genomic transgenes from *Drosophila pseudoobscura*

Langer CC*, Ejsmont RK*, **Schönbauer C***, Schnorrer F, Tomancak P.
PLoS One. 2010 Jan 28;5(1):e8928.

* These authors contributed equally to this work.

RNA interference (RNAi) provides a powerful reverse genetic tool to systematically analyze gene function both in cell culture and in tissues of whole organism, such as *Drosophila*. A major drawback of all RNAi-based approaches is the occurrence of potential false-positives caused by non-specific knockdown of genes other than the intended target gene (Kulkarni et al., 2006). The presence of such a potential off-target effect requires careful validation of the RNAi phenotype by additional independent experiments.

A good proof is the recapitulation of the RNAi phenotype with a classical mutant. However, this represents no universal approach, as it is limited by the availability of mutants and potential pleiotropic mutant phenotypes, which might prevent the study of tissue- and stage-specific gene functions. Alternatively, the phenotype can be confirmed by a second independent hairpin construct, targeting a different region of the target gene. Again, this approach is complicated by the fact that not all hairpins display the same knockdown efficiency, resulting in variable phenotypes. Moreover, it is not possible to design non-overlapping constructs for all genes.

Therefore, the gold standard in the RNAi field is to rescue the RNAi phenotype by a transgene immune to RNAi (Sarov and Stewart, 2005), for example, by using the homologous gene from a different related species, whose sequence is divergent enough from the host species to make it refractory to the RNAi construct. However, a caveat of this method is that over-expression of the rescue protein may itself exert an effect on the cell.

In this paper we evaluate the feasibility of rescuing *Drosophila melanogaster* RNAi phenotypes with genomic-clones from the related species *Drosophila*

pseudoobscura. We used clones from a genomic *Drosophila pseudoobscura* fosmid library (Ejsmont et al., 2009), ensuring close to endogenous gene expression levels, for rescue of muscle-specific RNAi phenotypes of five *Drosophila melanogaster* genes. We were able to successfully rescue three of them, demonstrating that cross-species rescue using fosmid transgenic libraries can be readily used to validate RNAi specificity in *Drosophila melanogaster*.

6.2 Summary of publication II

Three-dimensional reconstruction and segmentation of intact *Drosophila* by ultramicroscopy

Jährling N, Becker K, **Schönbauer C**, Schnorrer F , Dodt HU.
Front Syst Neurosci. 2010 Feb 8;4:1.

Combining ultramicroscopy (Siedentopf and Zsigmondy, 1902) with a newly developed procedure to clear fixed tissues, permits 3D visualization of entire specimens, such as whole mouse embryos, at single-cell-resolution, which cannot be obtained by other techniques allowing 3D reconstruction, like computer tomography or magnetic resonance imaging (Dodt et al., 2007). Here, we successfully applied this approach to visualize the entire nervous system, digestive system, and thoracic muscle pattern of whole adult *Drosophila*, demonstrating that this approach is a valuable tool for phenotypic characterization of internal *Drosophila* tissue and organ systems.

We used this technique to analyze thoracic muscles morphology in intact flies upon knockdown of candidate genes we have identified in the muscle RNAi screen (publication III).

6.3 Summary of publication III

Systematic genetic analysis of muscle morphogenesis and function in *Drosophila*

Schnorrer F, Schönbauer C, Langer CC, Dietzl G, Novatchkova M, Schernhuber K, Fellner M, Azaryan A, Radolf M, Stark A, Keleman K, Dickson BJ.

Nature. 2010 Mar 11;464(7286):287-91.

Here, we performed a genome-wide muscle-specific screen to delineate the genetic mechanisms, controlling *Drosophila* muscle formation and function using transgenic RNAi lines of the VDRC library (Dietzl et al., 2007). To achieve muscle-specific RNAi knockdown, we used the pan-mesodermal *Mef2-GALA* driver, which is expressed throughout *Drosophila* muscle development in muscles of both larva and adults (Ranganayakulu et al., 1996).

We successfully screened 17,759 RNAi lines, representing 10,461 distinct genes (75% of the *Drosophila* genome), and assayed for viability, locomotion and flight in over 25,000 flight tests. A total of 2,785 genes were scored as defective in one or more of these assays.

Of those genes we selected 436 genes, falling in the embryonic and larval lethal classes, and 315 genes that scored flightless, and performed a detailed morphological analysis of either their embryonic and larval body-wall-muscles (for the lethal genes) or their IFMs (for the flightless set), enabling us to assign these genes to specific functions in the organization of muscles, myofibrils and sarcomeres. I performed the morphological analysis and categorization into distinct phenotypic classes of the flightless set, leading to the discovery of about 200 genes with specific functions in formation or maintenance of fibrillar IFMs.

Many of the genes identified in the screen are conserved to mammals, among them genes known to be involved in sarcomere formation and/or genes that are implicated in human muscle diseases. Thus, our systematic approach not only defines the genetic basis of *Drosophila* muscle formation and function, but also represents a valuable resource for the identification of vertebrate muscle genes.

6.4 Summary of publication IV

Spalt mediates an evolutionarily conserved switch to fibrillar muscle fate in insects
Schönbauer C, Distler J, Jährling N, Radolf M, Dodt HU, Frasch M, Schnorrer F.
Nature. 2011 Nov 16;479(7373):406-9

Muscle-specific knockdown of the zinc finger transcription factor *spalt major (salm)* with *Mef2-GAL4* results in completely viable, but flightless animals, indicating an essential function of *salm* in fibrillar IFMs. Morphological analysis of *salm* RNAi IFMs indeed revealed a striking change in IFM fiber organization: instead of the fibrillar morphology with unaligned, not laterally connected myofibrils and nuclei localizing next to the myofibrils, the *salm* depleted IFMs possess a tubular arrangement of closely associated myofibrils, contain centrally positioned nuclei, and hence look indistinguishable to tubular leg muscles.

Moreover, analysis of the RNAi phenotype at stages, when myofibril and sarcomere assembly is initiated, showed that in *salm* knockdown flies fibrillar muscles are never formed, but tubular muscles develop in their place, demonstrating that *salm* is required to initiate the fibrillar muscle program.

Fibrillar IFM-specific expression of Salm protein is first detected in templates and forming myotubes, when myoblast fusion starts, and requires the upstream acting transcription factor *vestigial (vg)*, as no Spalt can be detected in *vg* mutants, which hence similarly display transformed tubular IFMs.

Strikingly, expression of *salm* alone is sufficient to induce the fibrillar muscle fate. Ectopic expression of *salm* switches fibrillar muscles into tubular ones by inducing IFM-specific and repressing tubular body-wall-muscle-specific proteins.

Microarray analysis identifying *salm* downstream genes revealed that *salm* switches the entire transcriptional program from tubular to fibrillar fate by regulating the expression as well as alternative splicing of key sarcomeric proteins specific to each muscle type.

Remarkably, *spalt* is similarly required for the specification of fibrillar IFMs in the Coleoptera *Tribolium* (red flour beetle) demonstrating that *spalt* function is conserved across insect species separated by 280 million years of evolution. Moreover, two of the four mammalian *spalt-like (sall)* genes are expressed in heart. Interestingly, mutations in human *SALL1* can cause heart abnormalities associated

with the Townes-Brocks syndrome leading us to speculate that Spalt might be similarly relevant for the function of stretch-activated vertebrate cardiac muscles.

7. Conclusion and outlook

We successfully conducted a genome-wide muscle-specific RNAi screen in which we identified *salm*, a conserved transcription factor, as a key regulator of fibrillar muscle fate. *Salm* is not only required for fibrillar muscle development, but its misexpression can convert other muscle types into fibrillar ones demonstrating *salm*'s remarkable ability to override other muscle differentiation programs. Even more remarkable, Spalt homologues are similarly required to promote differentiation of fibrillar flight muscles in other flying insects suggesting that *salm* initiates a conserved gene regulatory pathway possibly involved in specification of all muscles with stretch-activated myofibrils also including stretch-modulated cardiac muscles of vertebrates. Mechanistically *salm* mediates the switch to fibrillar muscle fate by regulating gene expression as well as splicing of muscle-type-specific proteins. The direct targets of *salm*, however, are still elusive.

Our work has demonstrated the power of transgenic RNAi for discovery of tissue-specific gene functions and further highlighted the *Drosophila* adult muscles as a valuable model for the generation of cell type diversity. The major implications of our findings are discussed in the attached publications. Some aspects, concerning the function of *salm* in fibrillar muscle fate specification, are discussed in more detail below.

7.1 Regulation of IFM-specific Salm expression

We showed that *salm* is not only essential for the specification of fibrillar IFMs, but can also switch tubular to fibrillar muscle fate upon its ectopic expression. Thus, the spatio-temporal expression of *salm* needs to be tightly regulated during adult muscle formation to ensure that its expression is restricted to developing IFMs.

Our data revealed that *salm* expression requires the transcription factor *vg* (publication IV). *vg* is expressed in a subset of AMPs only, beginning from embryonic stage 12 onwards (Sudarsan et al., 2001). At late larval stages, its expression is confined to IFM-forming AMPs (Sudarsan et al., 2001) and it continues

to be specifically expressed in the forming IFM myotubes during adult myogenesis in pupa (Bernard et al., 2006).

salm expression, however, is turned on only later in forming myotubes, shortly after myoblasts have started to fuse with either the templates (during DLM formation) or the founders (during DVM development), and - in contrast to *vg* - it is still absent at earlier stages in wing-disc-associated AMPs in larva. Moreover, ectopic expression of *vg* together with its cofactor *scalloped (sd)* cannot induce *salm* in leg muscles, suggesting the presence of additional regulatory mechanisms controlling the precise timing and position of *salm* expression (publication IV). However, the nature and source of these regulatory factors remains elusive.

Potentially, *salm* function is directed and confined to IFM-forming myotubes by intercellular signaling pathways well-known to mediate inductive interactions between different tissues and cell populations to coordinate organ development in various systems (Brook et al., 1996; Lawrence and Struhl, 1996; Curtiss et al., 2002; Furlong, 2004; Jukam and Desplan, 2010). These signaling pathways can either work instructively by directly inducing *salm* or set a permissive environment in which other genes (transcription factors, corepressors or coactivators, chromatin remodeling enzymes etc.) are necessary to drive *salm* expression. Another possible scenario is that an inhibitory signal must be shut down in order to turn on *salm* expression in a context-specific manner e.g. by making the cells competent to respond to yet another signaling pathway.

These patterning and cell specification events are carried out by only a few conserved signaling pathways (Gerhart, 1999) all of which have been studied in detail in *Drosophila* (Barolo and Posakony, 2002). Therefore, a lot of genetic tools are available for their tissue- and stage-specific manipulation, which can readily be exploited to delineate the regulatory mechanisms controlling the restricted expression of Salm in fibrillar IFMs.

7.2 Downstream targets of *salm*

salm belongs to the conserved Spalt-like gene family (de Celis and Barrio, 2009) and, in analogy to other members of this family, is thought to be a zinc finger transcription factor (Li et al., 2004; Wu et al., 2006; Zhang et al., 2006; Yamashita et al., 2007). As

such *salm* would specify fibrillar muscle fate by regulating the expression of target genes.

We performed microarray analysis and showed that *salm* regulates gene expression as well as alternative splicing of key sarcomeric components that are specific to each muscle-type. IFM-specific genes or gene-isoforms are positively regulated, whereas tubular leg-muscle-specific genes or gene-isoforms are negatively regulated (publication IV). However, we do not know, whether these effects on gene expression and splicing are direct or not.

In order to define the molecular mechanism of how *salm* switches between muscle fates, it will be crucial to identify genes directly bound by *salm* (the *salm* direct targets). Although *salm* function has been studied extensively in many tissue and cell systems (Frei et al., 1988; Kühnlein et al., 1994; Kühnlein and Schuh, 1996; Elstob et al., 2001; Mollereau et al., 2001; Grieder et al., 2009), *salm* direct targets and *salm* binding motifs in *Drosophila* are still elusive. The fact that *salm* is expressed in various tissues indicates that *salm* function is highly context-dependent, and, consequently, has different targets in distinct tissues and cell types. Performing cell-type-specific chromatin immunoprecipitation (ChIP) (Viens et al., 2004; Bonn et al., 2012) combined with high-throughput sequencing (ChIP-seq) (Park, 2009) to identify the IFM-specific *salm* targets, should shed light on the mechanisms by which *salm* initiates the fibrillar muscle program. Subsequent functional analysis of the identified targets should further reveal, how the fibrillar muscle program is executed.

7.3 Spalt and the evolution of fibrillar flight muscles

The evolution of asynchronous fibrillar flight muscles still is a matter of speculation, since to date no bona fida transitional forms between synchronous and asynchronous flight muscles have been identified (Pringle, 1981; Dudley, 2002). We could show that Spalt's function to specify fibrillar muscle fate is conserved from Diptera (true flies) to Coleoptera (beetles), suggesting that *spalt* is required to specify fibrillar muscle fate across insect species (publication IV).

The evolution of asynchronous flight muscles from synchronous muscles has occurred at least four times independently in the evolutionary history of insects

(Dickinson, 2006 Fig. 12), yet all asynchronous muscles are indirect flight muscles and have fibrillar morphology (Josephson, 2006), and, thus, presumably express *spalt*. In contrast, species with tubular flight muscles, such as the most ancient ones, the Odonata (dragonflies) and Ephemeroptera (mayflies) (Smith, 1965; 1966), should, accordingly, lack *spalt* expression in their flight muscles.

Interestingly, some insects with synchronous flight muscles, in particular the Lepidoptera (butterflies) and Orthoptera (grasshoppers, crickets, locusts), and some genera within the orders of Hymenoptera (bees, wasps and ants) and Homoptera (true bugs), possess yet a third, morphologically distinct muscle type beside tubular and fibrillar: the close-packed muscles. In these muscles the myofibrils and mitochondria are localized in the center and nuclei are arranged at the periphery. The diameter of their myofibrils is usually larger than that of myofibrils in tubular muscles, but is not as large as the one of myofibrils in fibrillar muscles (Smith, 1965). Since these insects display a somewhat “in-between” flight muscle morphology and some species within that class achieve high wing beat frequencies of about 160 Hz (Wootton and Newman, 1979), these genera could potentially comprise the missing transitional forms. Moreover, within the orders of Homoptera, Psocoptera (booklice) and Hymenoptera, related genera possess asynchronous as well as synchronous flight muscles, suggesting the potential transitional forms might as well be found within these orders (Daly, 1963; Pringle, 1981; Cullen, 2009). Thus, comparative morphological studies of flight muscles combined with expression and functional analysis of *spalt* in insect orders with either close-packed morphology or orders comprising asynchronous and synchronous species, may provide a good entry point to enhance our understanding of insect flight muscle evolution.

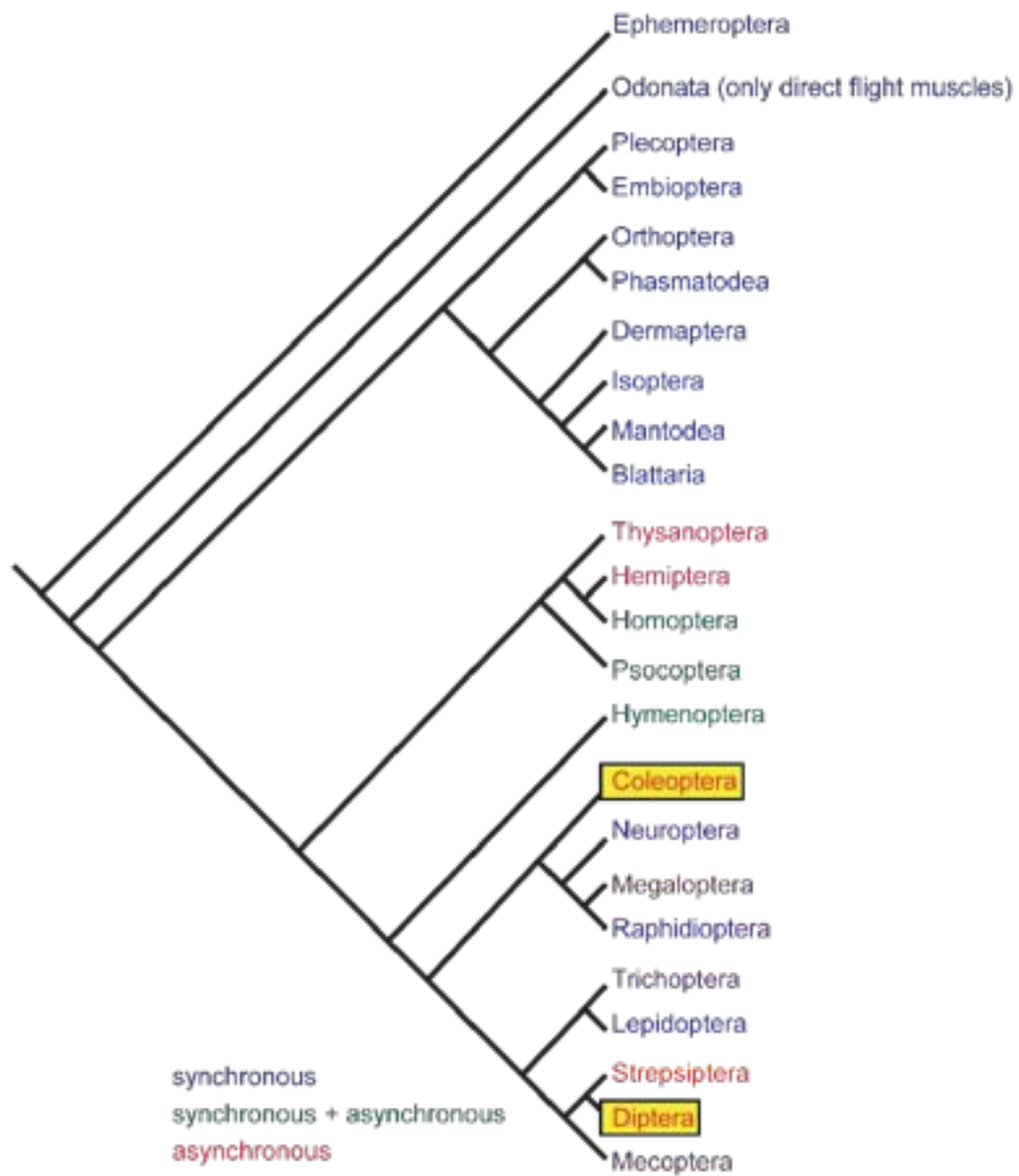


Fig. 12 | Flight muscle organization in insects

Phylogenetic tree of winged insects (from Schönbauer et al., 2011). Orders with synchronous IFMs are shown in blue, with asynchronous (fibrillar) IFMs in red and with both types in green. Yellow box marks orders tested to functionally require *spalt* for fibrillar muscle fate specification.

8. References

- Agianian, B., Krzic, U., Qiu, F., Linke, W.A., Leonard, K., and Bullard, B. (2004). A troponin switch that regulates muscle contraction by stretch instead of calcium. *EMBO J* 23, 772–779.
- Anant, S., Roy, S., and VijayRaghavan, K. (1998). Twist and Notch negatively regulate adult muscle differentiation in *Drosophila*. *Development* 125, 1361–1369.
- Atreya, K.B., and Fernandes, J.J. (2008). Founder cells regulate fiber number but not fiber formation during adult myogenesis in *Drosophila*. *Dev Biol* 321, 123–140.
- Ayme-Southgate, A., Lasko, P., French, C., and Pardue, M.L. (1989). Characterization of the gene for mp20: a *Drosophila* muscle protein that is not found in asynchronous oscillatory flight muscle. *J Cell Biol* 108, 521–531.
- Azpiazú, N., Lawrence, P.A., Vincent, J.P., and Frasch, M. (1996). Segmentation and specification of the *Drosophila* mesoderm. *Genes Dev* 10, 3183–3194.
- Barbas, J.A., Galceran, J., Krah-Jentgens, I., la Pompa, de, J.L., Canal, I., Pongs, O., and Ferrús, A. (1991). Troponin I is encoded in the haplolethal region of the Shaker gene complex of *Drosophila*. *Genes Dev* 5, 132–140.
- Barbas, J.A., Galceran, J., Torroja, L., Prado, A., and Ferrús, A. (1993). Abnormal muscle development in the heldup3 mutant of *Drosophila melanogaster* is caused by a splicing defect affecting selected troponin I isoforms. *Mol Cell Biol* 13, 1433–1439.
- Barolo, S., and Posakony, J.W. (2002). Three habits of highly effective signaling pathways: principles of transcriptional control by developmental cell signaling. *Genes Dev* 16, 1167–1181.
- Bataillé, L., Delon, I., Da Ponte, J.P., Brown, N.H., and Jagla, K. (2010). Downstream of identity genes: muscle-type-specific regulation of the fusion process. *Dev Cell* 19, 317–328.
- Bate, M. (1993). The mesoderm and its derivatives. In *The Development of Drosophila melanogaster*, Vol. 2, M. Bate and A. Martinez-Arias, Eds. (Cold Spring Harbor, NY: CSH Laboratory Press) 2, 1013–1019.
- Bate, M., Rushton, E., and Currie, D.A. (1991). Cells with persistent twist expression are the embryonic precursors of adult muscles in *Drosophila*. *Development* 113, 79–89.
- Baxendale, S., Davison, C., Muxworthy, C., Wolff, C., Ingham, P.W., and Roy, S. (2004). The B-cell maturation factor Blimp-1 specifies vertebrate slow-twitch muscle fiber identity in response to Hedgehog signaling. *Nat Genet* 36, 88–93.
- Baylies, M.K., and Bate, M. (1996). twist: a myogenic switch in *Drosophila*. *Science* 272, 1481–1484.

- Baylies, M.K., Bate, M., and Ruiz-Gómez, M. (1998). Myogenesis: a view from *Drosophila*. *Cell* *93*, 921–927.
- Bernard, F., Dutriaux, A., Silber, J., and Lalouette, A. (2006). Notch pathway repression by vestigial is required to promote indirect flight muscle differentiation in *Drosophila melanogaster*. *Dev Biol* *295*, 164–177.
- Bernard, F., Lalouette, A., Gullaud, M., Jeantet, A.Y., Cossard, R., Zider, A., Ferveur, J.F., and Silber, J. (2003). Control of apterous by vestigial drives indirect flight muscle development in *Drosophila*. *Dev Biol* *260*, 391–403.
- Bernstein, S.I., and Milligan, R.A. (1997). Fine tuning a molecular motor: the location of alternative domains in the *Drosophila* myosin head. *J Mol Biol* *271*, 1–6.
- Bodmer, R. (1993). The gene tinman is required for specification of the heart and visceral muscles in *Drosophila*. *Development* *118*, 719–729.
- Bodmer, R., Jan, L.Y., and Jan, Y.N. (1990). A new homeobox-containing gene, *msh-2*, is transiently expressed early during mesoderm formation of *Drosophila*. *Development* *110*, 661–669.
- Bonn, S., Zinzen, R.P., Perez-Gonzalez, A., Riddell, A., Gavin, A.-C., and Furlong, E.E.M. (2012). Cell type-specific chromatin immunoprecipitation from multicellular complex samples using BiTS-ChIP. *Nat Protoc* *7*, 978–994.
- Borkowski, O.M., Brown, N.H., and Bate, M. (1995). Anterior-posterior subdivision and the diversification of the mesoderm in *Drosophila*. *Development* *121*, 4183–4193.
- Bour, B.A., Chakravarti, M., West, J.M., and Abmayr, S.M. (2000). *Drosophila* SNS, a member of the immunoglobulin superfamily that is essential for myoblast fusion. *Genes Dev* *14*, 1498–1511.
- Brand, A.H., and Perrimon, N. (1993). Targeted gene expression as a means of altering cell fates and generating dominant phenotypes. *Development* *118*, 401–415.
- Brault, V., Reedy, M.C., Sauder, U., Kammerer, R.A., Aebi, U., and Schoenenberger, C. (1999). Substitution of flight muscle-specific actin by human (beta)-cytoplasmic actin in the indirect flight muscle of *Drosophila*. *J Cell Sci* *112* (Pt 21), 3627–3639.
- Braun, T., and Gautel, M. (2011). Transcriptional mechanisms regulating skeletal muscle differentiation, growth and homeostasis. *Nat Rev Mol Cell Biol* *12*, 349–361.
- Broadie, K.S., and Bate, M. (1991). The development of adult muscles in *Drosophila*: ablation of identified muscle precursor cells. *Development* *113*, 103–118.
- Brook, W.J., Diaz-Benjumea, F.J., and Cohen, S.M. (1996). Organizing spatial pattern in limb development. *Annu. Rev. Cell Dev. Biol.* *12*, 161–180.
- Brown, N.H. (1993). Integrins hold *Drosophila* together. *Bioessays* *15*, 383–390.
- Brown, N.H. (2000). Cell-cell adhesion via the ECM: integrin genetics in fly and worm. *Matrix Biol.* *19*, 191–201.

- Campbell, K.B. (2006). Functions of Stretch Activation in Heart Muscle. *J. Gen. Physiol.* *127*, 89–94.
- Carmena, A., Bate, M., and Jiménez, F. (1995). Lethal of scute, a proneural gene, participates in the specification of muscle progenitors during *Drosophila* embryogenesis. *Genes Dev* *9*, 2373–2383.
- Carmena, A., Gisselbrecht, S., Harrison, J., Jiménez, F., and Michelson, A.M. (1998). Combinatorial signaling codes for the progressive determination of cell fates in the *Drosophila* embryonic mesoderm. *Genes Dev* *12*, 3910–3922.
- Clark, K.A., McElhinny, A.S., Beckerle, M.C., and Gregorio, C.C. (2002). Striated muscle cytoarchitecture: an intricate web of form and function. *Annu. Rev. Cell Dev. Biol.* *18*, 637–706.
- Cripps, R.M., Black, B.L., Zhao, B., Lien, C.L., Schulz, R.A., and Olson, E.N. (1998). The myogenic regulatory gene Mef2 is a direct target for transcriptional activation by Twist during *Drosophila* myogenesis. *Genes Dev* *12*, 422–434.
- Cullen, M.J. (2009). The distribution of asynchronous muscle in insects with particular reference to the Hemiptera: an electron microscope study. *Journal of Entomology Series a, General Entomology* *49*, 17–41.
- Currie, D.A., and Bate, M. (1991). The development of adult abdominal muscles in *Drosophila*: myoblasts express twist and are associated with nerves. *Development* *113*, 91–102.
- Curtiss, J., Halder, G., and Mlodzik, M. (2002). Selector and signalling molecules cooperate in organ patterning. *Nat Cell Biol* *4*, E48–E51.
- Dabiri, G.A., Turnacioglu, K.K., Sanger, J.M., and Sanger, J.W. (1997). Myofibrillogenesis visualized in living embryonic cardiomyocytes. *Proc Natl Acad Sci USA* *94*, 9493–9498.
- Daly, H.V. (1963). Close-Packed and Fibrillar Muscles of the Hymenoptera. *Annals of the Entomological Society of America* *56*, 295–306.
- Davis, J.S., Hassanzadeh, S., Winitsky, S., Lin, H., Satorius, C., Vemuri, R., Aletras, A.H., Wen, H., and Epstein, N.D. (2001). The overall pattern of cardiac contraction depends on a spatial gradient of myosin regulatory light chain phosphorylation. *Cell* *107*, 631–641.
- de Celis, J.F., and Barrio, R. (2009). Regulation and function of Spalt proteins during animal development. *Int J Dev Biol* *53*, 1385–1398.
- DeSimone, S., Coelho, C., Roy, S., VijayRaghavan, K., and White, K. (1996). ERECT WING, the *Drosophila* member of a family of DNA binding proteins is required in imaginal myoblasts for flight muscle development. *Development* *122*, 31–39.
- Dickinson, M. (2006). Insect flight. *Curr Biol* *16*, R309–R314.

- Dietzl, G., Chen, D., Schnorrer, F., Su, K.-C., Barinova, Y., Fellner, M., Gasser, B., Kinsey, K., Oppel, S., Scheiblauer, S., et al. (2007). A genome-wide transgenic RNAi library for conditional gene inactivation in *Drosophila*. *Nature* *448*, 151–156.
- Dix, D.J., and Eisenberg, B.R. (1990). Myosin mRNA accumulation and myofibrillogenesis at the myotendinous junction of stretched muscle fibers. *J Cell Biol* *111*, 1885–1894.
- Dotd, H.-U., Leischner, U., Schierloh, A., Jährling, N., Mauch, C.P., Deininger, K., Deussing, J.M., Eder, M., Zieglgänsberger, W., and Becker, K. (2007). Ultramicroscopy: three-dimensional visualization of neuronal networks in the whole mouse brain. *Nature Methods* *4*, 331–336.
- Domingo, A., González-Jurado, J., Maroto, M., Díaz, C., Vinós, J., Carrasco, C., Cervera, M., and Marco, R. (1998). Troponin-T is a calcium-binding protein in insect muscle: in vivo phosphorylation, muscle-specific isoforms and developmental profile in *Drosophila melanogaster*. *J Muscle Res Cell Motil* *19*, 393–403.
- Dudley, R. (2002). Energetics and flight physiology. In *The Biomechanics of Insect Flight*, R. Dudley, ed. (Princeton, NJ: Princeton University Press) 159–202.
- Duffy, J.B. (2002). GAL4 system in *Drosophila*: a fly geneticist's Swiss army knife. *Genesis* *34*, 1–15.
- Dutta, D., Anant, S., Ruiz-Gomez, M., Bate, M., and VijayRaghavan, K. (2004). Founder myoblasts and fibre number during adult myogenesis in *Drosophila*. *Development* *131*, 3761–3772.
- Dutta, D., and VijayRaghavan, K. (2006). Metamorphosis and the Formation of the Adult Musculature. *Muscle Development in Drosophila*, H Sink, ed. (Georgetown, TX: Landes Bioscience) 125–142.
- Dutta, D., Shaw, S., Maqbool, T., Pandya, H., and VijayRaghavan, K. (2005). *Drosophila* Heartless acts with Heartbroken/Dof in muscle founder differentiation. *PLoS Biol* *3*, e337.
- Ehler, E., and Gautel, M. (2008). The sarcomere and sarcomerogenesis. *Adv Exp Med Biol* *642*, 1–14.
- Ejmont, R.K., Sarov, M., Winkler, S., Lipinski, K.A., and Tomancak, P. (2009). A toolkit for high-throughput, cross-species gene engineering in *Drosophila*. *Nature Methods* *6*, 435–437.
- Elstob, P.R., Brodu, V., and Gould, A.P. (2001). spalt-dependent switching between two cell fates that are induced by the *Drosophila* EGF receptor. *Development* *128*, 723–732.
- Falkenthal, S., Graham, M., and Wilkinson, J. (1987). The indirect flight muscle of *Drosophila* accumulates a unique myosin alkali light chain isoform. *Dev Biol* *121*, 263–272.
- Farrell, E.R., Fernandes, J., and Keshishian, H. (1996). Muscle organizers in

Drosophila: the role of persistent larval fibers in adult flight muscle development. *Dev Biol* 176, 220–229.

Fernandes, J., Bate, M., and VijayRaghavan, K. (1991). Development of the indirect flight muscles of *Drosophila*. *Development* 113, 67–77.

Fernandes, J.J., and Keshishian, H. (1996). Patterning the dorsal longitudinal flight muscles (DLM) of *Drosophila*: insights from the ablation of larval scaffolds. *Development* 122, 3755–3763.

Fernandes, J.J., Celniker, S.E., and VijayRaghavan, K. (1996). Development of the indirect flight muscle attachment sites in *Drosophila*: role of the PS integrins and the stripe gene. *Dev Biol* 176, 166–184.

Figeac, N., Jagla, T., Aradhya, R., Da Ponte, J.P., and Jagla, K. (2010). *Drosophila* adult muscle precursors form a network of interconnected cells and are specified by the rhomboid-triggered EGF pathway. *Development* 137, 1965–1973.

Figeac, N., Jagla, T., Aradhya, R., Da Ponte, J.P., and Jagla, K. (2011). Specification and behavior of AMPs, muscle-committed transient *Drosophila* stem cells. *Fly (Austin)* 5, 7–9.

Frasch, M. (1995). Induction of visceral and cardiac mesoderm by ectodermal Dpp in the early *Drosophila* embryo. *Nature* 374, 464–467.

Frei, E., Schuh, R., Baumgartner, S., Burri, M., Noll, M., Jürgens, G., Seifert, E., Nauber, U., and Jäckle, H. (1988). Molecular characterization of spalt, a homeotic gene required for head and tail development in the *Drosophila* embryo. *EMBO J* 7, 197–204.

Frommer, G., Vorbrüggen, G., Pasca, G., Jäckle, H., and Volk, T. (1996). Epidermal egr-like zinc finger protein of *Drosophila* participates in myotube guidance. *EMBO J* 15, 1642–1649.

Furlong, E.E. (2004). Integrating transcriptional and signalling networks during muscle development. *Curr Opin Genet Dev* 14, 343–350.

Fyrberg, E.A., Fyrberg, C.C., Biggs, J.R., Saville, D., Beall, C.J., and Ketchum, A. (1998). Functional nonequivalence of *Drosophila* actin isoforms. *Biochem. Genet.* 36, 271–287.

Fyrberg, E.A., Mahaffey, J.W., Bond, B.J., and Davidson, N. (1983). Transcripts of the six *Drosophila* actin genes accumulate in a stage- and tissue-specific manner. *Cell* 33, 115–123.

Gerhart, J. (1999). 1998 Warkany lecture: signaling pathways in development. *Teratology* 60, 226–239.

Ghazi, A., Anant, S., and VijayRaghavan, K. (2000). Apterous mediates development of direct flight muscles autonomously and indirect flight muscles through epidermal cues. *Development* 127, 5309–5318.

- Ghazi, A., Paul, L., and VijayRaghavan, K. (2003). Prepattern genes and signaling molecules regulate stripe expression to specify *Drosophila* flight muscle attachment sites. *Mech Dev* *120*, 519–528.
- Goldspink, G. (1968). Sarcomere length during post-natal growth of mammalian muscle fibres. *J Cell Sci* *3*, 539–548.
- Goldstein, M.A., and Entman, M.L. (1979). Microtubules in mammalian heart muscle. *J Cell Biol* *80*, 183–195.
- Gregorio, C.C., and Antin, P.B. (2000). To the heart of myofibril assembly. *Trends Cell Biol* *10*, 355–362.
- Gregorio, C.C., Granzier, H., Sorimachi, H., and Labeit, S. (1999). Muscle assembly: a titanic achievement? *Curr Opin Cell Biol* *11*, 18–25.
- Grieder, N.C., Morata, G., Affolter, M., and Gehring, W.J. (2009). Spalt major controls the development of the notum and of wing hinge primordia of the *Drosophila melanogaster* wing imaginal disc. *Dev Biol* *329*, 315–326.
- Groth, A.C., Fish, M., Nusse, R., and Calos, M.P. (2004). Construction of transgenic *Drosophila* by using the site-specific integrase from phage phiC31. *Genetics* *166*, 1775–1782.
- Hanson, J., and Huxley, H.E. (1953). Structural basis of the cross-striations in muscle. *Nature* *172*, 530–532.
- Hartenstein, V. (2006). The Muscle Pattern of *Drosophila*. *Muscle Development in Drosophila*, H Sink, Ed (Georgetown, TX: Landes Bioscience) 8–27.
- Hastings, G.A., and Emerson, C.P. (1991). Myosin functional domains encoded by alternative exons are expressed in specific thoracic muscles of *Drosophila*. *J Cell Biol* *114*, 263–276.
- Hofsten, von, J., Elworthy, S., Gilchrist, M.J., Smith, J.C., Wardle, F.C., and Ingham, P.W. (2008). Prdm1- and Sox6-mediated transcriptional repression specifies muscle fibre type in the zebrafish embryo. *EMBO Rep* *9*, 683–689.
- Holtzer, H., Hijikata, T., Lin, Z.X., Zhang, Z.Q., Holtzer, S., Protasi, F., Franzini-Armstrong, C., and Sweeney, H.L. (1997). Independent assembly of 1.6 microns long bipolar MHC filaments and I-Z-I bodies. *Cell Struct Funct* *22*, 83–93.
- Huxley, A.F., and Niedergerke, R. (1954). Structural changes in muscle during contraction; interference microscopy of living muscle fibres. *Nature* *173*, 971–973.
- Jaramillo, M.S., Lovato, C.V., Baca, E.M., and Cripps, R.M. (2009). Crossveinless and the TGFbeta pathway regulate fiber number in the *Drosophila* adult jump muscle. *Development* *136*, 1105–1113.
- Josephson, R. (2006). Comparative Physiology of Insect Flight Muscle. In *Nature's Versatile Engine: Insect Flight Muscle Inside and Out*, J. O. Vigoreaux, ed. (Georgetown, TX: Landes Bioscience) 35–43.

- Josephson, R.K., Malamud, J.G., and Stokes, D.R. (2000). Asynchronous muscle: a primer. *J. Exp. Biol.* *203*, 2713–2722.
- Jukam, D., and Desplan, C. (2010). Binary fate decisions in differentiating neurons. *Curr. Opin. Neurobiol.* *20*, 6–13.
- Karim, F.D., Guild, G.M., and Thummel, C.S. (1993). The *Drosophila* Broad-Complex plays a key role in controlling ecdysone-regulated gene expression at the onset of metamorphosis. *Development* *118*, 977–988.
- Karlik, C.C., and Fyrberg, E.A. (1986). Two *Drosophila melanogaster* tropomyosin genes: structural and functional aspects.
- Kossmann, C.E., and Fawcett, D.W. (1961). The Sarcoplasmic Reticulum of Skeletal and Cardiac Muscle. *Circulation* *24*, 336–348.
- Kozopas, K.M., and Nusse, R. (2002). Direct flight muscles in *Drosophila* develop from cells with characteristics of founders and depend on DWnt-2 for their correct patterning. *Dev Biol* *243*, 312–325.
- Kulkarni, M.M., Booker, M., Silver, S.J., Friedman, A., Hong, P., Perrimon, N., and Mathey-Prevot, B. (2006). Evidence of off-target effects associated with long dsRNAs in *Drosophila melanogaster* cell-based assays. *Nature Methods* *3*, 833–838.
- Kühnlein, R.P., and Schuh, R. (1996). Dual function of the region-specific homeotic gene *spalt* during *Drosophila* tracheal system development. *Development* *122*, 2215–2223.
- Kühnlein, R.P., Frommer, G., Friedrich, M., Gonzalez-Gaitan, M., Weber, A., Wagner-Bernholz, J.F., Gehring, W.J., Jäckle, H., and Schuh, R. (1994). *spalt* encodes an evolutionarily conserved zinc finger protein of novel structure which provides homeotic gene function in the head and tail region of the *Drosophila* embryo. *EMBO J* *13*, 168–179.
- Lawrence, P.A. (1982). Cell lineage of the thoracic muscles of *Drosophila*. *Cell* *29*, 493–503.
- Lawrence, P.A., and Brower, D.L. (1982). Myoblasts from *Drosophila* wing disks can contribute to developing muscles throughout the fly. *Nature* *295*, 55–57.
- Lawrence, P.A., and Struhl, G. (1996). Morphogens, compartments, and pattern: lessons from *drosophila*? *Cell* *85*, 951–961.
- Lee, J.C., VijayRaghavan, K., Celniker, S.E., and Tanouye, M.A. (1995). Identification of a *Drosophila* muscle development gene with structural homology to mammalian early growth response transcription factors. *Proc Natl Acad Sci USA* *92*, 10344–10348.
- Leptin, M., and Grunewald, B. (1990). Cell shape changes during gastrulation in *Drosophila*. *Development* *110*, 73–84.
- Levis, R., Hazelrigg, T., and Rubin, G.M. (1985). Effects of genomic position on the

expression of transduced copies of the white gene of *Drosophila*. *Science* 229, 558–561.

Li, D., Tian, Y., Ma, Y., and Benjamin, T. (2004). p150(Sal2) is a p53-independent regulator of p21(WAF1/CIP). *Mol Cell Biol* 24, 3885–3893.

Lilly, B., Galewsky, S., Firulli, A.B., Schulz, R.A., and Olson, E.N. (1994). D-MEF2: a MADS box transcription factor expressed in differentiating mesoderm and muscle cell lineages during *Drosophila* embryogenesis. *Proc Natl Acad Sci USA* 91, 5662–5666.

Lilly, B., Zhao, B., Ranganayakulu, G., Paterson, B.M., Schulz, R.A., and Olson, E.N. (1995). Requirement of MADS domain transcription factor D-MEF2 for muscle formation in *Drosophila*. *Science* 267, 688–693.

Lin, Z.X., Holtzer, S., Schultheiss, T., Murray, J., Masaki, T., Fischman, D.A., and Holtzer, H. (1989). Polygons and adhesion plaques and the disassembly and assembly of myofibrils in cardiac myocytes. *J Cell Biol* 108, 2355–2367.

Liotta, D., Han, J., Elgar, S., Garvey, C., Han, Z., and Taylor, M.V. (2007). The Him gene reveals a balance of inputs controlling muscle differentiation in *Drosophila*. *Curr Biol* 17, 1409–1413.

Mackenzie, J.M., Garcea, R.L., Zengel, J.M., and Epstein, H.F. (1978). Muscle development in *Caenorhabditis elegans*: mutants exhibiting retarded sarcomere construction. *Cell* 15, 751–762.

Maqbool, T., Soler, C., Jagla, T., Daczewska, M., Lodha, N., Palliyil, S., VijayRaghavan, K., and Jagla, K. (2006). Shaping leg muscles in *Drosophila*: role of ladybird, a conserved regulator of appendicular myogenesis. *PLoS ONE* 1, e122.

Marden, J.H. (2006). Functional and Ecological Meets of Isoform Variation in Insect Flight Muscle. In *Nature's Versatile Engine: Insect Flight Muscle Inside and Out*, J. O. Vignaux, ed. (Georgetown, TX: Landes Bioscience) 214–229.

Marino, T.A., Kuseryk, L., and Lauva, I.K. (1987). Role of contraction in the structure and growth of neonatal rat cardiocytes. *Am. J. Physiol.* 253, H1391–H1399.

Maroto, M., Arredondo, J., Goulding, D., Marco, R., Bullard, B., and Cervera, M. (1996). *Drosophila* paramyosin/miniparamyosin gene products show a large diversity in quantity, localization, and isoform pattern: a possible role in muscle maturation and function. *J Cell Biol* 134, 81–92.

Martín-Bermudo, M.D., Carmena, A., and Jiménez, F. (1995). Neurogenic genes control gene expression at the transcriptional level in early neurogenesis and in mesectoderm specification. *Development* 121, 219–224.

Matsumoto, A., Ukai-Tadenuma, M., Yamada, R.G., Houl, J., Uno, K.D., Kasukawa, T., Dauwalder, B., Itoh, T.Q., Takahashi, K., Ueda, R., et al. (2007). A functional genomics strategy reveals clockwork orange as a transcriptional regulator in the *Drosophila* circadian clock. *Genes Dev* 21, 1687–1700.

- McGuire, S.E., Mao, Z., and Davis, R.L. (2004). Spatiotemporal Gene Expression Targeting with the TARGET and Gene-Switch Systems in *Drosophila*. *Science Signaling* 2004, pl6–pl6.
- Miller, A. (1950). The Internal Anatomy and Histology of the Imago of *Drosophila melanogaster*. In *Biology of Drosophila*, M. Demerec, ed. (New York, NY: Hafner Publishing Company, Inc.) 420–531.
- Mollereau, B., Dominguez, M., Webel, R., Colley, N.J., Keung, B., de Celis, J.F., and Desplan, C. (2001). Two-step process for photoreceptor formation in *Drosophila*. *Nature* 412, 911–913.
- Neumüller, R.A., and Perrimon, N. (2011). Where gene discovery turns into systems biology: genome-scale RNAi screens in *Drosophila*. *Wiley Interdiscip Rev Syst Biol Med* 3, 471–478.
- Nguyen, H.T., Bodmer, R., Abmayr, S.M., McDermott, J.C., and Spoerel, N.A. (1994). *D-mef2*: a *Drosophila* mesoderm-specific MADS box-containing gene with a biphasic expression profile during embryogenesis. *Proc Natl Acad Sci USA* 91, 7520–7524.
- Ni, J.-Q., Liu, L.-P., Binari, R., Hardy, R., Shim, H.-S., Cavallaro, A., Booker, M., Pfeiffer, B.D., Markstein, M., Wang, H., et al. (2009). A *Drosophila* resource of transgenic RNAi lines for neurogenetics. *Genetics* 182, 1089–1100.
- Ni, J.-Q., Markstein, M., Binari, R., Pfeiffer, B., Liu, L.-P., Villalta, C., Booker, M., Perkins, L., and Perrimon, N. (2008). Vector and parameters for targeted transgenic RNA interference in *Drosophila melanogaster*. *Nature Methods* 5, 49–51.
- Niro, C., Demignon, J., Vincent, S., Liu, Y., Giordani, J., Sgarioto, N., Favier, M., Guillet-Deniau, I., Blais, A., and Maire, P. (2010). *Six1* and *Six4* gene expression is necessary to activate the fast-type muscle gene program in the mouse primary myotome. *Dev Biol* 338, 168–182.
- Nongthomba, U., Ansari, M., Thimmaiya, D., Stark, M., and Sparrow, J. (2007). Aberrant splicing of an alternative exon in the *Drosophila* troponin-T gene affects flight muscle development. *Genetics* 177, 295–306.
- Nüsslein-Volhard, C., and Wieschaus, E. (1980). Mutations affecting segment number and polarity in *Drosophila*. *Nature* 287, 795–801.
- Park, P.J. (2009). ChIP-seq: advantages and challenges of a maturing technology. *Nat Rev Genet* 10, 669–680.
- Perrimon, N., Ni, J.-Q., and Perkins, L. (2010). In vivo RNAi: today and tomorrow. *Cold Spring Harb Perspect Biol* 2, a003640.
- Poodry, C., and Schneiderman, H. (1970). The Ultrastructure of the Developing Leg of *Drosophila melanogaster*. *Wilhelm Roux's Archive* 166, 1–44.
- Potter, C.J., Tasic, B., Russler, E.V., Liang, L., and Luo, L. (2010). The Q system: a repressible binary system for transgene expression, lineage tracing, and mosaic

analysis. *Cell* 141, 536–548.

Pringle, J.W.S. (1981). The Bidder Lecture, 1980 The Evolution of Fibrillar Muscle in Insects. *J. Exp. Biol.* 94, 1–14.

Qiu, F., Brendel, S., Cunha, P.M.F., Astola, N., Song, B., Furlong, E.E.M., Leonard, K.R., and Bullard, B. (2005). Myofilin, a protein in the thick filaments of insect muscle. *J Cell Sci* 118, 1527–1536.

Qiu, F., Lakey, A., Agianian, B., Hutchings, A., Butcher, G.W., Labeit, S., Leonard, K., and Bullard, B. (2003). Troponin C in different insect muscle types: identification of two isoforms in *Lethocerus*, *Drosophila* and *Anopheles* that are specific to asynchronous flight muscle in the adult insect. *Biochem J* 371, 811–821.

Ranganayakulu, G., Schulz, R.A., and Olson, E.N. (1996). Wingless signaling induces nautilus expression in the ventral mesoderm of the *Drosophila* embryo. *Dev Biol* 176, 143–148.

Ray, R.P., Arora, K., Nüsslein-Volhard, C., and Gelbart, W.M. (1991). The control of cell fate along the dorsal-ventral axis of the *Drosophila* embryo. *Development* 113, 35–54.

Reed, C., Murphy, C., and Fristrom, D. (1975). The Ultrastructure of the Differentiating Pupal Leg of *Drosophila melanogaster*. *Wilhelm Roux's Archive* 178, 285–302.

Reedy, M.C., and Beall, C. (1993a). Ultrastructure of developing flight muscle in *Drosophila*. I. Assembly of myofibrils. *Dev Biol* 160, 443–465.

Reedy, M.C., and Beall, C. (1993b). Ultrastructure of Developing Flight Muscle in *Drosophila*. II. Formation of the Myotendon Junction. *Dev Biol* 160, 466–479.

Reedy, M.C., Bullard, B., and Vigoreaux, J.O. (2000). Flightin is essential for thick filament assembly and sarcomere stability in *Drosophila* flight muscles. *J Cell Biol* 151, 1483–1500.

Rhee, D., Sanger, J.M., and Sanger, J.W. (1994). The premyofibril: evidence for its role in myofibrillogenesis. *Cell Motil. Cytoskeleton* 28, 1–24.

Riechmann, V., Irion, U., Wilson, R., Grosskortenhaus, R., and Leptin, M. (1997). Control of cell fates and segmentation in the *Drosophila* mesoderm. *Development* 124, 2915–2922.

Roignant, J.-Y., Carré, C., Mugat, B., Szymczak, D., Lepesant, J.-A., and Antoniewski, C. (2003). Absence of transitive and systemic pathways allows cell-specific and isoform-specific RNAi in *Drosophila*. *RNA* 9, 299–308.

Roth, S., Stein, D., and Nüsslein-Volhard, C. (1989). A gradient of nuclear localization of the dorsal protein determines dorsoventral pattern in the *Drosophila* embryo. *Cell* 59, 1189–1202.

Roy, S., and VijayRaghavan, K. (1998). Patterning muscles using organizers: larval

- muscle templates and adult myoblasts actively interact to pattern the dorsal longitudinal flight muscles of *Drosophila*. *J Cell Biol* *141*, 1135–1145.
- Roy, S., and VijayRaghavan, K. (1999). Muscle pattern diversification in *Drosophila*: the story of imaginal myogenesis. *Bioessays* *21*, 486–498.
- Rubin, G.M., and Spradling, A.C. (1982). Genetic transformation of *Drosophila* with transposable element vectors. *Science* *218*, 348–353.
- Ruiz-Gómez, M., and Bate, M. (1997). Segregation of myogenic lineages in *Drosophila* requires numb. *Development* *124*, 4857–4866.
- Ruiz-Gómez, M., Coutts, N., Price, A., Taylor, M.V., and Bate, M. (2000). *Drosophila* dumbfounded: a myoblast attractant essential for fusion. *Cell* *102*, 189–198.
- Russell, B., Curtis, M.W., Koshman, Y.E., and Samarel, A.M. (2010). Mechanical stress-induced sarcomere assembly for cardiac muscle growth in length and width. *J Mol Cell Cardiol* *48*, 817–823.
- Sandstrom, D.J., and Restifo, L.L. (1999). Epidermal tendon cells require Broad Complex function for correct attachment of the indirect flight muscles in *Drosophila melanogaster*. *J Cell Sci* *112 (Pt 22)*, 4051–4065.
- Sandstrom, D.J., Bayer, C.A., Fristrom, J.W., and Restifo, L.L. (1997). Broad-complex transcription factors regulate thoracic muscle attachment in *Drosophila*. *Dev Biol* *181*, 168–185.
- Sanger, J.W., Kang, S., Siebrands, C.C., Freeman, N., Du, A., Wang, J., Stout, A.L., and Sanger, J.M. (2005). How to build a myofibril. *J Muscle Res Cell Motil* *26*, 343–354.
- Sanger, J.W., Wang, J., Holloway, B., Du, A., and Sanger, J.M. (2009). Myofibrillogenesis in skeletal muscle cells in zebrafish. *Cell Motil. Cytoskeleton* *66*, 556–566.
- Sarov, M., and Stewart, A.F. (2005). The best control for the specificity of RNAi. *Trends Biotechnol.* *23*, 446–448.
- Schaeffer, P., Conley, K., and Lindstedt, S. (1996). Structural correlates of speed and endurance in skeletal muscle: the rattlesnake tailshaker muscle. *J. Exp. Biol.* *199*, 351–358.
- Schiaffino, S., and Reggiani, C. (1996). Molecular diversity of myofibrillar proteins: gene regulation and functional significance. *Physiol. Rev.* *76*, 371–423.
- Schiaffino, S., Sandri, M., and Murgia, M. (2007). Activity-dependent signaling pathways controlling muscle diversity and plasticity. *Physiology (Bethesda)* *22*, 269–278.
- Schnorrer, F., and Dickson, B.J. (2004). Muscle building; mechanisms of myotube guidance and attachment site selection. *Dev Cell* *7*, 9–20.

- Schnorrer, F., Schönbauer, C., Langer, C.C.H., Dietzl, G., Novatchkova, M., Schernhuber, K., Fellner, M., Azaryan, A., Radolf, M., Stark, A., et al. (2010). Systematic genetic analysis of muscle morphogenesis and function in *Drosophila*. *Nature* *464*, 287–291.
- Schönbauer, C., Distler, J., Jährling, N., Radolf, M., Dodt, H.-U., Frasch, M., and Schnorrer, F. (2011). Spalt mediates an evolutionarily conserved switch to fibrillar muscle fate in insects. *Nature* *479*, 406–409.
- Shiels, H.A., and White, E. (2008). The Frank-Starling mechanism in vertebrate cardiac myocytes. *J. Exp. Biol.* *211*, 2005–2013.
- Shishido, E., Higashijima, S., Emori, Y., and Saigo, K. (1993). Two FGF-receptor homologues of *Drosophila*: one is expressed in mesodermal primordium in early embryos. *Development* *117*, 751–761.
- Siedentopf, H., and Zsigmondy, R. (1902). Über Sichtbarmachung und Größenbestimmung ultramikroskopischer Teilchen, mit besonderer Anwendung auf Goldrubingläser. *Annalen Der Physik* *315*, 1–39.
- Smith D.S. (1965). The organization of flight muscle in an aphid, *Megoura viciae* (Homoptera). With a discussion on the structure of synchronous and asynchronous striated muscle fibers. *J Cell Biol* *27*, 379–393.
- Smith, D.S. (1966). The organization of flight muscle fibers in the Odonata. *J Cell Biol* *28*, 109–126.
- Smith, D.S. (1965). The Flight Muscles of Insects. *Sci Am* *212*, 77–88.
- Snodgrass, R. (1935). *Principles of Insect Morphology* (New York: McGraw-Hill Book Company, inc.).
- Soler, C., and Taylor, M.V. (2009). The Him gene inhibits the development of *Drosophila* flight muscles during metamorphosis. *Mech Dev* *126*, 595–603.
- Soler, C., Daczewska, M., Da Ponte, J.P., Dastugue, B., and Jagla, K. (2004). Coordinated development of muscles and tendons of the *Drosophila* leg. *Development* *131*, 6041–6051.
- Sparrow, J.C., and Schöck, F. (2009). The initial steps of myofibril assembly: integrins pave the way. *Nat Rev Mol Cell Biol* *10*, 293–298.
- Stahling-Hampton, K., Hoffmann, F.M., Baylies, M.K., Rushton, E., and Bate, M. (1994). dpp induces mesodermal gene expression in *Drosophila*. *Nature* *372*, 783–786.
- Steiger, G.J. (1971). Stretch activation and myogenic oscillation of isolated contractile structures of heart muscle. *Pflugers Arch.* *330*, 347–361.
- Steiger, G.J. (1977). Tension transients in extracted rabbit heart muscle preparations. *J Mol Cell Cardiol* *9*, 671–685.

- Stelzer, J.E., Larsson, L., Fitzsimons, D.P., and Moss, R.L. (2006). Activation dependence of stretch activation in mouse skinned myocardium: implications for ventricular function. *J. Gen. Physiol.* *127*, 95–107.
- Sudarsan, V., Anant, S., Guptan, P., VijayRaghavan, K., and Skaer, H. (2001). Myoblast diversification and ectodermal signaling in *Drosophila*. *Dev Cell* *1*, 829–839.
- Swank, D.M., Bartoo, M.L., Knowles, A.F., Iliffe, C., Bernstein, S.I., Molloy, J.E., and Sparrow, J.C. (2001). Alternative Exon-encoded Regions of *Drosophila* Myosin Heavy Chain Modulate ATPase Rates and Actin Sliding Velocity.
- Swank, D.M., Knowles, A.F., Suggs, J.A., Sarsoza, F., Lee, A., Maughan, D.W., and Bernstein, S.I. (2002). The myosin converter domain modulates muscle performance. *Nat Cell Biol* *4*, 312–317.
- Taylor, M.V., Beatty, K.E., Hunter, H.K., and Baylies, M.K. (1995). *Drosophila* MEF2 is regulated by twist and is expressed in both the primordia and differentiated cells of the embryonic somatic, visceral and heart musculature. *Mech Dev* *50*, 29–41.
- Thisse, C., Perrin-Schmitt, F., Stoetzel, C., and Thisse, B. (1991). Sequence-specific transactivation of the *Drosophila* twist gene by the dorsal gene product. *Cell* *65*, 1191–1201.
- Tiegs, O.W. (1955). The Flight Muscles of Insects-Their Anatomy and Histology; with Some Observations on the Structure of Striated Muscle in General. *Philosophical Transactions of the Royal Society B: Biological Sciences* *238*, 221–348.
- Timmons, L. (2003). Inducible Systemic RNA Silencing in *Caenorhabditis elegans*. *Mol Biol Cell* *14*, 2972–2983.
- Tonino, P., Pappas, C.T., Hudson, B.D., Labeit, S., Gregorio, C.C., and Granzier, H. (2010). Reduced myofibrillar connectivity and increased Z-disk width in nebulin-deficient skeletal muscle. *J Cell Sci* *123*, 384–391.
- Vemuri, R., Lankford, E.B., Poetter, K., Hassanzadeh, S., Takeda, K., Yu, Z.X., Ferrans, V.J., and Epstein, N.D. (1999). The stretch-activation response may be critical to the proper functioning of the mammalian heart. *Proc Natl Acad Sci USA* *96*, 1048–1053.
- Viens, A., Mechold, U., Lehrmann, H., Harel-Bellan, A., and Ogryzko, V. (2004). Use of protein biotinylation in vivo for chromatin immunoprecipitation. *Anal Biochem* *325*, 68–76.
- Vincent, S.D., and Buckingham, M.E. (2010). How to make a heart: the origin and regulation of cardiac progenitor cells. *Curr. Top. Dev. Biol.* *90*, 1–41.
- Volk, T., and VijayRaghavan, K. (1994). A central role for epidermal segment border cells in the induction of muscle patterning in the *Drosophila* embryo. *Development* *120*, 59–70.
- Vorbrüggen, G., and Jäckle, H. (1997). Epidermal muscle attachment site-specific

target gene expression and interference with myotube guidance in response to ectopic stripe expression in the developing *Drosophila* epidermis. *Proc Natl Acad Sci USA* *94*, 8606–8611.

Wang, K., and Ramirez-Mitchell, R. (1983). A network of transverse and longitudinal intermediate filaments is associated with sarcomeres of adult vertebrate skeletal muscle. *J Cell Biol* *96*, 562–570.

Williams, P.E., and Goldspink, G. (1971). Longitudinal growth of striated muscle fibres. *J Cell Sci* *9*, 751–767.

Wootton, R.J., and Newman, D. (1979). Whitefly have the highest contraction frequencies yet recorded in non-fibrillar flight muscles. *Nature* *280*, 402–403.

Wu, Q., Chen, X., Zhang, J., Loh, Y.-H., Low, T.-Y., Zhang, W., Zhang, W., Sze, S.-K., Lim, B., and Ng, H.-H. (2006). Sall4 interacts with Nanog and co-occupies Nanog genomic sites in embryonic stem cells. *The Journal of Biological Chemistry* *281*, 24090–24094.

Yagi, R., Mayer, F., and Basler, K. (2010). Refined LexA transactivators and their use in combination with the *Drosophila* Gal4 system. *Proc Natl Acad Sci USA* *107*, 16166–16171.

Yamashita, K., Sato, A., Asashima, M., Wang, P.-C., and Nishinakamura, R. (2007). Mouse homolog of SALL1, a causative gene for Townes-Brocks syndrome, binds to A/T-rich sequences in pericentric heterochromatin via its C-terminal zinc finger domains. *Genes Cells* *12*, 171–182.

Zhang, J., Tam, W.-L., Tong, G.Q., Wu, Q., Chan, H.-Y., Soh, B.-S., Lou, Y., Yang, J., Ma, Y., Chai, L., et al. (2006). Sall4 modulates embryonic stem cell pluripotency and early embryonic development by the transcriptional regulation of Pou5f1. *Nat Cell Biol* *8*, 1114–1123.

9. Supplements

In the following publications I to IV are reprinted. Supplementary videos and Excel tables are provided in the online versions of the publisher's homepage and can also be found on the enclosed CD.

Publication I

In Vivo RNAi Rescue in *Drosophila melanogaster* with Genomic Transgenes from *Drosophila pseudoobscura*

Christoph C. H. Langer¹*, Radoslaw K. Ejsmont²*, Cornelia Schönbauer¹*, Frank Schnorrer¹*, Pavel Tomancak²*

1 Max-Planck-Institute of Biochemistry, Martinsried, Germany, **2** Max-Planck-Institute of Molecular Cell Biology and Genetics, Dresden, Germany

Abstract

Background: Systematic, large-scale RNA interference (RNAi) approaches are very valuable to systematically investigate biological processes in cell culture or in tissues of organisms such as *Drosophila*. A notorious pitfall of all RNAi technologies are potential false positives caused by unspecific knock-down of genes other than the intended target gene. The ultimate proof for RNAi specificity is a rescue by a construct immune to RNAi, typically originating from a related species.

Methodology/Principal Findings: We show that primary sequence divergence in areas targeted by *Drosophila melanogaster* RNAi hairpins in five non-melanogaster species is sufficient to identify orthologs for 81% of the genes that are predicted to be RNAi refractory. We use clones from a genomic fosmid library of *Drosophila pseudoobscura* to demonstrate the rescue of RNAi phenotypes in *Drosophila melanogaster* muscles. Four out of five fosmid clones we tested harbour cross-species functionality for the gene assayed, and three out of the four rescue a RNAi phenotype in *Drosophila melanogaster*.

Conclusions/Significance: The *Drosophila pseudoobscura* fosmid library is designed for seamless cross-species transgenesis and can be readily used to demonstrate specificity of RNAi phenotypes in a systematic manner.

Citation: Langer CCH, Ejsmont RK, Schönbauer C, Schnorrer F, Tomancak P (2010) In Vivo RNAi Rescue in *Drosophila melanogaster* with Genomic Transgenes from *Drosophila pseudoobscura*. PLoS ONE 5(1): e8928. doi:10.1371/journal.pone.0008928

Editor: Bassem A. Hassan, VIB, Belgium

Received: November 2, 2009; **Accepted:** January 8, 2010; **Published:** January 28, 2010

Copyright: © 2010 Langer et al. This is an open-access article distributed under the terms of the Creative Commons Attribution License, which permits unrestricted use, distribution, and reproduction in any medium, provided the original author and source are credited.

Funding: This work was supported by the Max-Planck Society and the Human Frontier Science Program. The funders had no role in study design, data collection and analysis, decision to publish, or preparation of the manuscript.

Competing Interests: The authors have declared that no competing interests exist.

* E-mail: schnorrer@biochem.mpg.de (FS); tomancak@mpi-cbg.de (PT)

† These authors contributed equally to this work.

Introduction

Classical forward genetic mutagenesis screens pioneered the understanding of animal development in particular by using *Drosophila* as a model system [1]. The availability of the fly genome together with the discovery of RNA interference (RNAi) started an era of systematic reverse genetics, recently fuelled by the generation of genome-wide RNAi libraries in *Drosophila* [2,3,4]. Since RNAi can be achieved in a tissue specific manner in *Drosophila* [5] these genome-wide libraries have been used to study organ development [6,7,8]; and neuronal function [9] in an intact fly and will undoubtedly find many more applications in the near future.

A major pitfall of any RNAi approach are potential false positives resulting from unspecific knock-down of other genes than the anticipated target, the so called “off-target” effect. In case of randomly inserted hairpin transgenes false positives may arise from miss-expression of neighbouring genes. Despite the relatively low false positive rate in the systematic screens performed thus far (5–7%) ([7,8]), its presence necessitates the confirmation of the association of a RNAi phenotype with a particular gene by an independent method. The best proof is the recapitulation of the RNAi phenotype by a classical mutant, however such an approach is not universal as mutants are either not available or may display un-interpretable, pleiotropic phenotypes. Alternatively, the RNAi

phenotype can be confirmed by a second hairpin construct targeting a different region of the target gene that should show no or a different off-target effect. However, not all hairpins work to the same efficiency of knock-down and hence the observed phenotypes may differ despite the fact that only the correct on-target is knocked-down. Furthermore, not all genes are suited to generate several optimal 300 bp long hairpin sequences without overlap.

A conclusive proof of RNAi specificity is a rescue with a transgene that is immune to the RNAi and complements the loss of function of the target gene [10]. A convenient source of a RNAi-immune transgene is an orthologous gene from another closely related species that is divergent enough on the nucleotide sequence level to diminish RNAi efficiency while still functionally complementing the knock-down of the endogenous gene activity. This approach was successfully applied in human tissue culture RNAi using BAC transgenes from mouse [11] and in *C. elegans* with subcloned genomic BAC from *C. briggsae* [12]. When attempting RNAi rescue in living organisms, it is important to ensure that the rescue transgene gets expressed in the same cells and tissues in which RNAi was activated. Using the same driver for both RNAi and the gene rescue construct is one possibility, but the cDNA may not function properly when expressed from an artificial promoter. Recent advances in transgenesis of the *Drosophila* genome

allow transformation of large BAC sized transgenes [13] and make it possible to test cross-species rescue using genomic transgenes that recapitulate endogenous gene expression patterns [14].

Here we evaluate computationally and experimentally the performance of genomic clones from non-melanogaster species in rescue of RNAi phenotypes in *Drosophila melanogaster* (*D. melanogaster*). We identify *Drosophila pseudoobscura* (*D. pseudoobscura*) as a species suitable for RNAi rescue in terms of hairpin sequence divergence and make use of *D. pseudoobscura* FlyFos genomic fosmid library [15] to test RNAi specificity *in vivo*. We assayed for rescue of muscle specific knock-down phenotypes for five genes and were able to rescue three, suggesting that cross-species fosmid rescue is a useful strategy for establishing the specificity of RNAi phenotypes *in vivo* that can be easily applied to genome-wide RNAi screens in combination with the FlyFos library.

Materials and Methods

Bioinformatics Analysis of Hairpin Sequence Divergence

We downloaded pair-wise alignments between *D. melanogaster* and the 5 non-melanogaster species from the UCSC database (*D. melanogaster* release dm3 (UCSC)/Release 5 (FlyBase), non-melanogaster assembly releases by UCSC droSim1 (*D. simulans*), droAna3 (*D. ananassae*), dp4 (*D. pseudoobscura*), droPer1 (*D. persimilis*), droVir3 (*D. virilis*)). Using custom Perl scripts we extracted the portions of the pair-wise genome alignments covered by annotated Release 5 *D. melanogaster* transcripts (in case of multiple isoforms we selected the longest transcript to represent the gene) and collected the pair-wise alignment into single 'multiple' alignment file for each gene. These files were then searched with 12,591 hairpin sequences from genome wide transgenic RNAi library [2] (the library contains 15,059 hairpins; for simplicity only a single hairpin for each gene in the library was used for the analysis). 273 genes were not mapped because an alignment file was missing. Of the remaining genes 86% (10,858) mapped to the *D. melanogaster* sequence in the alignment files with 100% accuracy along the entire length of the hairpin. The 1733 hairpins that did not map completely were ignored in subsequent analysis. For the 10,858 fully mapped hairpins we counted the number of nucleotides conserved and the longest uninterrupted nucleotide stretch, both relative to *D. melanogaster* sequence. The collected counts were analyzed in Excel.

The multiple sequence alignments shown in **Figure 1c** and **Figure 2** were generated using EBI clustalw web-server and decorated in Jalview [16].

Fosmid Selection and Transgenesis

At the time when the genes for the rescue experiments were selected we had mapped 2,592 *D. pseudoobscura* fosmids. These fosmids fully include 1278 predicted *D. pseudoobscura* genes with exactly one ortholog in *D. melanogaster* genome. The genome-wide transgenic RNAi screen for muscle phenotypes with *Mef2-Gal4* driver resulted in 764 hits showing a defect in larval or flight muscle morphology [8]. 87 of these hits had a *D. pseudoobscura* ortholog covered by a fosmid and we manually selected five genes for the rescue experiment based on the RNAi phenotype and the placement of the ortholog within the fosmid (**Table 1** and **Figure S1**). Identifiers of the different data sources (fosmids, orthologs, RNAi hits) were matched using FlyMine [17]. The fosmid DNA was isolated as described in Ejsmont et al. [15]. The

transgenesis was performed by Genetic Services (<http://www.geneticservices.com/>).

Fly Strains and Genetics

All crosses were done at 27°C to increase *GAL4* activity. All hairpins were obtained from the VDRC stock centre. All fosmids were inserted at the same site on the third chromosome (attP2 [18]) using site specific phiC31 integrase [19] and were recombined with *Mef2-GAL4* also located on the third chromosome [20]. Recombinants were easily identified by dsRed expression in the ocelli (expression in the eye is quenched by [white +]). If the hairpin was located on the third chromosome it was also recombined with the fosmid enabling to test for rescue in the presence of two copies of the fosmid. *Mical*^{k1496} and *Mical*^{l666} are described in [21], *Cg25C*, *sar1*, *shg* and *vkg* mutants as well as *Df(2L)Exel7022* deleting both *vkg* and *Cg25C* were obtained from Bloomington. A GFP trap in *CG6416* was used to label the Z-line in larvae [22]. *w[1119]* was used as wild type and is indicated by "+". Recombinant chromosomes are indicated by ";"; homologous chromosomes by "/".

Phenotypic Analysis of Larval and Adult Flight Muscles, and Embryos

The larva-files for immuno-stainings of larval muscles were prepared as described [23]. All dissections were done in relaxing solution (20 mM phosphate buffer, pH 7.0; 5 mM MgCl₂, 5 mM EGTA, 5 mM ATP). Samples were fixed with 4% paraformaldehyde (PFA) in relaxing solution. Antibody incubations and subsequent washing steps were performed in PBS with 0,2% Triton X-100 instead of PBS-Tween. Samples were stained with rabbit anti-Kettin Ig 1/3 (1:100) [24], mouse anti-Mhc 3e8 (1:100) [25], mouse anti-Collagen IV (1:100) [26], and rhodamine phalloidin or Alexa dye labelled secondary antibodies (Molecular Probes). To image flight muscles hemi-thoraces of adults were prepared by removing wings, head and abdomen with fine scissors, fixing the thoraces in 4% PFA in relaxing solution for 10 min and bisecting them sagittally with a sharp microtome blade. Thorax halves were then incubated in relaxing solution for 15 min, fixed for 10 min in PFA, washed twice in PBS+0,2% Triton X-100, incubated in rhodamine phalloidin (1:500, in PBS +0,2% Triton X-100) for 30 min, washed two times in PBS +0,2% Triton X-100 and mounted in Vectashield. Embryos were fixed and stained as described [27] with rat anti-Mhc MAC147 (1:100) (Babraham Institute) and mouse anti-CollagenIV (1:100) [26]. Images were acquired with a Leica SP2 or Leica SP5 with 10x and 63x objectives to analyse flight muscles and myofibrils, and 40x objective to analyse embryos and larval muscles. Images were processed with ImageJ and Photoshop.

To analyse muscles of intact larvae the larvae carrying the *CG6416* GFP trap were immobilised by dipping in 65°C water for about 1 sec, and then mounted in 50% glycerol. Images were acquired on a Zeiss AxioImagerZ1 at 20x and analysed with ImageJ software.

To score for larval growth well fed, mated males and females were incubated in a vial for about 24 h, adults were removed and the vial was incubated for another 48 h or 72 h depending on the strength of the RNAi phenotype. All relevant crosses were done in parallel at the same time blind to the genotype. Larvae were immobilised by placing into 65°C water for about 1 sec, and then mounted in 50% glycerol. Images were acquired on a Leica M2FLIII with a ProgRes C14 at 1.25x magnification

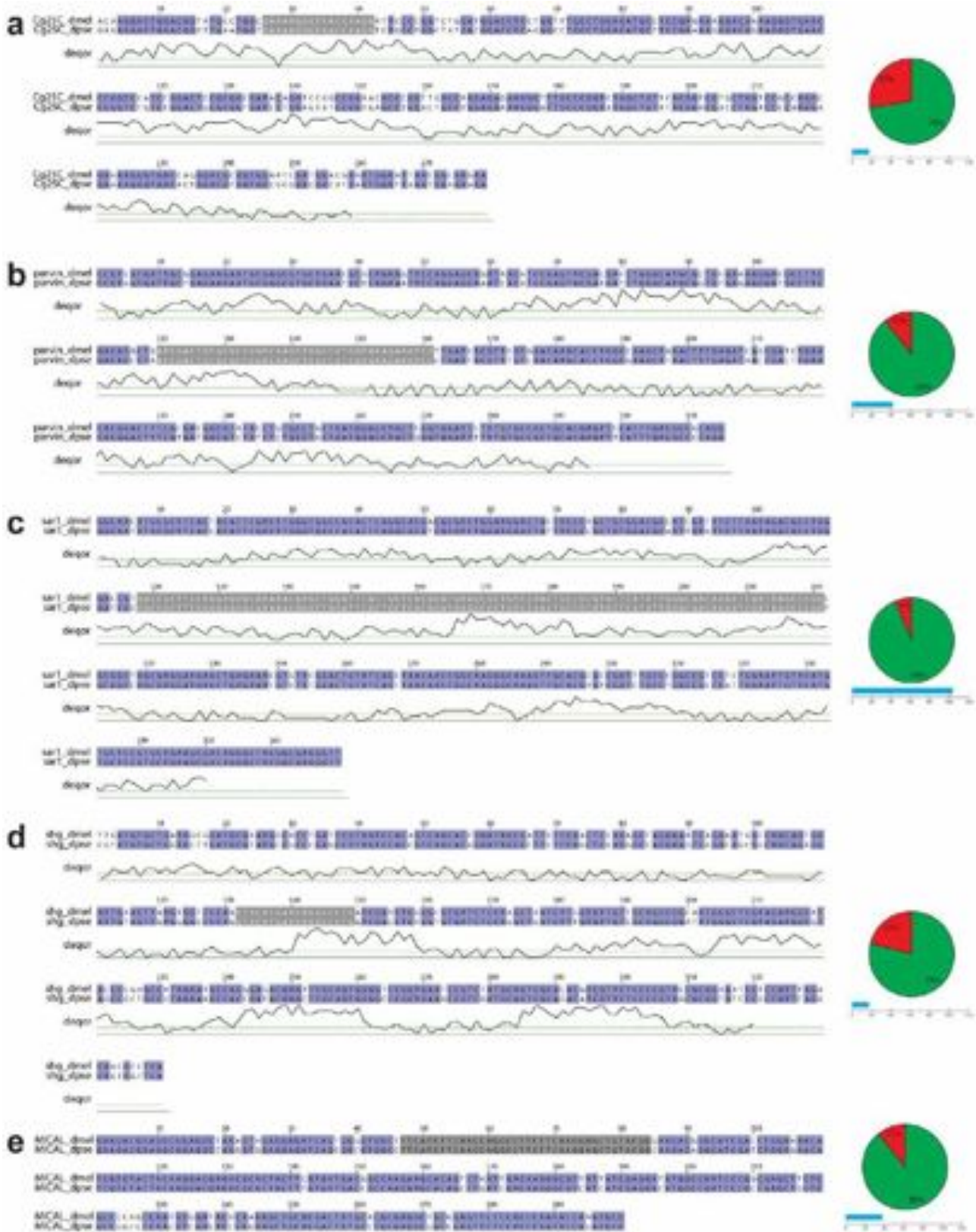


Figure 2. Pairwise sequence alignment of hairpins used in rescue experiments. Alignments between *D. melanogaster* and *D. pseudoobscura* for hairpins targeting (a) *Cg25c* (collagen IV), (b) *CG32528* (*parvin*), (c) *sar1*, (d) *shg* and (e) *Mical*. The extent of homology and the longest identical nucleotide stretch are graphically depicted next to each alignment. Matching nucleotides are shaded purple, mismatches white and the longest identical stretches are shaded grey within the alignments. The DEQOR scores are plotted below the alignments (a–d) and the score 5 cut-off above which the siRNA at that position is considered RNAi inefficient is depicted by a green line. doi:10.1371/journal.pone.0008928.g002

Table 1. Overview of genes and fosmids.

<i>D. mel.</i> Gene	Trans- formant ID	FlyFos ID	RNAi phenotype	RNAi fosmid rescue?	Mutant allelic combination	Mutant phenotype	Mutant fosmid rescue?
<i>Cg25C</i> (<i>collagen IV</i>)	104536	045318	larval lethal	larval growth rescued; few pupa and adults	<i>Cg25C^{h00405}/</i> <i>Df(2L)Exel7022</i>	embryo or larval lethal	n. a.
<i>CG32528</i> (<i>parvin</i>)	11670	044975	myospheroid phenotype; early larval lethal	myospheroid phenotype rescued; 2x fosmid survive until early pupae	---	---	---
<i>sar1</i>	34191	045459	sarcomere defect; larval lethal	larval growth and sarcomere phenotype rescued; survive until early pupae	<i>sar1⁰⁵⁷¹²/Df</i> (<i>3R</i>) <i>ED6085</i>	embryo or larval lethal	few adult survivors (small size, can fly)
<i>shg</i>	27081	045685	missing flight muscles	no rescue	<i>shg^{E17D}/shg²</i>	embryo or larval lethal	viable adults that fly
<i>Mical</i>	25372	045847	irregular flight muscle myofibrils	no rescue	<i>Mical^{k1496}/Dr</i> (<i>3R</i>) <i>Exel6155</i>	Irregular flight muscle myofibrils	no rescue

Overview of all genes, RNAi constructs and fosmids used. The degree of homology between the genes in the targeted region is indicated. The RNAi and mutant phenotypes and their rescue by the fosmids is summarized.

doi:10.1371/journal.pone.0008928.t001

and larval length from head to tail was measured with Photoshop.

Results

Evaluation of Sequenced *Drosophila* Species for Transgenic RNAi Rescue Experiment

In order to identify the species best suited for RNAi rescue we performed comparative analysis of the divergence of *D. melanogaster* hairpin sequences in 5 different non-melanogaster species (Figure 1a) that sample the evolutionary tree of the sequenced *Drosophilid* genomes [28,29]. We first mapped all hairpin sequences onto pair-wise, global genome alignments between *D. melanogaster* and the 5 non-melanogaster species available from UCSC [30] and extracted the percent identity for each pair (Figure 1b). As expected the pattern of hairpin sequence divergence follows the phylogeny; *D. simulans* sequences closely resemble *D. melanogaster* (94.75% are more than 90% conserved, i.e. 90th percentile), the sister species *D. pseudoobscura* and *D. persimilis* are almost indistinguishable (90th percentile 1.78% and 1.63% respectively), *D. annanassae* similarity falls in between the *D. simulans* and the *obscura* group (90th percentile 2.98%) and *D. virilis* is most divergent with respect to *D. melanogaster* (90th percentile 0.41%). Overall the sequence homology of the species outside of *melanogaster* subgroup is quite comparable as 32.38% (*D. virilis*) to 55.61% (*D. annanassae*) of the hairpins have more than 75% of the nucleotides conserved relative to *D. melanogaster*.

We next asked how sensitive would the sequences from non-melanogaster species be to the *melanogaster* RNAi hairpins. It is broadly accepted in the RNAi field that stretches of 19 and more identical nucleotides can cause an ‘off-target’ effect [31,32,33]. Therefore we extracted the longest identity stretches from the pair-wise hairpin alignments for each species (Figure 1c) and analyzed their distribution. Vast majority (98.62%) of the longest identical stretches in *D. simulans* are longer than 18 nucleotides (Figure 1d) which allows us to conclude that this species would be a poor choice for *in vivo* RNAi rescue. Among the remaining species *D. virilis* has the largest proportion of hairpins that contain identity stretches shorter than 19 nucleotides (67.22%), making the clones likely refractory to RNAi. However the differences are not large; using the same criterion, 47.75% of *annanassae* clones, 53.58% of *D. persimilis* and 53.58% of *D. pseudoobscura* genes would also be refractory (Figure 1e). Altogether 81% of the genes in the VDR

hairpin collection have an ortholog with less than 19 nt identity stretch in at least one of the 5 non-melanogaster species. Since 94% of the refractory orthologs come from either *D. pseudoobscura* or *D. virilis* which are established model systems, we conclude that they are both well suited to serve as a donor for RNAi rescue experiment from the sequence divergence point of view.

Besides sequence divergence, the second important criterion for successful RNAi rescue is the ability of the transgene to complement the RNAi phenotype. The *D. virilis* life cycle is significantly longer than in *D. melanogaster* whereas *D. pseudoobscura* develops at a more similar pace [34]. Comparative micro-array time-course analysis of embryogenesis revealed that 24.7% of *D. virilis* genes exhibits differential gene expression profiles relative to *D. melanogaster* compared to 18.8% for *D. pseudoobscura* (P.T. manuscript in preparation). Based on these considerations we decided that *D. pseudoobscura* genomic transgenes are more likely to complement *D. melanogaster* loss-of-function phenotypes and are thus best suited for RNAi rescue.

Selection of FlyFos Clones for *In Vivo* RNAi Rescue

We previously constructed a *D. pseudoobscura* genomic fosmid library, which we call FlyFos, in a vector containing 3xP3 dsRed dominant selection cassette [35] and attB sites for phiC31-mediated site-specific transgenesis [15,18]. We thus far mapped end-sequences of 5,855 fosmid clones to *D. pseudoobscura* genome that cover 67.28% of the annotated *D. pseudoobscura* genes including at least 10 kb upstream and 5 kb downstream of the predicted gene model [15].

In order to select *D. pseudoobscura* FlyFos fosmids for RNAi rescue experiments we compared the complete list of hits from a genome-wide transgenic RNAi screen for muscle specific phenotypes induced by knocked-down with *Mef2-GALA* driver [8], with the mapped *D. pseudoobscura* fosmids by linking annotated gene orthologs [36]. We selected five genes that lead either to larval lethality or a flightless phenotype (Table 1, see methods). All selected fosmids span at least to the next gene 5' and 3' from the gene assayed (Figure S1). The sequence similarity between *D. melanogaster* and *D. pseudoobscura* for the gene regions targeted by the used hairpins ranges from 73–94% (Figure 2). The largest stretch of exact match varies from 17–104 nucleotides. In order to estimate the ability of the siRNAs derived from the hairpins to function in RNAi we ran DEQOR analysis on the sequences [37]

(**Figure 2**). DEQOR evaluates all possible 19mers from the hairpin sequence for a number of criteria (GC content, GC balance across the length of the siRNA and polynucleotide stretches) resulting in a score that reflects the efficiency of each 19mer in RNAi (the lower the score, the better RNAi performance, siRNAs below score 5 are considered suitable for RNAi). We used here DEQOR scores to ask whether the long identical stretches between *D. melanogaster* and *D. pseudoobscura* sequences are efficient in RNAi and thus likely to cross-silence the rescue transgene. Interestingly we found that most of the long identical stretch sequences (see **Figure 2c**) are predicted to perform poorly in RNAi suggesting that used hairpins will not significantly affect the *D. pseudoobscura* transgenes.

Drosophila pseudoobscura Fosmids Rescue In Vivo RNAi Phenotypes in *Drosophila melanogaster*

We obtained *D. melanogaster* transgenics for all five fosmids by selecting for the dsRed expression in the eye, which is easily identifiable in *white* genetic background. In case of the *Mical* fosmid instead of the eye we observed expression of dsRed in the thorax. As this fosmid was not able to rescue a *Mical* mutant allelic combination that recapitulates our observed RNAi phenotype, causing very irregular myofibrils in the indirect flight muscles (**Figure S2** and [21]), we judged this fosmid as non functional and did not investigate it further.

To test cross-species functionality of the *D. pseudoobscura* fosmid in *D. melanogaster* we rescued classical mutants of *shotgun* (*shg*) and *sar1* to viability and flight ability with the *shg* and *sar1* fosmids, respectively (**Table 1**) demonstrating that the *D. pseudoobscura* genes are fully functional in *D. melanogaster*.

For *shg* RNAi in muscle we observed a flightless phenotype caused by missing indirect flight muscles in the thorax [8]. The *shg* fosmid does not rescue this phenotype, indicating that the RNAi phenotype is either unspecific or the *D. pseudoobscura* gene is also targeted by the hairpin.

Three of our selected genes, the collagen IV homolog *Cg25C*, the parvin homolog *CG32528* and the small GTPase *sar1* lead to larval lethality upon knock-down with *Mef2-GAL4* [8], **Table 1**). *Cg25C* is strongly expressed in embryonic hemocytes and supposedly has an important role in basement membrane function. We first analyzed P-element mutants to test if our collagen IV antibody recognizes *Cg25C* or *Vkg*, the second *Drosophila* collagen IV which is present in the basement membrane around the larval muscles [38]. As both genes face each other “head to head” the available P-elements located 5' of each gene may also affect expression of the other more distant gene if enhancer elements are shared (**Figure S3a**). We find the expected strong collagen IV signal in hemocytes of wild-type stage 16 and stage 17 embryos with the collagen IV antibody (**Figure S3b,e**). This signal is absent in *Cg25C^{k00405}/Df(2L)Exel7022* stage 16 and stage 17 embryos (**Figure S3c,f**). We also found no signal in *vkg⁰¹²⁰⁹/Df(2L)Exel7022* at stage 16, but detect a robust signal at stage 17 in these embryos (**Figure S3d,g**), suggesting that the collagen IV antibody does recognise *Cg25C* and not *Vkg*.

This conclusion is further corroborated by RNAi knock-down of both genes in muscle. We detect a collagen IV containing basement membrane around the growing larval muscles in wild type (**Figure 3a**). This collagen IV signal is severely reduced when *Cg25C* is knocked-down in muscle with *Mef2-GAL4* (**Figure 3b**) but not in *vkg* knock-down larvae (**Figure 3d**), which die at a comparable stage as *Cg25C* knock-down larvae [8]. This demonstrates that the collagen IV antibody indeed recognizes *Cg25C* and suggests an essential role for *Cg25C* in basement membrane function around growing muscles. The *D. pseudoobscura*

Cg25C fosmid (*FlyFos-pse-Cg25C*) rescues larval growth significantly but not completely compared to knock-down and wild type (**Figure 3e**, **Table 1**) demonstrating the specificity of the RNAi knock-down. This incomplete rescue suggests that the *FlyFos-pse-Cg25C* fosmid is either not fully functional or not entirely immune to the *Cg25C* hairpin. Antibody staining against collagen IV/*Cg25C* argue for the latter as its localisation around the muscles is still markedly reduced in the rescued larvae (**Figure 3c**). In conclusion we demonstrate that the muscle specific RNAi knock-down of *Cg25C* can be rescued by the *FlyFos-pse-Cg25C*.

Muscles require the integrin complex for stable attachment to tendons [39]. We found that *parvin* knock-down results in early larval lethality with body muscles displaying a myospheroid phenotype (**Figure 4a**). This myospheroid phenotype is entirely rescued by the *D. pseudoobscura parvin* fosmid (*FlyFos-pse-parvin*) (**Figure 4b–d**). Similarly the growth defect in *parvin* knock-down larva is rescued; interestingly two copies of the fosmid increase the level of rescue (**Figure 4e** and **Figure S4**). We conclude that *Drosophila parvin* is required for muscle attachment, most likely via an integrin dependent mechanism as mouse parvin is an important member of the integrin complex [40] and integrin mutant *Drosophila* embryos display a myospheroid phenotype [39].

Finally we investigated the small GTPase *sar1* implicated in vesicle transport [41] and heart formation in the embryo [42]. Knock-down of *sar1* in muscle causes a muscle sarcomere phenotype. Both the myosin thick filaments and the Z-line anchoring the actin filaments show a “fading-Z” phenotype or in extreme cases we observe a partial loss of sarcomeres (**Figure 5a–c**). The *FlyFos-pse-sar1* completely rescues this sarcomere phenotype (**Figure 5d**) demonstrating a specific role of *sar1* for sarcomere formation and in turn larval growth (**Figure 5e**).

Discussion

In this study we present a systematic evaluation of cross-species rescue with genomic transgenes for testing the specificity of transgenic RNAi knock-down in *Drosophila melanogaster*. We identified *D. pseudoobscura* and *D. virilis* as suitable, although not optimal, species for transgenic RNAi rescue and chose *D. pseudoobscura* FlyFos fosmid library to test the rescue performance. Despite the sequence similarity, which in some cases goes well beyond the 19 nt threshold (*sar1* 104 nt stretch), we were able to demonstrate rescue of the RNAi phenotype for three of the five genes tested. Similarly we showed rescue of classical mutants for *shg* and *sar1*. Overall, our strategy of cross-species RNAi rescue worked successfully for three of four cases in which the fosmid is functional.

We did not obtain a full rescue of the RNAi phenotypes. Since we observed full rescue of classical mutant phenotypes in two out of three cases and Kondo et. al [14] reported successful rescue in four out of four cases, we believe that in most cases the *D. pseudoobscura* gene products are able to functionally replace the *D. melanogaster* gene. We hypothesize that the incompleteness of the RNAi rescue is mainly caused by the sequence similarity of the genes between *D. melanogaster* and *D. pseudoobscura* which still results in knock-down of the *pseudoobscura* gene to some extent. In case of *parvin* we have strong evidence supporting this notion as two copies of the fosmid rescue better than a single copy. Kondo et. al. [14] reports full rescue of a rough-eye phenotype induced by over-expressing dsRNA directed against apoptotic gene *diap1* with an eye specific driver (GMR-GAL4) raising the possibility that the efficiency of the cross-species RNAi rescue will depend on the strength of the *GAL4* driver, the tissue and the gene tested.

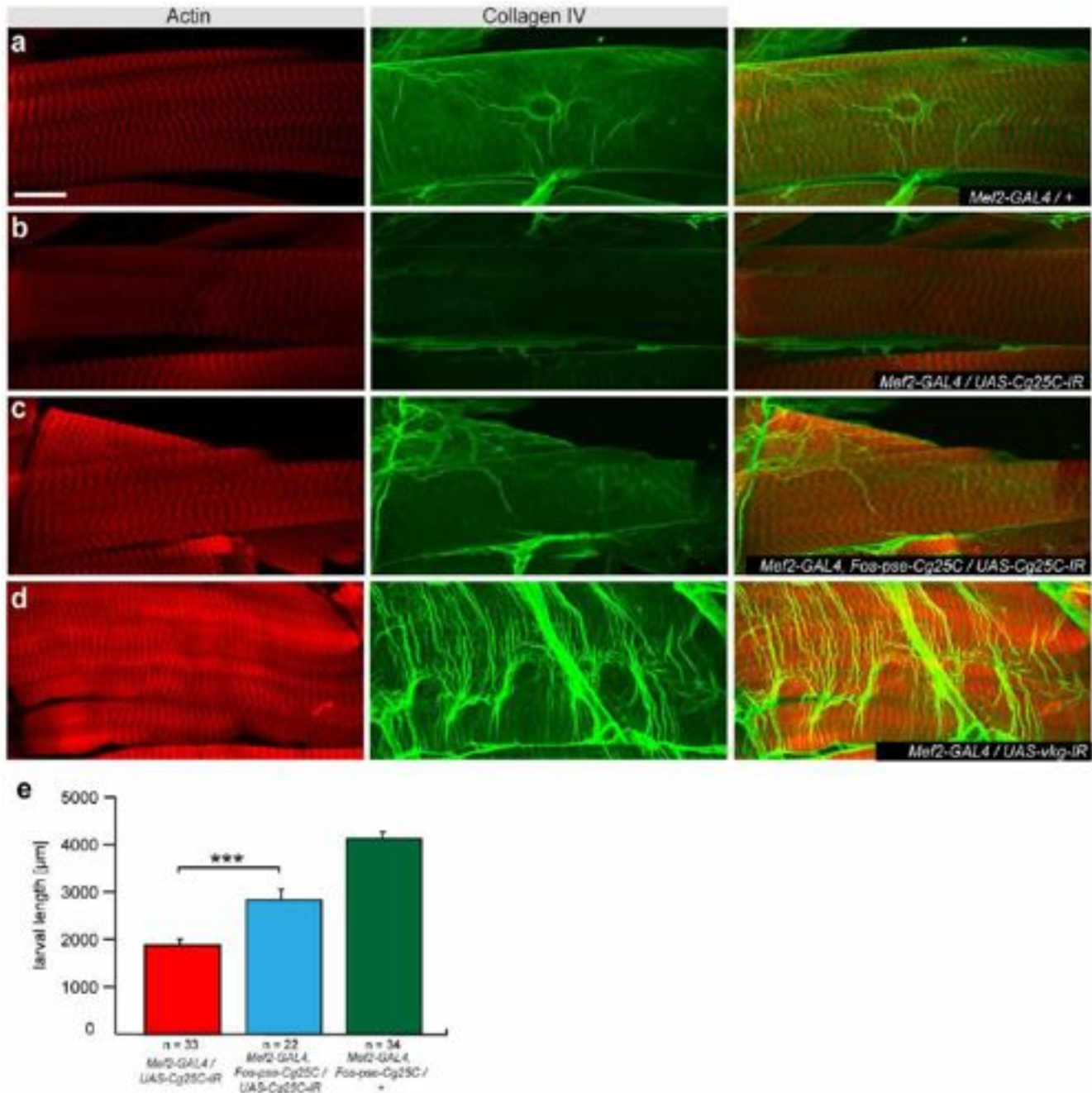


Figure 3. Rescue of *Cg25C* phenotype by *D. pseudoobscura* fosmid. (a–d) Collagen IV (green) wraps the larval muscles in wild type (a) and is strongly reduced in *Mef2-GAL4/UAS-Cg25C-IR* (TF104536) (b) but rescued by *FlyFos-pse-Cg25C* (c); Collagen IV levels are not altered in *Mef2-GAL4/UAS-vkg-IR* (TF106812) (d); actin is visualised with phalloidin; size bar corresponds to 25 μm. (e) Quantification of larval size in *Mef2-GAL4/UAS-Cg25C-IR* (TF104536) larvae (red) rescued by *FlyFos-pse-Cg25C* (blue) and wild type (green). ***p < 0.0001 (unpaired two-tailed t-test). 72–96 h after egg laying were assayed. Error bars indicate standard error of the mean (SEM). doi:10.1371/journal.pone.0008928.g003

Interestingly, the extent of the rescue does not necessarily correlate with the similarity of the hairpin-targeted sequences as measured by longest identity stretches (Figure 2, and Table 1). It appears that the ‘naïve’ application of 19 nt threshold generally thought to be sufficient for cross-silencing may strongly underestimate the proportion of refractory orthologs. In contrary, data from cell culture indicate that even miss-matches every 12 bp can still result in some RNAi mediated silencing [43]. Hence assessing the efficiency of theoretical siRNAs generated from the hairpin by

the DEQOR protocol may represent a more realistic measure of cross-silencing potential. Analysis of larger sets of cross-species rescue experiments will be required to evaluate the predictive power of the DEQOR analysis.

We observed a broad range of outcomes in our cross-species RNAi rescue experiments that allow us to define simple rules for their interpretation. We propose that if a phenotypic rescue, albeit incomplete, is observed, the specificity of the RNAi knock-down need not be questioned any longer. If, however, no

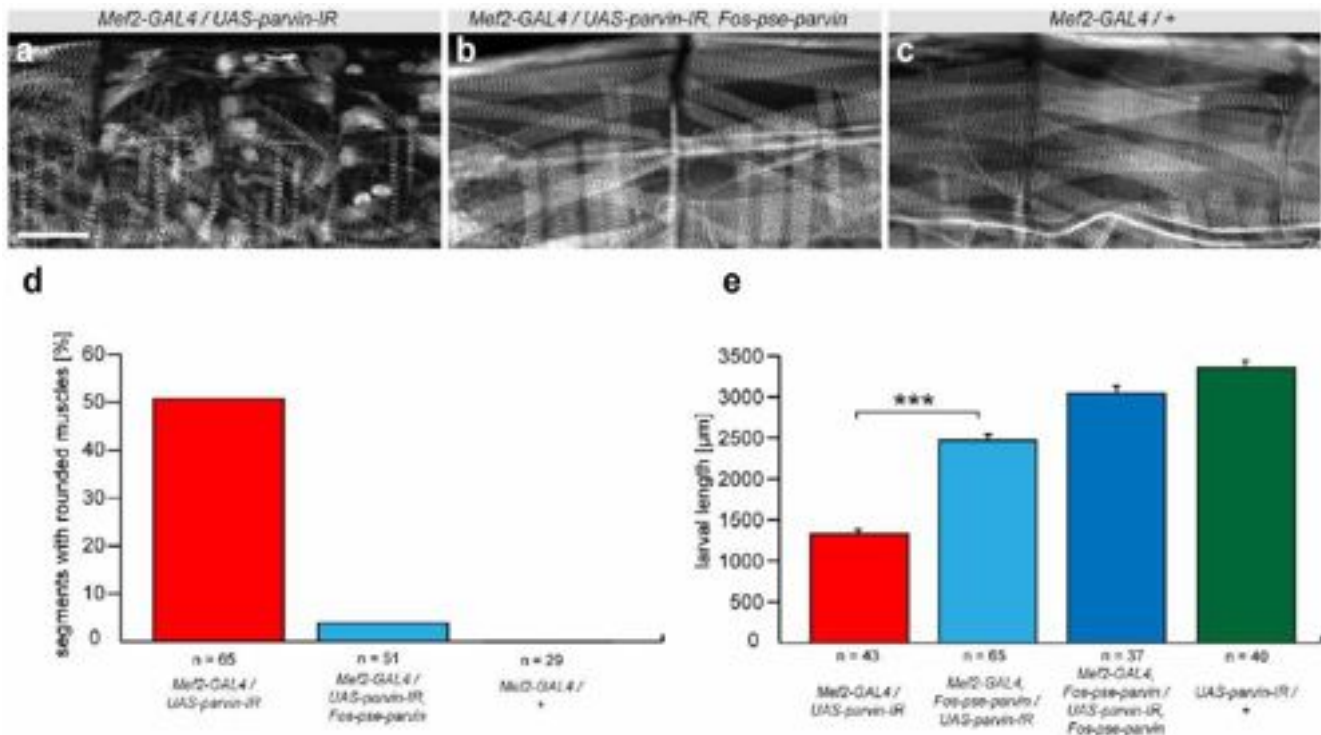


Figure 4. Phenotypic rescue of *parvin* by *D. pseudoobscura* fosmid. (a–c) Rounded/myospheroid muscle phenotype in *Mef2-GAL4/UAS-parvinIR* (TF11670) (a) is rescued by *FlyFos-pse-parvin* (b) to wild type (c); size bar corresponds to 100 μm. (d) Quantification of myospheroid phenotype rescue, percentage of segments containing rounded muscles are shown, below the total numbers of segments scored. (e) Quantification of larval size in *Mef2-GAL4/UAS-parvinIR* larva (red), rescued by one (light blue) or two copies of *FlyFos-pse-parvin* (dark blue), compared to wild type (green). Larvae 48–72 h after egg laying were assayed. Error bars indicate standard error of the mean (SEM), *** $p < 0.0001$ (unpaired two-tailed t-test) compared to rescued larvae.

doi:10.1371/journal.pone.0008928.g004

rescue is observed, it is necessary to determine whether the rescuing construct is active. This can be done by rescuing a classical mutant allele if available, or by showing, using antibody staining or RNA *in situ*, that the expression of the hetero-specific transgene mimics the expression of wild-type ortholog and is unperturbed in the RNAi genetic background. For the purpose of visualizing the rescue construct in a straightforward manner, it may be useful to tag the construct with a reporter such as GFP [15]. When these controls establish that the rescue construct is functional, the absence of RNAi rescue indicates that the observed phenotype is caused by an off-target knock-down.

In the future we plan to establish a fosmid library for *D. virilis* to expand the spectrum of genes in which cross-species RNAi rescue is an option. However our bioinformatics analysis indicates that for approximately 1/3 of the genes even the distantly related *Drosophilids* diverged insufficiently to attempt cross-species RNAi rescue with confidence. It may be possible to optimize the placement of the targeting hairpin within the gene model to enable efficient cross-species rescue, but the existing transgenic RNAi libraries cannot benefit from this approach. Alternatively one can use recombineering manipulation to render *D. melanogaster* fosmid sequences RNAi immune by introducing silent mutations in the stretch covered by the hairpin [43]. Such strategy is costly and laborious despite the advances in high-throughput manipulation of large clones in bacteria.

The *D. pseudoobscura* fosmid library is freely available at <http://transgenome.mpi-cbg.de/>. The rescue with FlyFos clones is very simple; once a suitable clone containing the gene of interest is

identified, it can be directly injected into *D. melanogaster* without additional modification. Hence, our system is simpler than the fosmid retrofitting approach developed by Kondo et. al. [14]. After transgenesis, that can be efficiently performed by a company, the fosmids marked with dsRed in eyes and ocelli can be easily recombined with most existing GAL4 lines or hairpin constructs.

In conclusion, cross-species rescue is a valid approach to demonstrate RNAi specificity and thus may complement the vast number of *in vivo* RNAi studies done in *Drosophila* [6,7,8,9]. It may go beyond the mere rescue of an RNAi loss of function phenotype as it can also be applied to perform structure-function analysis in an RNAi knock-down background [44]. The fosmids can easily be engineered by liquid culture recombineering to delete or modify specific protein domains or single critical amino acids [13,15,45]. This will enable systematic structure-function studies for genes, for which no mutants are available, or more importantly mutants that display highly pleiotropic phenotypes.

Supporting Information

Figure S1 Genomic region of *D. pseudoobscura* fosmids. Screenshots of gbrowse representations of the genomic regions of *D. pseudoobscura* genome corresponding to extent of the fosmids used in rescue experiments. The gene orthologous to the *D. melanogaster* gene knocked-down by RNAi is marked by the presence of its transcript and CDS. The FlyFos identifier and mapping coordinates of end-sequences of the fosmid on *D. pseudoobscura* genome are shown on top of each gbrowse view.

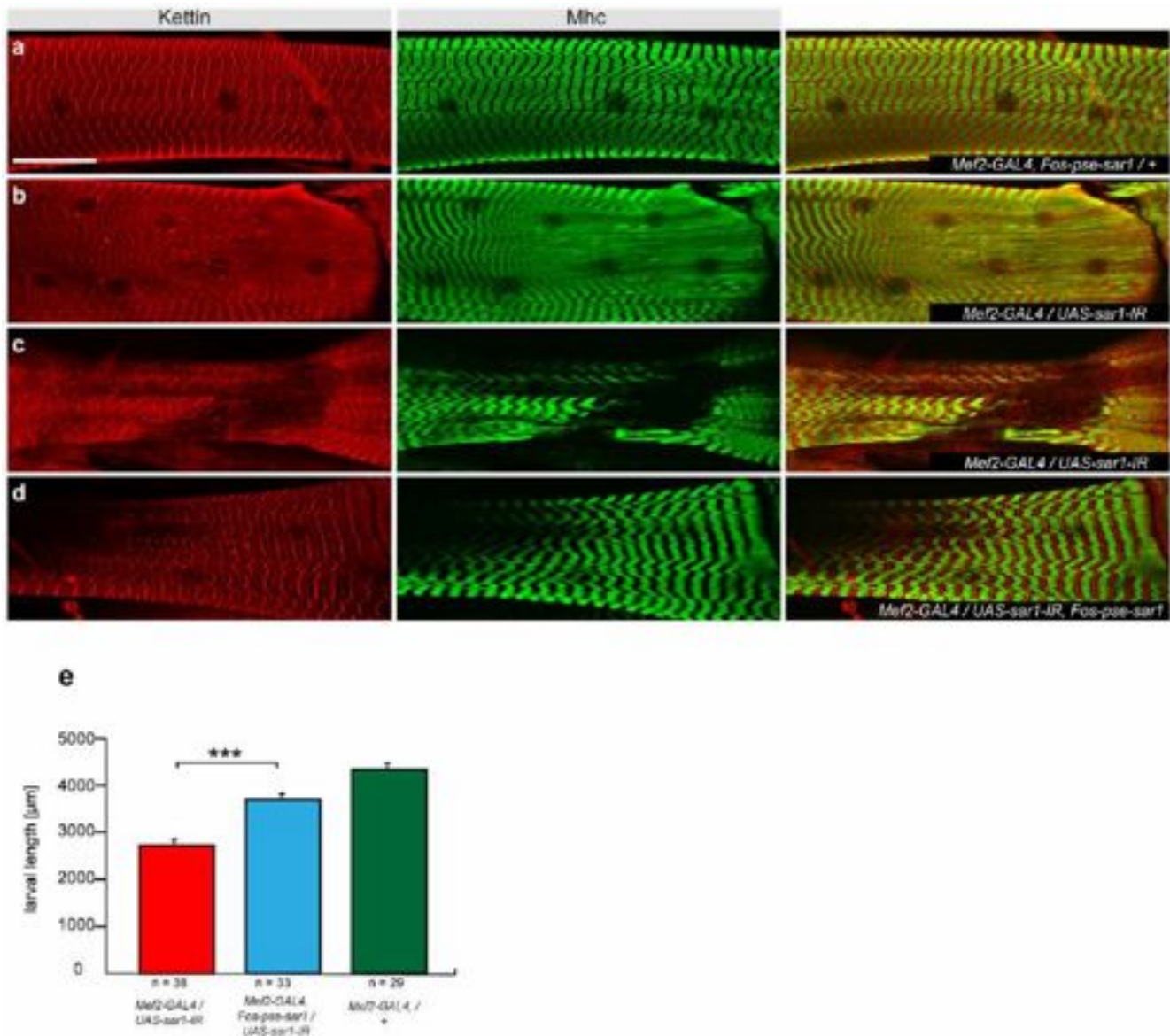


Figure 5. Phenotypic rescue of *sar1* by *D. pseudoobscura* fosmid. (a–d) Fading Z- and M-line or loss of sarcomeres in *Mef2-GAL4/UAS-sar1-IR* (TF34191) (b, c) is rescued by *FlyFos-pse-sar1*(d) to wild type (a). Z-lines are visualised with anti-Kettin (red), M-lines with anti-Mhc antibody (green); size bar corresponds to 50 μm. (e) Quantification of larval length in *Mef2-GAL4/UAS-sar1-IR* larvae (red), compared to *FlyFos-pse-sar1* rescued (blue) and wild type (green). Larvae 72–96 h after egg laying were assayed. Error bars indicate standard error of the mean (SEM), ***p<0.0001 (unpaired two-tailed t-test) compared to rescued larvae. doi:10.1371/journal.pone.0008928.g005

Found at: doi:10.1371/journal.pone.0008928.s001 (0.93 MB TIF)

Figure S2 Mical mutant and RNAi phenotype Indirect flight muscles (a–d) and myofibrils of these IFMs (e–g) in wild type (a, e) *Mical* mutants (b, f), *Mef2-GAL4/UAS-Mical-IR* (TF25372) (c, g) and *Mical* mutants carrying the *FlyFos-pse-Mical* (d, h). Actin is visualised by phalloidin; size bar in (a–d) corresponds to 100 μm, in (e–g) to 10 μm.

Found at: doi:10.1371/journal.pone.0008928.s002 (2.19 MB TIF)

Figure S3 *Cg25C* and *vkg* genomic locus and collagen IV protein expression. (a) Screenshot of gbrowse representation of the genomic regions of *D. melanogaster Cg25C* and *vkg*; the position of the P-elements *vkg*⁰¹²⁰⁹ and *Cg25C*^{k00405} are indicated accord-

ing to Flybase. (b–g) Stage 16 (b–d) and stage 17 (e–g) wild-type (b, e), *Cg25C*^{k00405}/*Df(2L)Exel7022* (c, f) and *vkg*⁰¹²⁰⁹/*Df(2L)Exel7022* (d, g) embryos are stained for Mhc in green and Collagen IV in red; size bar corresponds to 50 μm.

Found at: doi:10.1371/journal.pone.0008928.s003 (3.37 MB TIF)

Figure S4 Rescue of *parvin* knock-down. Larva of 48–72 h (a–c) or 72–96 h (d–f) were imaged at the same magnification. *Mef2-GAL4/UAS-parvinIR* (TF11670) (a, d) stay tiny compared to *Mef2-GAL4/UAS-parvinIR*, *FlyFos-pse-parvin* (b, e) and *UAS-parvin-IR/+* control larvae (c, f). Size bar corresponds to 1 mm.

Found at: doi:10.1371/journal.pone.0008928.s004 (1.94 MB TIF)

Acknowledgments

We thank VDRRC, the Bloomington stock centre and Hermann Aberle for fly stocks. We are grateful to Elisabeth Knust, Judith Saide, Bellinda Bullard and John Fessler for discussions and generous gift of antibodies. We thank Vineeth Surendranath for help with DEQOR analysis.

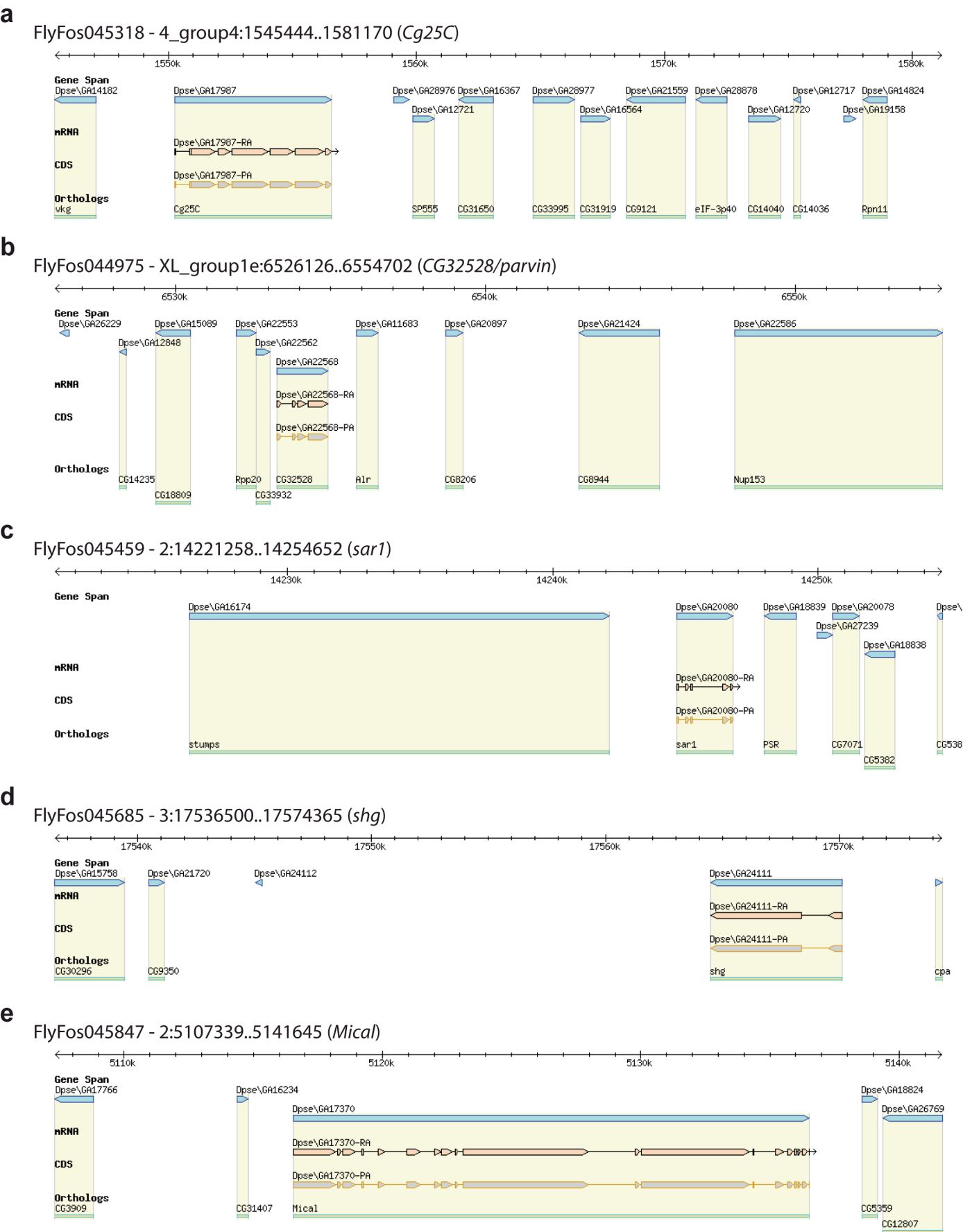
References

- Nüsslein-Volhard C, Wieschaus E (1980) Mutations affecting segment number and polarity in *Drosophila*. *Nature* 287: 795–801.
- Dietzl G, Chen D, Schnorrer F, Su KC, Barinova Y, et al. (2007) A genome-wide transgenic RNAi library for conditional gene inactivation in *Drosophila*. *Nature* 448: 151–156.
- Matsumoto A, Ukai-Tadenuma M, Yamada RG, Houli J, Uno KD, et al. (2007) A functional genomics strategy reveals clockwork orange as a transcriptional regulator in the *Drosophila* circadian clock. *Genes Dev* 21: 1687–1700.
- Ni J-Q, Liu L-P, Binari R, Hardy R, Shim H-S, et al. (2009) A *Drosophila* resource of transgenic RNAi lines for neurogenetics. *Genetics* 182: 1089–1100.
- Roignant J-Y, Carré C, Mugat B, Szymczak D, Lepesant J-A, et al. (2003) Absence of transitive and systemic pathways allows cell-specific and isoform-specific RNAi in *Drosophila*. *RNA* 9: 299–308.
- Cronin SJF, Nehme NT, Limmer S, Liegeois S, Pospisilik JA, et al. (2009) Genome-wide RNAi screen identifies genes involved in intestinal pathogenic bacterial infection. *Science* 325: 340–343.
- Mummary-Widmer JL, Yamazaki M, Stoeger T, Novatchkova M, Bhalerao S, et al. (2009) Genome-wide analysis of Notch signalling in *Drosophila* by transgenic RNAi. *Nature* 458: 987–992.
- Schnorrer F, Schönbauer C, Langer CCH, Dietzl G, Novatchkova M, et al. (2010) Systematic genetic analysis of muscle morphogenesis and function in *Drosophila*. *Nature*.
- Yapici N, Kim Y-J, Ribeiro C, Dickson BJ (2008) A receptor that mediates the post-mating switch in *Drosophila* reproductive behaviour. *Nature* 451: 33–37.
- Sarov M, Stewart AF (2005) The best control for the specificity of RNAi. *Trends Biotechnol* 23: 446–448.
- Kittler R, Pelletier L, Ma C, Poser I, Fischer S, et al. (2005) RNA interference rescue by bacterial artificial chromosome transgenesis in mammalian tissue culture cells. *Proc Natl Acad Sci U S A* 102: 2396–2401.
- Sarov M, Schneider S, Pozniakovski A, Roguev A, Ernst S, et al. (2006) A recombineering pipeline for functional genomics applied to *Caenorhabditis elegans*. *Nat Methods* 3: 839–844.
- Venken KJ, He Y, Hoskins RA, Bellen HJ (2006) P[acman]: a BAC transgenic platform for targeted insertion of large DNA fragments in *D. melanogaster*. *Science* 314: 1747–1751.
- Kondo S, Booker M, Perrimon N (2009) Cross-species RNAi Rescue Platform in *Drosophila melanogaster*. *Genetics*.
- Ejsmont RK, Sarov M, Winkler S, Lipinski KA, Tomancak P (2009) A toolkit for high-throughput, cross-species gene engineering in *Drosophila*. *Nat Methods*.
- Waterhouse AM, Procter JB, Martin DMA, Clamp M, Barton GJ (2009) Jalview Version 2—a multiple sequence alignment editor and analysis workbench. *Bioinformatics* 25: 1189–1191.
- Lyne R, Smith R, Rutherford K, Wakeling M, Varley A, et al. (2007) FlyMine: an integrated database for *Drosophila* and *Anopheles* genomics. *Genome Biol* 8: R129.
- Groth AC, Fish M, Nusse R, Calos MP (2004) Construction of transgenic *Drosophila* by using the site-specific integrase from phage phiC31. *Genetics* 166: 1775–1782.
- Bischof J, Maeda RK, Hediger M, Karch F, Basler K (2007) An optimized transgenesis system for *Drosophila* using germ-line-specific phiC31 integrases. *Proc Natl Acad Sci U S A* 104: 3312–3317.
- Ranganayakulu G, Schulz RA, Olson EN (1996) Wingless signaling induces nautilus expression in the ventral mesoderm of the *Drosophila* embryo. *Dev Biol* 176: 143–148.
- Beuchle D, Schwarz H, Langegger M, Koch I, Aberle H (2007) *Drosophila* MICAL regulates myofilament organization and synaptic structure. *Mech Dev* 124: 390–406.
- Quinones-Coello AT, Petrella LN, Ayers K, Melillo A, Mazzalupo S, et al. (2007) Exploring strategies for protein trapping in *Drosophila*. *Genetics* 175: 1089–1104.

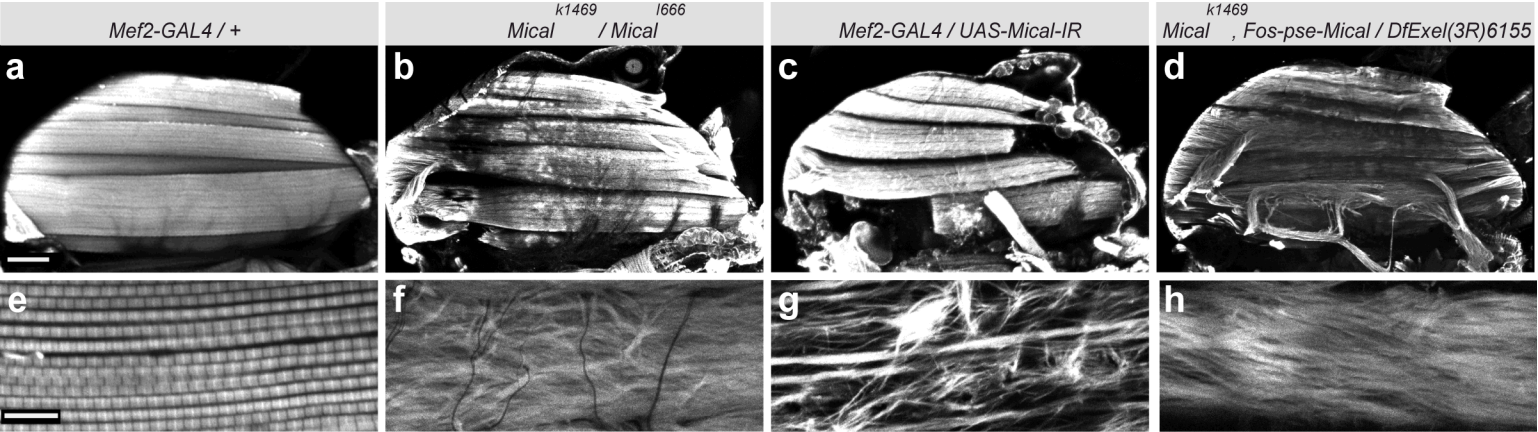
Author Contributions

Conceived and designed the experiments: FS PT. Performed the experiments: CCHL RE CS. Analyzed the data: CCHL RE CS FS PT. Contributed reagents/materials/analysis tools: FS PT. Wrote the paper: FS PT.

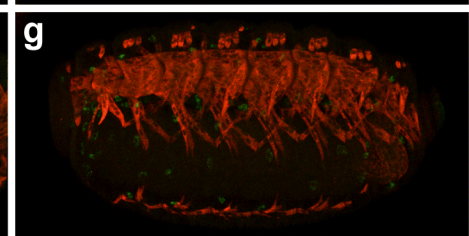
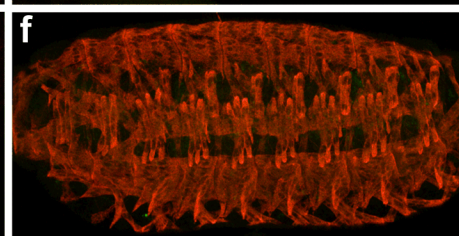
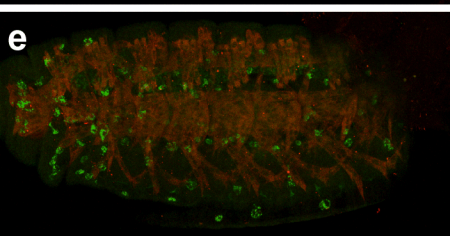
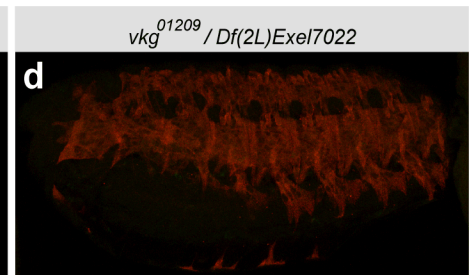
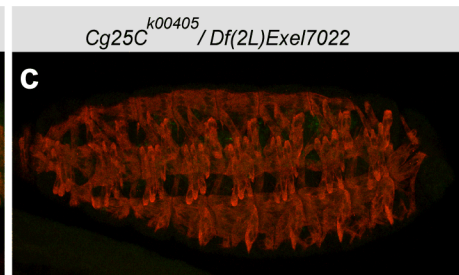
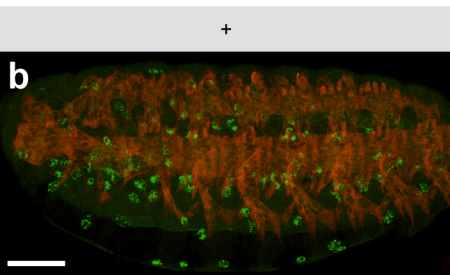
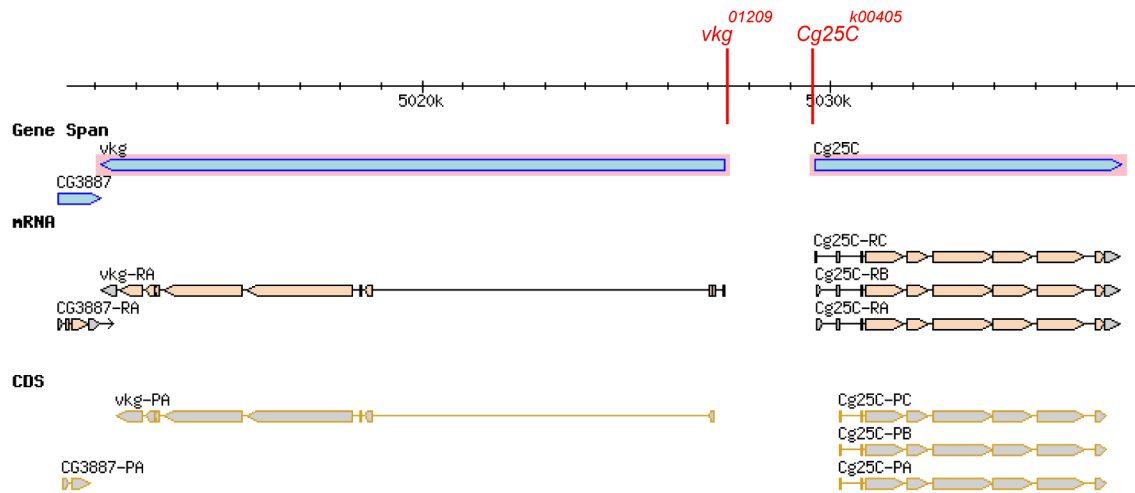
- Schmid A, Sigrist SJ (2008) Analysis of neuromuscular junctions: histology and in vivo imaging. *Methods Mol Biol* 420: 239–251.
- Burkart C, Qiu F, Brendel S, Benes V, Haag P, et al. (2007) Modular proteins from the *Drosophila* *sals* gene and their expression in muscles with different extensibility. *J Mol Biol* 367: 953–969.
- Saide JD, Chin-Bow S, Hogan-Sheldon J, Busquets-Turner L, Vigoreaux JO, et al. (1989) Characterization of components of Z-bands in the fibrillar flight muscle of *Drosophila melanogaster*. *J Cell Biol* 109: 2157–2167.
- Fessler LI, Nelson RE, Fessler JH (1994) *Drosophila* extracellular matrix. *Genes Dev* 8: 271–294.
- Schnorrer F, Kalchauer I, Dickson BJ (2007) The transmembrane protein Kon-tiki couples to Dgrip to mediate myotube targeting in *Drosophila*. *Dev Cell* 12: 751–766.
- Consortium DG, Clark AG, Eisen MB, Smith DR, Bergman CM, et al. (2007) Evolution of genes and genomes on the *Drosophila* phylogeny. *Nature* 450: 203–218.
- Stark A, Lin MF, Kheradpour P, Pedersen JS, Parts L, et al. (2007) Discovery of functional elements in 12 *Drosophila* genomes using evolutionary signatures. *Nature* 450: 219–232.
- Karolchik D, Kuhn RM, Baertsch R, Barber GP, Clawson H, et al. (2008) The UCSC Genome Browser Database: 2008 update. *Nucleic Acids Res* 36: D773–779.
- Kulkarni MM, Booker M, Silver SJ, Friedman A, Hong P, et al. (2006) Evidence of off-target effects associated with long dsRNAs in *Drosophila melanogaster* cell-based assays. *Nat Methods* 3: 833–838.
- Ma Y, Creanga A, Lum L, Beachy PA (2006) Prevalence of off-target effects in *Drosophila* RNA interference screens. *Nature* 443: 359–363.
- Perrimon N, Mathey-Prevot B (2007) Matter arising: off-targets and genome-scale RNAi screens in *Drosophila*. *Fly (Austin)* 1: 1–5.
- Markow TA, O'Grady PM (2007) *Drosophila* biology in the genomic age. *Genetics* 177: 1269–1276.
- Berghammer AJ, Klingler M, Wimmer EA (1999) A universal marker for transgenic insects. *Nature* 402: 370–371.
- Tweedie S, Ashburner M, Falls K, Leyland P, McQuilton P, et al. (2009) FlyBase: enhancing *Drosophila* Gene Ontology annotations. *Nucleic Acids Res* 37: D555–559.
- Henschel A, Buchholz F, Habermann B (2004) DEQOR: a web-based tool for the design and quality control of siRNAs. *Nucleic Acids Res* 32: W113–120.
- Alves-Silva J, Hahn I, Huber O, Mende M, Reissaus A, et al. (2008) Prominent actin fiber arrays in *Drosophila* tendon cells represent architectural elements different from stress fibers. *Mol Biol Cell* 19: 4287–4297.
- Bökel C, Prokop A, Brown NH (2005) Papillote and Piopio: *Drosophila* ZP-domain proteins required for cell adhesion to the apical extracellular matrix and microtubule organization. *J Cell Sci* 118: 633–642.
- Montanez E, Wickström S, Altstätter J, Chu H, Fässler R (2009) alpha-parvin controls vascular mural cell recruitment to vessel wall by regulating RhoA/ROCK signalling. *EMBO J*.
- Aridor M, Fish KN, Bannykh S, Weissman J, Roberts TH, et al. (2001) The Sar1 GTPase coordinates biosynthetic cargo selection with endoplasmic reticulum export site assembly. *J Cell Biol* 152: 213–229.
- Olson EN (2006) Gene regulatory networks in the evolution and development of the heart. *Science* 313: 1922–1927.
- Schulz JG, David G, Hassan BA (2009) A novel method for tissue-specific RNAi rescue in *Drosophila*. *Nucleic Acids Res* 37: e93.
- Bird AW, Hyman AA (2008) Building a spindle of the correct length in human cells requires the interaction between TPX2 and Aurora A. *J Cell Biol* 182: 289–300.
- Venken KJ, Kasprowitz J, Kuenen S, Yan J, Hassan BA, et al. (2008) Recombineering-mediated tagging of *Drosophila* genomic constructs for in vivo localization and acute protein inactivation. *Nucleic Acids Res* 36: e114.



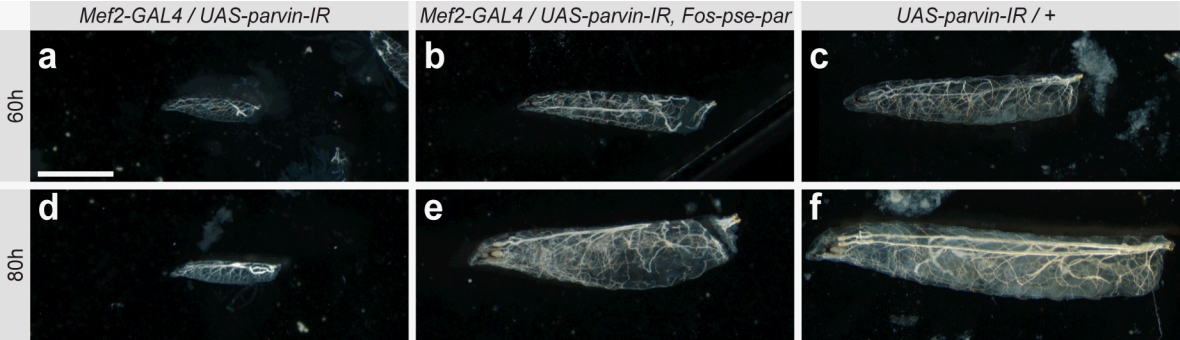
Suppl. Figure 1



Suppl. Figure 2

a

Suppl. Figure 3



Suppl. Figure 4

Publication II



Three-dimensional reconstruction and segmentation of intact *Drosophila* by ultramicroscopy

Nina Jährling^{1,2,3*}, Klaus Becker^{1,2}, Cornelia Schönbauer⁴, Frank Schnorrer⁴ and Hans-Ulrich Dodt^{1,2}

¹ Department of Bioelectronics, FKE, Vienna University of Technology, Vienna, Austria

² Bioelectronics, Center for Brain Research, Medical University of Vienna, Vienna, Austria

³ Department of Neurobiology, University of Oldenburg, Oldenburg, Germany

⁴ Max-Planck-Institute of Biochemistry, Muscle Dynamics, Martinsried, Germany

Edited by:

Randolf Menzel, Freie Universität Berlin, Germany

Reviewed by:

Jean-Christophe Sandoz, CNRS University Paul Sabatier, France

*Correspondence:

Nina Jährling, Center for Brain Research, Department of Bioelectronics, Spitalgasse 4, 1090 Vienna, Austria.
e-mail: nina.jaehrling@medunivien.ac.at

Genetic mutants are invaluable for understanding the development, physiology and behaviour of *Drosophila*. Modern molecular genetic techniques enable the rapid generation of large numbers of different mutants. To phenotype these mutants sophisticated microscopy techniques are required, ideally allowing the 3D-reconstruction of the anatomy of an adult fly from a single scan. Ultramicroscopy enables up to cm fields of view, whilst providing micron resolution. In this paper, we present ultramicroscopy reconstructions of the flight musculature, the nervous system, and the digestive tract of entire, chemically cleared, *Drosophila* in autofluorescent light. The 3D-reconstructions thus obtained verify that the anatomy of a whole fly, including the filigree spatial organization of the direct flight muscles, can be analysed from a single ultramicroscopy reconstruction. The recording procedure, including 3D-reconstruction using standard software, takes no longer than 30 min. Additionally, image segmentation, which would allow for further quantitative analysis, was performed.

Keywords: ultramicroscopy, imaging, *Drosophila*, segmentation, light sheet microscopy, morphology, phenotyping, flight muscle

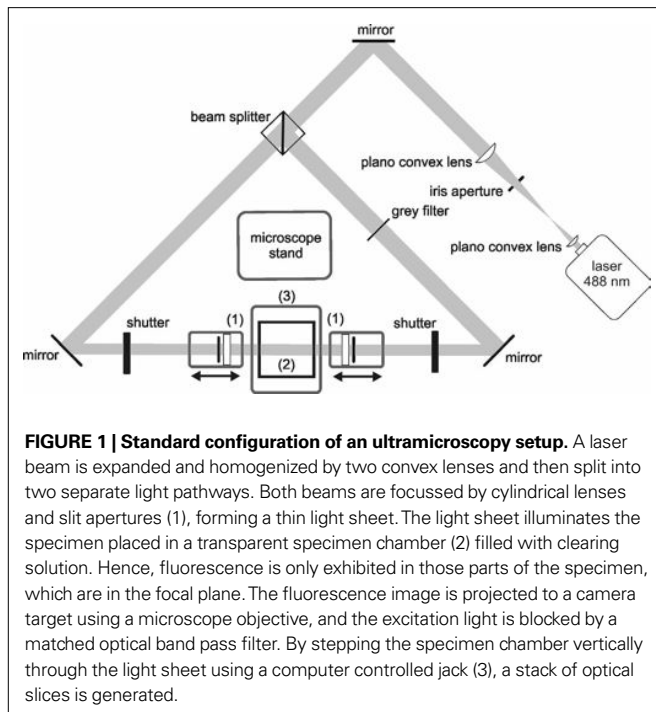
INTRODUCTION

For several decades, *Drosophila melanogaster* serves as an outstanding model organism in genetic research. Its high fecundity and its simple cultivation make *Drosophila* optimally suited for high-throughput screening of the many defined genetic aberrations generated by modern molecular biology approaches. Ideally, a microscopy device for high-throughput phenotyping of *Drosophila* mutants should allow the 3D-reconstruction of virtually the whole anatomy of a fly in a single scan taking no longer than several minutes. Standard confocal or two photon microscopes provide the required resolution, but since both work best with high magnification objectives the provided fields of view are too small to image a complete fly in a single pass. Ultramicroscopy (Figure 1) works also well with low power objectives, providing excellent spatial resolution and optical sectioning quality, comparable to confocal microscopy (Dodt et al., 2007; Jährling et al., 2008). In this paper we present 3D-reconstructions and segmentations of *Drosophila* organs obtained from an ultramicroscopy scan of an intact, chemically cleared adult fly.

A detailed anatomical atlas about the internal anatomy of *Drosophila* was first presented by Miller (1950), and later extended by Hartenstein (1993). The basic organ systems of *Drosophila* are the nervous system, the intestinal tract and the musculature. The *Drosophila*'s muscular system consists of multiple contractile fibres arranged in distinct groups or layers (Miller, 1950). In the thorax flight, jump and leg muscles are the most prominent. Flight muscles are classified into direct flight muscles (DFMs) and indirect flight muscles (IFMs), according to their functional role in wing

movement. The large IFMs of the mesothorax function as a single contractile unit, generating the main propulsion during flight (Dutta et al., 2004). They are formed by the dorsal longitudinal muscles (DLMs) consisting of six fibres, and three groups of dorsal-ventral muscles (DVM-I, DVM-II, and DVM-III) in each half of the thorax. DVM-I consists of three fibres, DVM-II and DVM-III consist of two fibres, each (Dutta et al., 2004). The largest muscle of the mesothorax is the tergal depressor of the trochanter (TDT), also called jump muscle enabling jump start of the fly (Dutta et al., 2004). Unlike the IFMs, which generate the power for the wing beat, the DFMs are responsible for adjusting the orientation of the wings during flight. They are attached to the wing base in such a way that they can generate subtle torsions of the wings, which are responsible for controlling the direction of flight. Due to their filigree structure and their complex spatial arrangement, 3D-reconstructions of the DFMs in the entire fly are challenging, demonstrating the strengths of ultramicroscopy. The central nervous system (CNS) of *Drosophila* comprises the dorsally located brain enclosed by the head capsule, the thoracico-abdominal ganglion (ThAGI), and the cervical connective (CN), which connects the brain with the ThAGI (Hartenstein, 1993). In *Drosophila* the different thoracic ganglia are merged into two bonded masses of neural tissue, no ganglia exist in the abdomen (Miller, 1950).

3D-reconstructions of chemically cleared entire *Drosophila* were performed, using the ultramicroscopy setup described in Becker et al. (2008). The obtained reconstructions give detailed insight into the anatomy of the flight musculature, the nervous system, and the intestinal tract.



MATERIALS AND METHODS

PREPARATION AND CLEARING

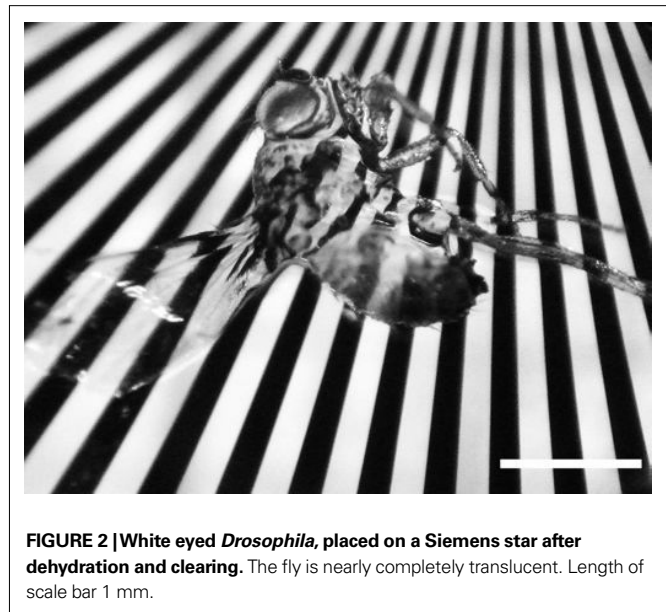
Adult white eyed *Drosophila*, *w*[1118], were killed by ether and fixed at 4°C in 4% paraformaldehyde overnight. Flies were dehydrated in a graded ethanol series (50, 70, 96, 100% for 1 h, last step overnight), and incubated in clearing solution, consisting of two parts benzyl benzoate and one part benzyl alcohol (BABB, Spalteholz, 1914) for at least 4 h, until they became almost transparent (**Figure 2**).

ULTRAMICROSCOPY

For ultramicroscopy, the setup described in Becker et al. (2008) was used. Imaging was performed by exciting autofluorescence using a 488-nm, 200 mW diode laser (Sapphire, Coherent, Germany). Images were recorded using a 10× objective (N.A. 0.3), and a CoolSnap K4 camera with 2048 × 2048 pixels (Roper Scientific, Germany).

SEGMENTATION AND 3D-RECONSTRUCTION

Manual image segmentation was performed, based on the visual shape of anatomical structures of interest. These structures were marked using an interactive pen display (Wacom Cintiq 12WX, Germany) in three orthogonal spatial orientations. The borders of the encircled structures were smoothed using a 6 × 6 Gaussian filter. The visualization software Amira 5.2 (Visage Imaging, Germany), running on a computer with two quad-core processors a 2.5-GHz, 32 GB RAM, and an FX-5800 (NVIDIA, Germany) graphic processor board, was used for all image processing.



RESULTS

An adult fly was three dimensionally reconstructed from an ultramicroscopy stack consisting of 579 images of 2048 × 2048 pixels each, and 1.66 μm vertical spacing (**Figure 3**). The surface (**Figure 3A**), the situs of various inner organs, and the musculature (**Figures 3B,D**) of the entire fly is demonstrated. **Figures 3B,C** show the six pairs of DLMs forming the IFMs. The brain and the ThAGl are well visible. The six DFM attached to the base of each wing (Ghazi et al., 2000) are easily addressed as DFM49–DFM54 (D). DFM52 can only rudimentarily be identified, because it is clipped by the viewing plane.

The raw optical sections underlying **Figure 3**, and additional virtual sections from two directions orthogonal to the recording plane were used for manual segmentation (**Figures 4A–C**). Different organs were marked in different colours. From the segmented planes we generated a 3D model and superimposed it on a digitally reconstructed radiography of the fly (**Figures 5A,B**). **Figures 5C,D** show the DLMs in dark blue. Laterally, three further groups of DVMs (DVM-I, DVM-II, DVM-II) are shown in light blue. The DFMs are coloured in yellow. The brain, the CN, and the ThAGl, being the fundamental parts of the CNS, are marked in three dissimilar green tones. Above the ThAGl parts of the intestinal system are shown in red and brown colours. The cibarium (CB) crosses the brain, leading to the oesophagus (ES), which connects to the proventriculus (PV). It is followed by the gut, and the unpaired asymmetrically located crop (CR).

DISCUSSION

We have demonstrated that ultramicroscopy allows the 3D-reconstruction of the inner anatomy of entire, cleared *Drosophila*. The time needed for a complete scan of a single

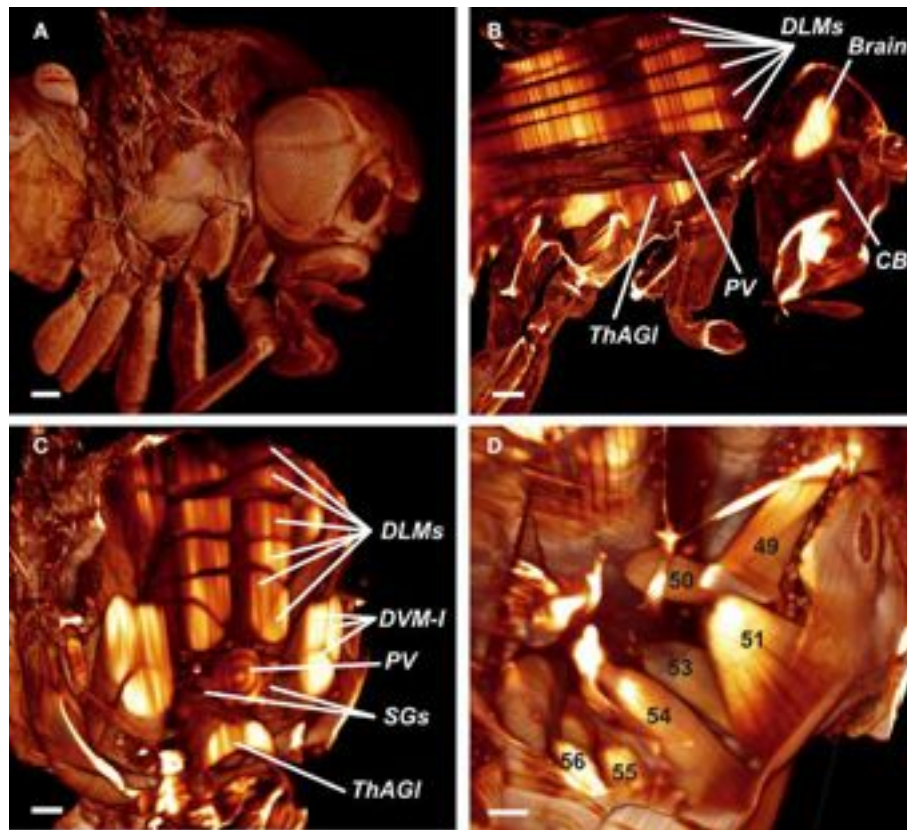


FIGURE 3 | (A) Reconstructed surface of an entire fly. Scale bar 100 μ m. **(B)** Sagittal view of the fly's inner anatomy, showing parts of the flight muscles, the nervous, and the cardiac system. DLMs, dorso longitudinal muscles; ThAGI, thoracico-abdominal ganglion; PV, proventriculus; CB, cibarium. Scale bar: 100 μ m.

(C) Detail of the fly virtually sectioned along a transversal plane through the thorax. DVM-I, dorsal-ventral muscles; SGs, salivary glands. Scale bar: 100 μ m. **(D)** Detail showing the direct flight muscles DFM49–DFM56. DFM52 is only rudimentarily visible, because it is clipped by the viewing plane. Scale bar 40 μ m.

fly, including 3D-reconstruction using Amira, is below 30 min. As mechanical slicing of the specimen is avoided, artefacts, such as tissue disruptions or dislocations due to the microtome knife do not occur. 3D-reconstructions of entire cleared *Drosophila* have previously been performed by McGurk et al. (2007) using optical projection tomography (OPT), mainly focussing on the IFMs. Our method not only provides a much more detailed 3D-reconstruction of the IFMs and the TDT, but also highlights the organization of the DFMs. The filigree muscles DFM49 up to DFM54 can be clearly visualized. Ultramicroscopy allows resolutions of $<10 \mu$ m, and can resolve structures down to the size of single dendritic spines (Dodt et al., 2007). By combining ultramicroscopy with GFP expression (Dodt et al., 2007), immunolabeling (Jährling et al., 2008), or lectin-staining (Jährling et al., 2009) morphological structures not visible by observations in autofluorescent light can be visualized. The instrumentation effort for an ultramicroscopy setup is moderate. Standard software developed for confocal microscopy can be used for 3D-reconstruction.

Ultramicroscopy data can be segmented for further analysis with respect to various anatomical structures. We presented segmentations of the major parts of the nervous system, the musculature and the intestinal tract. While such segmentations on a manual basis presently still are relatively costly in terms of labour, future developments in the field of computational bioimage processing may allow a semi-automatic processing of anatomical structures of interest. A promising approach in this field may be model based segmentation algorithms, which contain some integrated 'knowledge' about the general geometry of various anatomical structures and their variability (Peng, 2009; Heimann and Meinzer, 2009).

Drosophila is an important model organism for studying the function of genes linked to neuro-degenerative diseases and how these mutations lead to dysfunction (Lu and Vogel, 2009). Recent development of RNAi libraries allows now the systematic, genome-wide analysis of tissue morphogenesis (Dietzl et al., 2007). Since these questions are now in the focus of current molecular genetic research, ultramicroscopy may become important as an appropriate tool for rapid scanning of experimentally generated fly mutants.

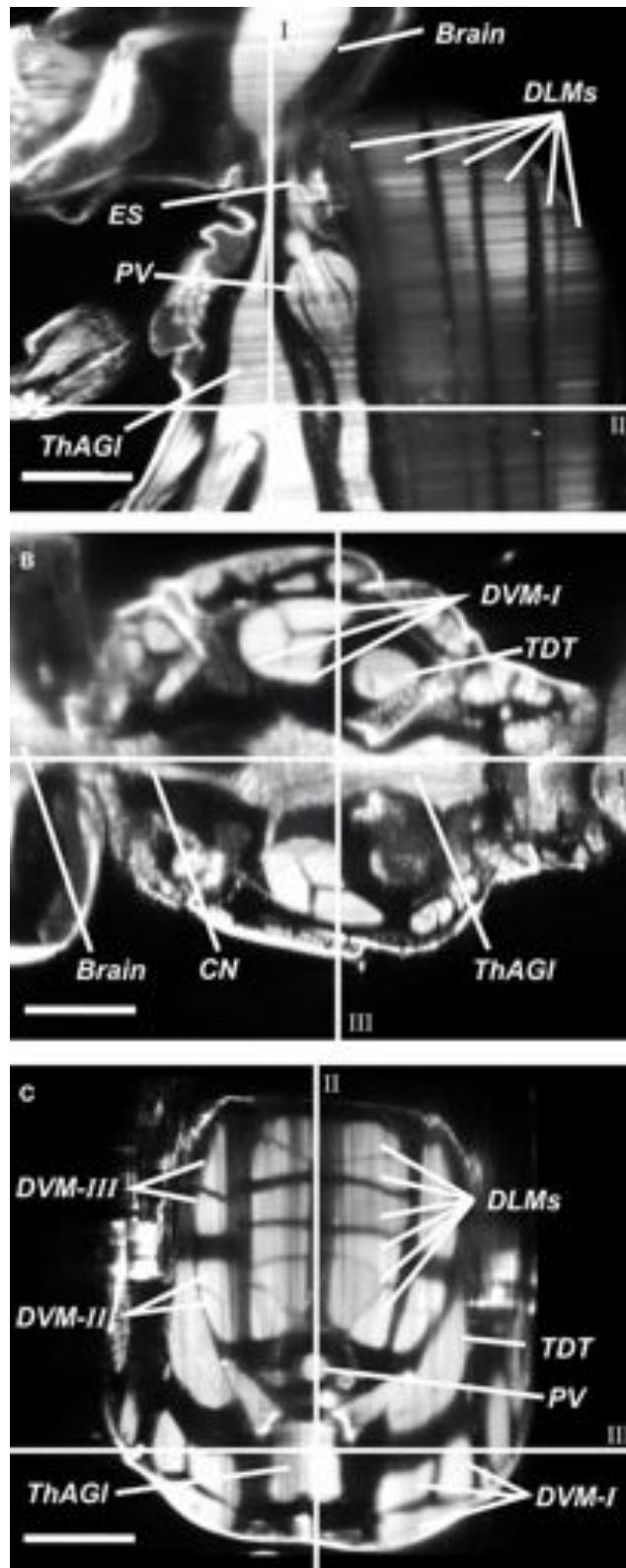


FIGURE 4 | Cross sections in three orthogonal directions (A–C) were used to segment anatomical structures in three different orientations.

ES, oesophagus; CN, cervical connective; DLMs, dorsal longitudinal muscles; DVM-I/II/III, dorsal–ventral muscles; PV, proventriculus; TDT, tergal depressor

of the trochanter; ThAGI, thoracico-abdominal ganglion. I: Sagittal plane, II: transversal plane, III: coronal plane. **(A)** Sagittal optical slice.

(B) Computed coronal slice. **(C)** Computed transversal slice. Length of scale bars 100 μ m.

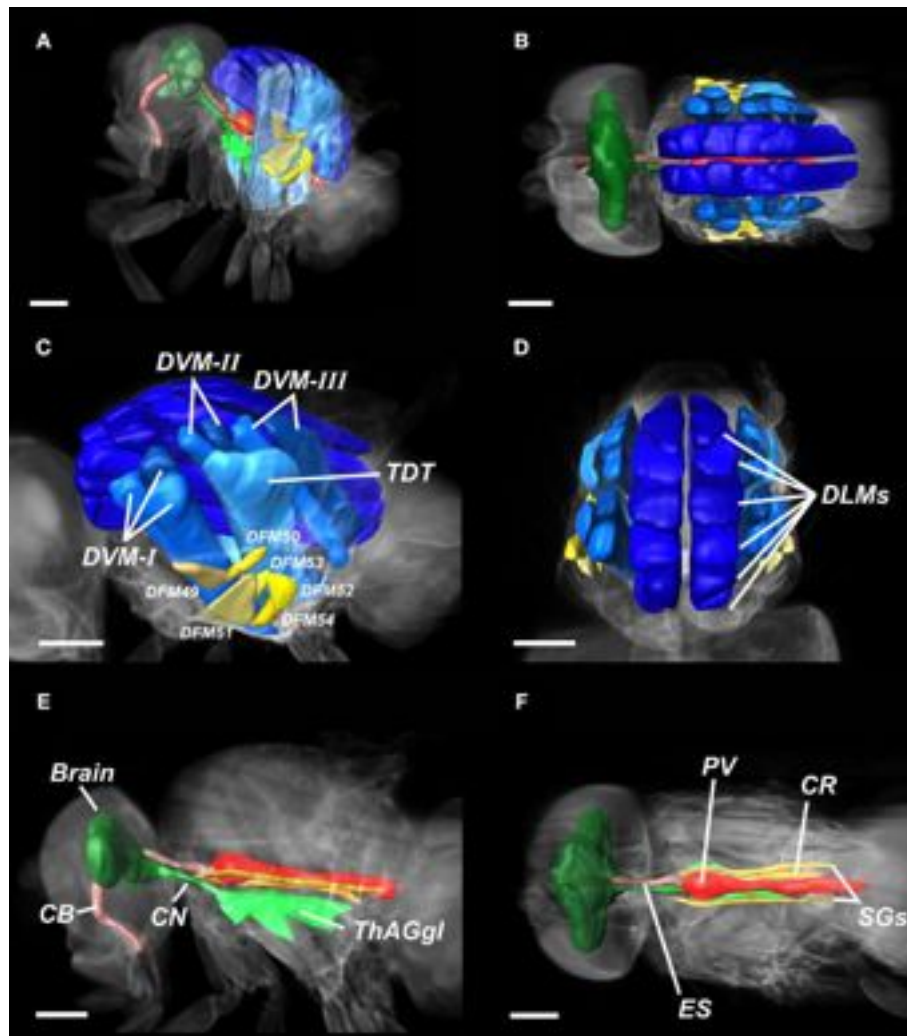


FIGURE 5 | Segmentation of *Drosophila* organs. (A,B) Overview of the entire fly, illustrating major components of the nervous system, the intestinal tract, and the musculature. **(C,D)** Detail of the flight musculature. DLM, dorsal longitudinal muscles (dark-blue); DVM-I/II/III, dorsal-ventral muscles (blue); DFM49–DFM54, direct flight muscles (yellow); TDT, tergal depressor of the

trochanter (light-blue). **(E-F)** Detail of the CNS and the intestinal system. Brain (dark green), CN, cervical connective (green); ThAGl, thoraco-abdominal ganglion, (light-green); CB, cibarium (light-rose); ES, oesophagus (rose); PV, proventriculus (red); SGs, pair of salivary glands (brown); CR, crop (orange). Length of scale bar 200 μ m.

ACKNOWLEDGMENTS

We thank T. K. Stackhouse for carefully reading this manuscript. This study was supported by SFB391, the Hertie Foundation and the Max-Planck Society.

SUPPLEMENTARY MATERIAL

The Supplementary Material for this article can be found online at <http://www.frontiersin.org/systemsneuroscience/paper/10.3389/neuro.06/001.2010/>

REFERENCES

Becker, K., Jährling, N., Kramer, E. R., Schnorrer, F., and Dodt, H.-U. (2008). Ultramicroscopy: 3D-reconstruction of large microscopic specimens. *J. Biophoton.* 1, 36–42.

Dietzl, G., Chen, D., Schnorrer, F., Su, K.-C., Barinova, Y., Fellner, M., Gasser, B., Kinsey, K., Oppel, S., Scheiblauer, S., Couto, A., Marra, V., Keleman, K., and

Dickson, B. J. (2007). A genome-wide transgenic RNAi library for conditional gene inactivation in *Drosophila*. *Nature* 448, 151–156

Dodt, H.-U., Leischner, U., Schierloh, A., Jährling, N., Mauch, C.P., Deininger, K., Deusing, J.M., Eder, M., Zieglgänsberger, W., and Becker, K. (2007). Ultramicroscopy: three-dimensional visualization of neural networks in the whole mouse brain. *Nat. Methods* 4, 331–336.

Dutta, D., Anant, S., Ruiz-Gomez, M., Bate, M., and VijayRaghavan, K. (2004). Founder myoblasts and fibre number during myogenesis in *Drosophila*. *Development* 131, 3761–3772.

Ghazi, A., Anant, S., and VijayRaghavan, K. (2000). Apterous mediates development of direct muscles autonomously and indirect flight muscles through epidermal cues. *Development* 127, 5309–5318.

Hartenstein, V. (1993). *Atlas of Drosophila*. Development. New York, Cold Spring Harbor Laboratory Press.

Heimann, T., and Meinzer, H.-P. (2009). Statistical shape models for 3D medical image segmentation: a review. *Med. Image Anal.* 13, 543–563.

- Jährling, N., Becker, K., and Dodt, H.-U. (2009). 3D-reconstruction of blood vessels by ultramicroscopy. *Organogenesis* 5, 227–230.
- Jährling, N., Becker, K., Kramer, E. R., and Dodt, H.-U. (2008). 3D-visualization of nerve fiber bundles by ultramicroscopy. *Med. Laser Appl.* 23, 209–215.
- Lu, B., and Vogel, H. (2009). *Drosophila* models of neurodegenerative diseases. *Annu. Rev. Pathol. Mech. Dis.* 4, 315–342.
- McGurk, L., Morrison, H., Keegan, L. P., Sharpe, J., and O'Connell, M. A. (2007). Three-dimensional imaging of *Drosophila melanogaster*. *PLoS ONE* 2, e834. doi: 10.1371/journal.pone.0000834.
- Miller, A. (1950). The internal anatomy and histology of the imago of *Drosophila melanogaster*. In *Biology of Drosophila*, M. Demerec, ed. (New York, Wiley), pp. 420–534.
- Peng, H. (2009). Bioimage informatics: a new area engineering biology. *Bioinformatics* 24, 1827–1836.
- Spalteholz, W. (1914). Über das Durchsichtigmachen von menschlichen und tierischen Präparaten. Leipzig, S. Hirzel.
- Conflict of Interest Statement:** The authors declare that the research was conducted in the absence of any commercial or financial relationships that could be construed as a potential conflict of interest.
- Received: 04 September 2009; paper pending published: 29 October 2009; accepted: 13 January 2010; published online: 08 February 2010.
- Citation: Jährling N, Becker K, Schönbauer C, Schnorrer F and Dodt H-U (2010) Three-dimensional reconstruction and segmentation of intact *Drosophila* by ultramicroscopy. *Front. Syst. Neurosci.* 4:1. doi: 10.3389/neuro.06.001.2010
- Copyright © 2010 Jährling, Becker, Schönbauer, Schnorrer and Dodt. This is an open-access article subject to an exclusive license agreement between the authors and the Frontiers Research Foundation, which permits unrestricted use, distribution, and reproduction in any medium, provided the original authors and source are credited.

Publication III

Systematic genetic analysis of muscle morphogenesis and function in *Drosophila*

Frank Schnorrer^{1,2}, Cornelia Schönbauer¹, Christoph C. H. Langer¹, Georg Dietzl², Maria Novatchkova², Katharina Schernhuber², Michaela Fellner², Anna Azaryan², Martin Radolf², Alexander Stark², Krystyna Keleman² & Barry J. Dickson²

Systematic genetic approaches have provided deep insight into the molecular and cellular mechanisms that operate in simple unicellular organisms. For multicellular organisms, however, the pleiotropy of gene function has largely restricted such approaches to the study of early embryogenesis. With the availability of genome-wide transgenic RNA interference (RNAi) libraries in *Drosophila*^{1,2}, it is now possible to perform a systematic genetic dissection of any cell or tissue type at any stage of the lifespan. Here we apply these methods to define the genetic basis for formation and function of the *Drosophila* muscle. We identify a role in muscle for 2,785 genes, many of which we assign to specific functions in the organization of muscles, myofibrils or sarcomeres. Many of these genes are phylogenetically conserved, including genes implicated in mammalian sarcomere organization and human muscle diseases.

Muscle biology is an attractive target for analysis by genome-wide transgenic RNAi. The basic cell and developmental biology of muscles is largely conserved from insects to mammals^{3–6}, and their multinuclear architecture renders them inaccessible to conventional genetic mosaic strategies. To systematically disrupt gene functions exclusively in the muscles of intact animals, we crossed the muscle-specific *Mef2-GAL4* driver to each of the *UAS-IR* transgenic RNAi lines in our genome-wide library¹. Progeny from these crosses were assayed for viability, posture, locomotion and flight. We screened a total of 17,759 RNAi lines, representing 10,461 distinct genes. A total of 3,909 lines and 2,785 genes were scored as defective in one or more of these assays (Fig. 1, Supplementary Fig. 1 and Supplementary Tables 1 and 2).

This screen identified 73 of 77 positive control genes (Supplementary Table 3), suggesting a false-negative rate of just 5%. To assess the false-positive rate, we compiled a negative control list of 79 genes shown by classical genetic studies to have no function in muscles. Of the 121 RNAi lines available for these genes, only one scored positive in our assays (Supplementary Table 4). We thus estimate that our screen has a false-positive rate of 1.3% of genes (a false-discovery rate of 5%).

We selected 1,004 of the positive genes at random for validation using a second, independent hairpin construct. These lines were obtained from a second RNAi library currently under construction using the phiC31 site-specific integrase system (K.K. and B.J.D., unpublished observations). A total of 874 genes (87.1%) were again positive (Supplementary Table 5), consistent with the estimated 5% false-discovery rate in our primary screen and a false-negative rate comparable to that observed with the first library (~5%).

We began the detailed analysis of these muscle phenotypes by examining the morphology of the larval body wall muscles (Supplementary Fig. 1). Reasoning that defects in these muscles are most likely to result in embryonic or larval lethality, we focused on the 436 genes that fell into these phenotypic classes in the primary

screen (excluding for technical reasons those lines that were not viable as homozygotes). For each of these lines, muscle organization was visualized in live animals using a green fluorescent protein (GFP) marker that specifically labels the sarcomeric Z-line⁷. Defects were readily observed for 190 genes, either in overall muscle morphology (Fig. 2a and Supplementary Table 6) or sarcomeric organization (Fig. 2b and Supplementary Table 7).

We distinguished three classes of defect in muscle morphology (Fig. 2c–k): ‘split myofibril’ (53 genes), ‘missing muscles’ (8 genes) and ‘rounded muscles’ (13 genes), in which muscles are either split into thinner myofibrils, are missing or have the rounded appearance characteristic of muscles that undergo normal morphogenesis but fail to form stable attachments. The ‘split myofibril’ class includes several signalling molecules, such as the FGF receptor *heartless*, *Anxb11*, the actin regulator α -*actinin* and several RNA-binding proteins (for example, *CG5800*; Fig. 2g). In these mutants, the muscles still generally attach to the appropriate tendon cells. The ‘missing muscles’ class includes splicing factors and *His2A* (Fig. 2f). The ‘rounded muscles’ class includes known muscle attachment factors such as integrins, ILK

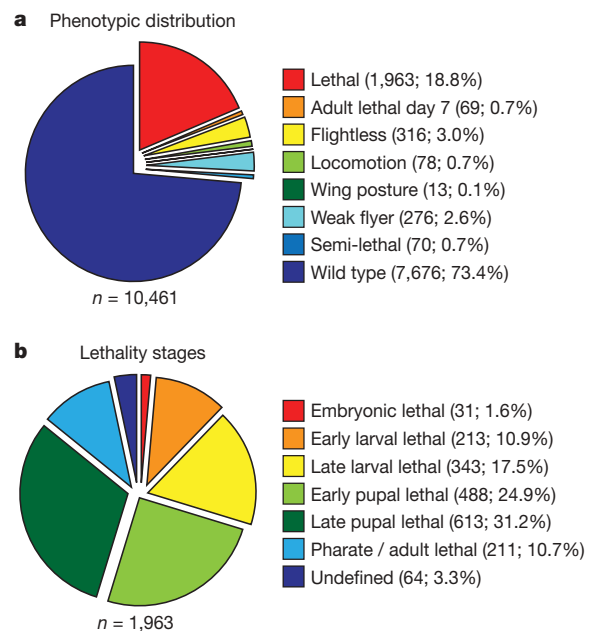


Figure 1 | Phenotypic classification of primary screen. a, Distribution of genes into phenotypic classes in the primary muscle screen. **b**, Distribution of the lethality stages for all essential genes.

¹Max-Planck-Institute of Biochemistry, Am Klopferspitz 18, 82152 Martinsried, Germany. ²Research Institute of Molecular Pathology (IMP), Dr. Bohr-Gasse 7, A-1030 Vienna, Austria.

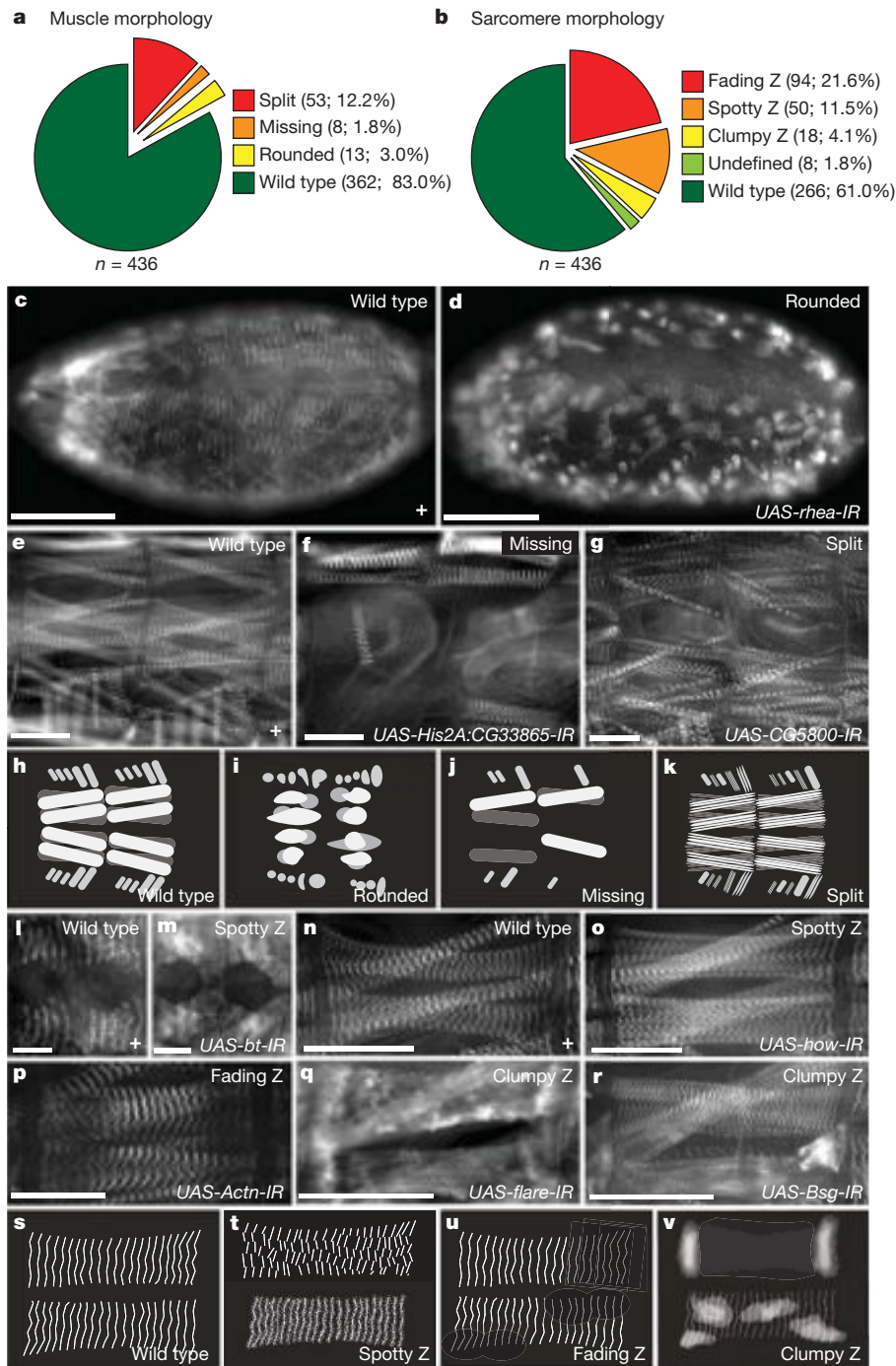


Figure 2 | Larval muscle screen. **a, b**, Muscle (**a**) and sarcomere (**b**) morphology classes of the larval body muscles. **c–k**, Wild-type and mutant phenotypes: normal muscles in wild-type embryos (**c, h**) compared with rounded muscles in *UAS-rhea-IR* (TF40400) (**d, i**), wild-type L3 larval muscles (**e**), missing muscles in *UAS-CG33865-IR* (TF39116) (**f, j**) and split muscles in *UAS-CG5800* (TF27519) (**g, k**). **l–r**, Sarcomere morphology

and *rhea*, the fly Talin orthologue (Fig. 2d), as well as the fly Parvin orthologue.

We also defined three classes of defect in sarcomeric organization (Fig. 2l–v): ‘fading Z’ (94 genes), ‘spotty Z’ (50 genes) and ‘clumpy Z’ (18 genes), in which the Z-lines are either reduced, discontinuous or appear as large irregular aggregates, respectively. The ‘fading Z’ class is exemplified by α -actinin (*Actn*; Fig. 2p), and the ‘spotty Z’ class by *how* (Fig. 2o), which encodes an RNA-binding protein required for muscle development⁸, and *bent* (Fig. 2m), which encodes a titin- or projectin-like protein⁹. Most of the known sarcomeric components (*bt*, *sls*, *Mhc*, actin, *Tm2*, *TpnC47D*, and *TpnC73F*) fell into the spotty

phenotypes: wild-type embryonic sarcomeres (**l, s**) compared with *UAS-bt-IR* (TF46253) displaying spotty Z sarcomeres (**m, t**), and wild-type L3 sarcomeres (**n**) compared with spotty Z in *UAS-how-IR* (TF13756) (**o**), fading Z in *UAS-Actn-IR* (TF7760) (**p, u**), and clumpy Z in *UAS-flare* (TF22851) (**q, v**) and *UAS-Bsg-IR* (TF43307) (**r**). Scale bars, 100 μ m (**c, d**) and 50 μ m (**e–g, i–r**).

Z class. The ‘clumpy Z’ class includes *flare* (CG10724), the recently identified fly orthologue of actin interacting protein 1 (AIP1), a regulator of F-actin disassembly¹⁰ and *Basigin* (*Bsg*), a muscle transmembrane protein required for formation of the neuromuscular junction¹¹ (Fig. 2q, r). We confirmed efficient knockdown of several of these proteins by antibody staining (Supplementary Fig. 2).

We performed a similar analysis of muscle morphology in adults, using phalloidin staining to visualize the indirect flight muscles (IFMs) for all RNAi lines that scored as flightless in the primary screen (Supplementary Fig. 1 and Fig. 1a). The large regular structure of the IFMs and their critical role in flight make them ideal models for

studying muscle structure and function^{12,13}. Moreover, unlike the larval body wall muscles, IFMs resemble vertebrate muscles in their construction from multiple fibres, each composed of many myofibrils¹⁴. Defects in IFMs were observed in 196 of the 328 flightless genes tested. We assigned each of these genes to one or more of nine distinct phenotypic categories, based on defects in overall muscle morphology (Fig. 3a and Supplementary Table 8), myofibril morphology (Fig. 3b and Supplementary Table 9) or sarcomeric organization (Fig. 3c and Supplementary Table 10).

The two classes of defect in overall IFM morphology were ‘missing IFMs’ (55 genes) and ‘irregular IFMs’ (12 genes). The ‘missing IFM’ class includes *parkin* (*park*) and *flightin* (*fln*) (Fig. 3e), both previously associated with IFM degeneration^{15,16}, as well as several transcription factors that may contribute to the specification of individual muscles (Supplementary Table 8). The ‘irregular IFM’ class includes *flightless I* (*flii*; Fig. 3f, g) and MICAL, which serve as positive controls^{17,18}, as well as *CG8578*, the mouse orthologue of which (LRRFIP2) interacts with the leucine-rich repeats of mouse *Flii*¹⁹.

We defined four classes of myofibril defect: ‘degenerate’ (39 genes), ‘irregular’ (7 genes), ‘frayed’ (97 genes) and ‘trapezoid’ (29 genes). Most genes in the ‘degenerate’ myofibril class were also classified as ‘missing IFMs’. Distinct myofibrils are difficult to discern in these lines, as is observed upon knockdown of the band 4.1 septate junction protein encoded by *coracle*²⁰ (Fig. 3l). The ‘irregular’ myofibril class is characterized by misoriented and disorganized myofibrils, as seen with *flii* (Fig. 3j) and Supplementary Fig. 3) or its interactor *CG8578* (Fig. 3o).

of which are severely disrupted upon knockdown of *flii* or *CG8578* (Fig. 3o and Supplementary Fig. 3a, b), and in *flii* mutants (Fig. 3n). In the ‘frayed’ class, myofibrils are unusually thin and often frayed at the edges, as for example upon knockdown of the actin regulator *coronin* (Fig. 3i), and the M- and Z-lines are also thinner and appear bent at the frayed edges of the myofibril (Supplementary Fig. 4d). The ‘trapezoid’ class is characterized by myofibrils with a zigzag-like structure, usually with thick Z-lines and thinner actin filaments towards the M-lines. One gene in this class is the adducin homologue *hts* (Fig. 3k and Supplementary Fig. 4f, g). For 49 genes, mostly of the ‘trapezoid’ and ‘frayed’ classes, we also observed large actin aggregates (Fig. 3m and Supplementary Table 9) that are reminiscent of so-called zebra bodies²¹, possibly collapsed Z-lines, that are commonly observed in human nemaline myopathies²².

Three further phenotypic classes were based on sarcomere organization: ‘no sarcomere’ (39 genes), ‘no M’ (12 genes) and ‘fuzzy Z’ (99 genes). The ‘no sarcomere’ set generally coincides with the degenerate myofibril and missing IFM classes (Fig. 3s, w and Supplementary Fig. 3e). The ‘no M’ class is characterized by sarcomeres with an apparently normal Z-line, but no discernable M-line in phalloidin stainings (Fig. 3q, u). This is seen upon knockdown of the obscurin homologue *unc-89* (Fig. 3q), and in *unc-89* mutants (B. Bullard, personal communication). Staining *unc-89* knockdown IFMs with the M-line marker anti-Mhc revealed that the M-line is indeed present, but is significantly broadened and invaded by thin actin filaments (Supplementary Fig. 5a, b). Knockdown of the potassium channel *eag* leads to a more severe M-line phenotype with complete absence of

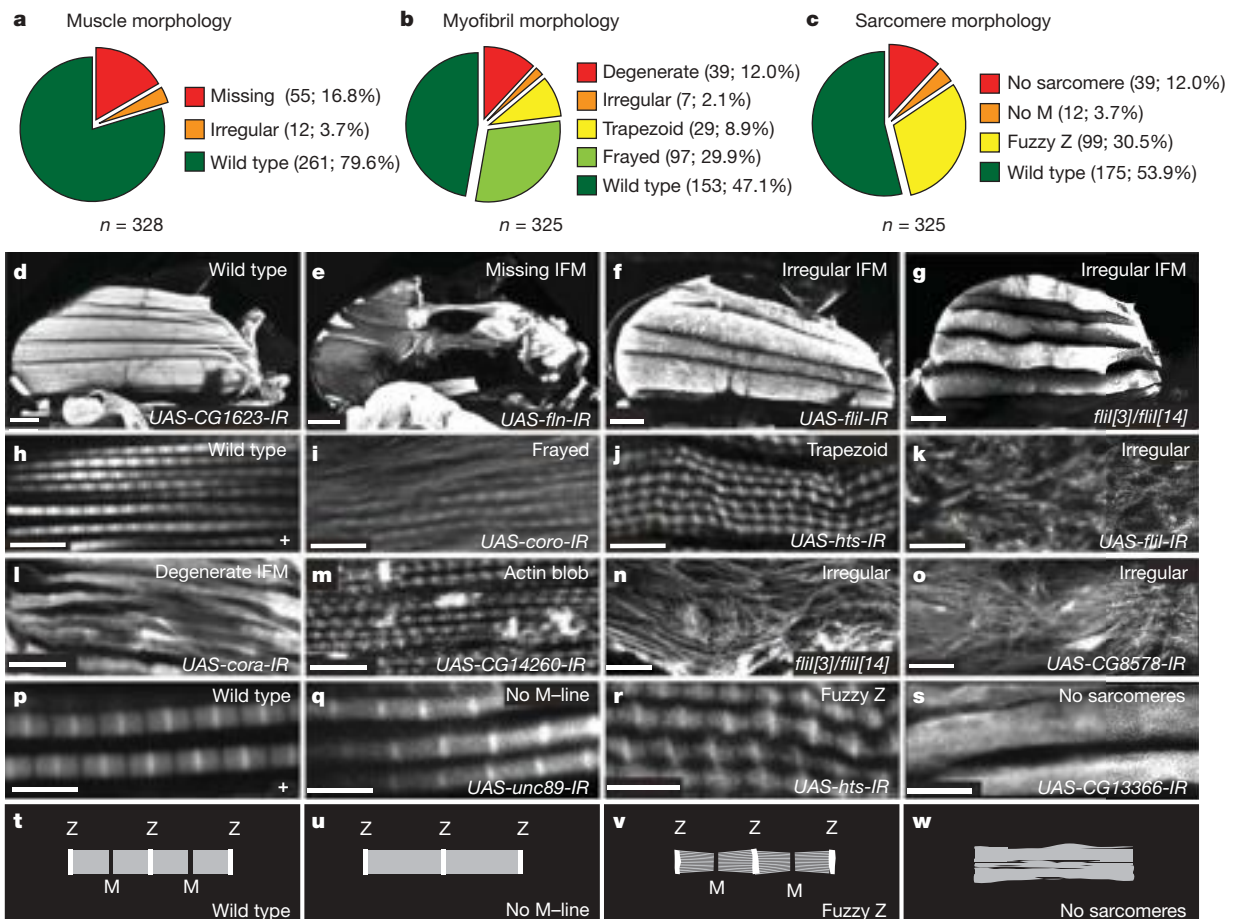


Figure 3 | Adult muscle screen. **a–c**, Distribution of muscle (**a**), myofibril (**b**) and sarcomere (**c**) morphology of the adult IFMs. **d–g**, Normal IFMs in wild type (**d**), missing IFMs in *UAS-fln-IR* (TF46153) (**e**), irregular IFMs in *UAS-flii-IR* (TF39528) (**f**) and *flii* mutant (**g**). **h–o**, Normal myofibril morphology in wild type (**h**), frayed in *UAS-coro-IR* (TF44671) (**i**), trapezoid in *UAS-hts-IR* (29101) (**j**), irregular in *UAS-flii-IR* (TF39528) (**k**), *flii*

mutants (**n**) and *UAS-CG8578-IR* (TF35968) (**o**), degenerated IFMs in *UAS-cora-IR* (TF9787) (**l**) and actin blobs in *UAS-CG14260* (TF17452) (**m**). **p–w**, Normal sarcomere morphology in wild type (**p**), no visible M-line in *UAS-unc89-IR* (TF29412) (**q**), fuzzy Z in *UAS-hts-IR* (TF29101) (**r**) and no sarcomeres in *UAS-CG13366* (TF29606) (**s**), and the respective schematics (**t–w**). Scale bars, 100 μ m (**d–g**), 10 μ m (**h–o**), 5 μ m (**p–s**).

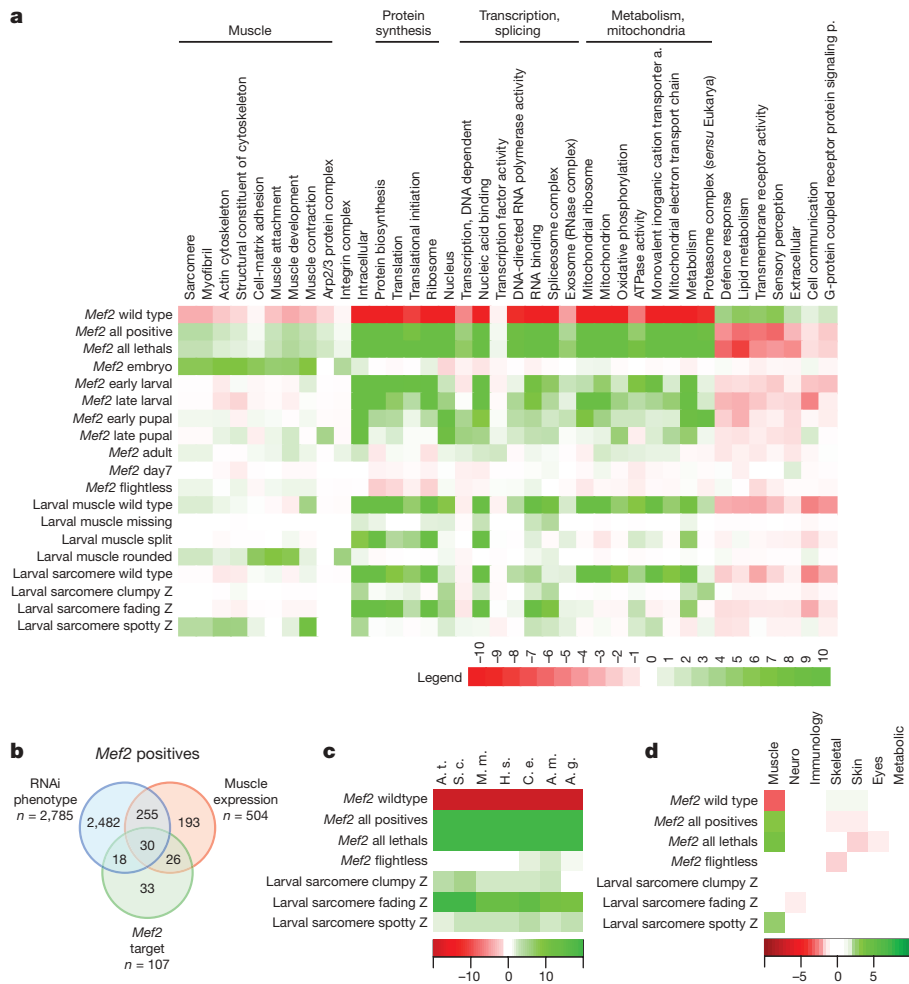


Figure 4 | Bioinformatic analyses. **a**, GO-term enrichment in the various phenotypic classes. **b**, Overlap of genes expressed in muscles, predicted *Mef2* targets and positives in the *Mef2* RNAi screen. Only genes tested in the RNAi screen are included ($n = 10,460$ for *Mef2*), and only *Mef2* high-confidence targets for which expression data were available are included ($n = 107$).

Mhc at the M-line (Supplementary Fig. 5c). This may explain why *eag* mutants display severe flight defects²³. Surprisingly, we find upon knockdown of the Par domain transcription factor *pdp1* an overlap of Z- and M-lines (Supplementary Fig. 5d), suggesting that mesodermal *pdp1* (ref. 24) regulates correct sarcomere assembly. The ‘fuzzy Z’ class is characterized by a broadening of the Z-line (Fig. 3r, v), and generally coincides with the frayed and trapezoidal classes of myofibril defect. We analysed RNA levels in isolated flight muscles for selected genes of the ‘irregular’ myofibril class and the ‘no M’ class. This analysis confirmed a significant knockdown of the target messenger RNA. In contrast, mRNA levels of predicted off-target genes (defined as having at least one perfect 16 nucleotide match to the hairpin) were not altered any more than mRNA levels of other randomly selected genes (Supplementary Fig. 6).

We examined the gene ontology (GO) database (www.geneontology.org) to assess the representation of various gene classes in each of our phenotypic categories (Fig. 4a). GO terms related to muscles are all significantly enriched in the set of *Mef2*-positive genes, particularly in the embryonic lethals. We also note an enrichment of the GO terms ‘muscle attachment’ and ‘cell-matrix adhesion’ in the ‘rounded’ phenotype class, consistent with the failure to form a stable muscle attachment in these lines. Another noticeable enrichment is the GO term ‘muscle contraction’ within the ‘spotty Z’ class of sarcomeric defects, suggesting that the actin defects in these lines correlate with impaired contractility.

c, d, Conservation across species (**c**) and link to clinical diseases (**d**) in *Mef2* lethal as well as the sarcomere phenotypic sets. A. t., *Arabidopsis thaliana*; S. c., *Saccharomyces cerevisiae*; M. m., *Mus musculus*; H. s., *Homo sapiens*; C. e., *Caenorhabditis elegans*; A. m., *Apis mellifera*; A. g., *Anopheles gambiae*.

Previous studies have sought to identify muscle genes systematically either by expression profiling (<http://www.fruitfly.org/cgi-bin/ex/insitu.pl>) or chromatin immunoprecipitation of *Mef2*-binding sites²⁵, both of which have been focused on embryos. More than half of the muscle-expressed genes (285 of 504, $P < 10^{-47}$, Fig. 4b) and almost half of the *Mef2* targets (48 of 107, $P < 10^{-4}$, Fig. 4b) were functionally validated in our screen. A total of 30 genes are positive in all three data sets, representing a set of *Mef2* target genes with confirmed muscle expression and function (Supplementary Table 11). Almost half of these had no functional assignment before this study. Similar large-scale gene expression and *Mef2* target data are not yet available for later developmental stages, but we note that our RNAi screen has assigned functions to 10 of 12 genes known to be differentially expressed in adult muscle precursors²⁶ (Supplementary Table 11), and to 10 of 14 genes predicted to function in terminally differentiated muscle²⁷ (Supplementary Table 12).

Finally, we found that the genes with a muscle RNAi phenotype are, on average, much better conserved than those with no phenotype (Fig. 4c). Moreover, examination of the OMIM database (<http://www.ncbi.nlm.nih.gov/omim>) revealed that these conserved genes are enriched for genes implicated in human muscle diseases, but not diseases that affect other tissues (Fig. 4d). Thus, our work not only lays a foundation for a comprehensive analysis of muscle biology in *Drosophila*, but also for the systematic analysis of gene function in vertebrate muscles.

METHODS SUMMARY

All RNAi crosses to *Mef2-GAL4* were performed at 27 °C and males were assayed at day 7 of adult life blind to the genotype. Positives were also retested blind, along with previously untested lines in the primary screen. Where multiple RNAi lines for the same gene resulted in different phenotypes, the gene was assigned the strongest of these phenotypes. Larval muscles were visualized with *ZCCL0663*, a GFP trap in *CG6416* labelling the Z-line²; adult flight muscles were bisected and stained with phalloidin.

Received 14 January; accepted 30 December 2009.

- Dietzl, G. *et al.* A genome-wide transgenic RNAi library for conditional gene inactivation in *Drosophila*. *Nature* **448**, 151–156 (2007).
- Matsumoto, A. *et al.* A functional genomics strategy reveals clockwork orange as a transcriptional regulator in the *Drosophila* circadian clock. *Genes Dev.* **21**, 1687–1700 (2007).
- Schnorrer, F. & Dickson, B. J. Muscle building; mechanisms of myotube guidance and attachment site selection. *Dev. Cell* **7**, 9–20 (2004).
- Hartenstein, V. in *Muscle Development in Drosophila* (ed. Sink, H.) 8–27 (Landes Biosciences, 2006).
- Taylor, M. V. in *Muscle Development in Drosophila* (ed. Sink, H.) 169–203 (Landes Biosciences, 2006).
- Buckingham, M. Myogenic progenitor cells and skeletal myogenesis in vertebrates. *Curr. Opin. Genet. Dev.* **16**, 525–532 (2006).
- Quinones-Coello, A. T. *et al.* Exploring strategies for protein trapping in *Drosophila*. *Genetics* **175**, 1089–1104 (2007).
- Zaffran, S., Astier, M., Gratecos, D. & Semeriva, M. The held out wings (how) *Drosophila* gene encodes a putative RNA-binding protein involved in the control of muscular and cardiac activity. *Development* **124**, 2087–2098 (1997).
- Ayme-Southgate, A., Vigoreaux, J., Benian, G. & Pardue, M. L. *Drosophila* has a twitchin/titin-related gene that appears to encode projectin. *Proc. Natl Acad. Sci. USA* **88**, 7973–7977 (1991).
- Ren, N., Charlton, J. & Adler, P. N. The *flare* gene, which encodes the AIP1 protein of *Drosophila*, functions to regulate F-actin disassembly in pupal epidermal cells. *Genetics* **176**, 2223–2234 (2007).
- Besse, F. *et al.* The Ig cell adhesion molecule Basigin controls compartmentalization and vesicle release at *Drosophila melanogaster* synapses. *J. Cell Biol.* **177**, 843–855 (2007).
- Vigoreaux, J. O. in *Muscle Development in Drosophila* (ed. Sink, H.) 143–156 (Landes Biosciences, 2006).
- Vigoreaux, J. O. Genetics of the *Drosophila* flight muscle myofibril: a window into the biology of complex systems. *Bioessays* **23**, 1047–1063 (2001).
- Bate, M. in *The development of Drosophila melanogaster*, Vol. 2 (eds Bate, M. & Martinez-Arias, A.) 1013–1090 (Cold Spring Harbor Press, 1993).
- Park, J. *et al.* Mitochondrial dysfunction in *Drosophila* PINK1 mutants is complemented by parkin. *Nature* **441**, 1157–1161 (2006).
- Reedy, M. C., Bullard, B. & Vigoreaux, J. O. Flightin is essential for thick filament assembly and sarcomere stability in *Drosophila* flight muscles. *J. Cell Biol.* **151**, 1483–1500 (2000).
- Campbell, H. D. *et al.* The *Drosophila melanogaster flightless-I* gene involved in gastrulation and muscle degeneration encodes gelsolin-like and leucine-rich repeat domains and is conserved in *Caenorhabditis elegans* and humans. *Proc. Natl Acad. Sci. USA* **90**, 11386–11390 (1993).
- Beuchle, D., Schwarz, H., Langegger, M., Koch, I. & Aberle, H. *Drosophila* MICAL regulates myofilament organization and synaptic structure. *Mech. Dev.* **124**, 390–406 (2007).
- Fong, K. S. & de Couet, H. G. Novel proteins interacting with the leucine-rich repeat domain of human flightless-I identified by the yeast two-hybrid system. *Genomics* **58**, 146–157 (1999).
- Lamb, R. S., Ward, R. E., Schweizer, L. & Fehon, R. G. *Drosophila* coracle, a member of the protein 4.1 superfamily, has essential structural functions in the septate junctions and developmental functions in embryonic and adult epithelial cells. *Mol. Biol. Cell* **9**, 3505–3519 (1998).
- Nongthomba, U., Ansari, M., Thimmaiya, D., Stark, M. & Sparrow, J. Aberrant splicing of an alternative exon in the *Drosophila troponin-T* gene affects flight muscle development. *Genetics* **177**, 295–306 (2007).
- North, K. N., Laing, N. G. & Wallgren-Pettersson, C. Nematine myopathy: current concepts. The ENMC International Consortium and Nematine Myopathy. *J. Med. Genet.* **34**, 705–713 (1997).
- Homyk, T. & Sheppard, D. E. Behavioral mutants of *Drosophila melanogaster*. I. Isolation and mapping of mutations which decrease flight ability. *Genetics* **87**, 95–104 (1977).
- Reddy, K. L. *et al.* The *Drosophila* PAR domain protein 1 (*Pdp1*) gene encodes multiple differentially expressed mRNAs and proteins through the use of multiple enhancers and promoters. *Dev. Biol.* **224**, 401–414 (2000).
- Sandmann, T. *et al.* A temporal map of transcription factor activity: *mef2* directly regulates target genes at all stages of muscle development. *Dev. Cell* **10**, 797–807 (2006).
- Butler, M. J. *et al.* Discovery of genes with highly restricted expression patterns in the *Drosophila* wing disc using DNA oligonucleotide microarrays. *Development* **130**, 659–670 (2003).
- Arbeitman, M. N. *et al.* Gene expression during the life cycle of *Drosophila melanogaster*. *Science* **297**, 2270–2275 (2002).

Supplementary Information is linked to the online version of the paper at www.nature.com/nature.

Acknowledgements We thank the Vienna *Drosophila* RNAi Center for transgenic RNAi lines, and H. Bellen, B. Bullard, J. Saide and T. Volk for their gifts of various antibodies. This work was supported by Boehringer Ingelheim GmbH, the Max-Planck Society and a postdoctoral fellowship to F.S. from the Human Frontier Science Program. Generation of a second set of RNAi lines was supported by a grant from the European Union 7th Framework Programme. A.S. and M.N. were supported by the Austrian Ministry for Science and Research (GEN-AU Bioinformatics Integration Network).

Author Contributions F.S. designed and performed the screen and other experiments, analysed the data and wrote the manuscript with B.J.D. C.S. and C.C.H.L. analysed selected muscle phenotypes in detail. G.D., K.S., M.F. and A.A. assisted in the primary screen, and G.D. also in the initial data analysis. M.R. performed the RNA microarrays. M.N. and A.S. performed the bioinformatic analyses. K.K. led the team that generated the second RNAi hairpin lines.

Author Information Reprints and permissions information is available at www.nature.com/reprints. The authors declare no competing financial interests. Correspondence and requests for materials should be addressed to F.S. (schnorrer@biochem.mpg.de) or B.J.D. (dickson@imp.ac.at).

SUPPLEMENTARY METHODS

***Mef2* primary screen.** RNAi hairpins from the VDRC collection were crossed to *Mef2-GAL4* at 27°C. After 2 weeks lethality rate and stage was scored, and if possible 20 - 30 males containing *Mef2-GAL4* and *UAS-IR* were sorted and incubated for another 7 days at 27°C, at which time adult viability, wing posture and flight were scored as previously described¹. Every positive line was retested once or twice, blind to both the genotype and the outcome of the initial assay. Scores were averaged. Only lines with a s_{19} score¹ better than 0.5 were scored in this work to avoid unspecific phenotypes (Supplementary Fig. 7). For a gene with two *UAS-IR* lines, the stronger phenotype was used to assign the phenotypic class.

Larval assay. RNAi hairpins were crossed to *Mef2-GAL4*, *ZCL0663*, a GFP trap in *CG6416* labelling the Z-line⁷, and progeny assayed after 2–5 days at 27°C, depending on the lethality stage observed in the initial screen. Larvae were immobilised by placing them into 65°C water for about 1 sec, and then mounted in 50% glycerol. Images were acquired on a Zeiss Axiophot or Zeiss AxioImagerZ1 at 10x and 20x and analysed with Metamorph software.

Embryo and larval staining. Embryos were stained as described²⁸ with mouse anti-Mhc 3e8 (1:100; ref. 29) and rat anti-Projectin MAC150 (1:100) (Babraham Institute). For larval stainings larva-filets were prepared as described³⁰ with the modification that dissections were done in relaxing solution (20mM phosphate buffer, pH 7.0; 5 mM MgCl₂; 5 mM EGTA, 5 mM ATP). Samples stained with rat anti-How (1:100; ref. 31) were fixed with 4% paraformaldehyde (PFA), samples stained with rat anti- α -Actinin MAK276 (1:3; ref. 32) (Babraham Institute) were fixed with ice cold MeOH. All incubations were performed in PBST (PBS + 0,2% Tx100) instead of PBSTween. Mouse anti-Mhc 3e8 was used (1:30; ref. 29). Images were taken with a Leica SP2 with a 40x objective and processed with ImageJ and Photoshop.

Adult muscle assay. Hemi-thoraces from 7–10 day old *Mef2-GAL4 UAS-IR* adults were prepared by removing head, legs and abdomen with scissors, fixing the thorax in 4% paraformaldehyde (PFA) in relaxing solution (20mM phosphate buffer, pH 7.0; 5 mM MgCl₂; 5 mM EGTA) for 5–10 min and bisecting the thoraces sagittally with a sharp microtome blade. Hemi-thoraces were incubated for 15–20 min in relaxing solution, fixed for 10 min in 4% PFA in relaxing solution, washed 2x in PBST (PBS + 0,1% Tween) and incubated with rhodamine phalloidin (Molecular Probes) for 30 min (1:500 in PBST). After washing 2x for 10 min in PBST, samples were mounted in 50% glycerol and imaged with a Zeiss LSM 510 or Leica SP2 with 10x and 100x objectives to analyze muscle fibers and myofibrils, respectively. For immunohistochemistry hemi-thoraces were prepared as above, apart from incubating the thorax in relaxing solution supplemented with 3 % normal goat serum for 20 min before fixation. Hemi-thoraces were incubated with primary and secondary antibodies for 1 h each in PBS with 0.2 % Triton-X100 and mounted in Vectashield. Mouse anti-Mhc 3e8 was used (1:50; ref. 29), rabbit anti-FliI sc-30046 were used 1:50 (Santa Cruz), rabbit anti-Unc-89 (1:500; ref. 33), rat anti- α -Actinin MAK276 (1:3; ref. 32, Brabraham Institute) and guinea pig anti-Tmod (1:100; ref 34).

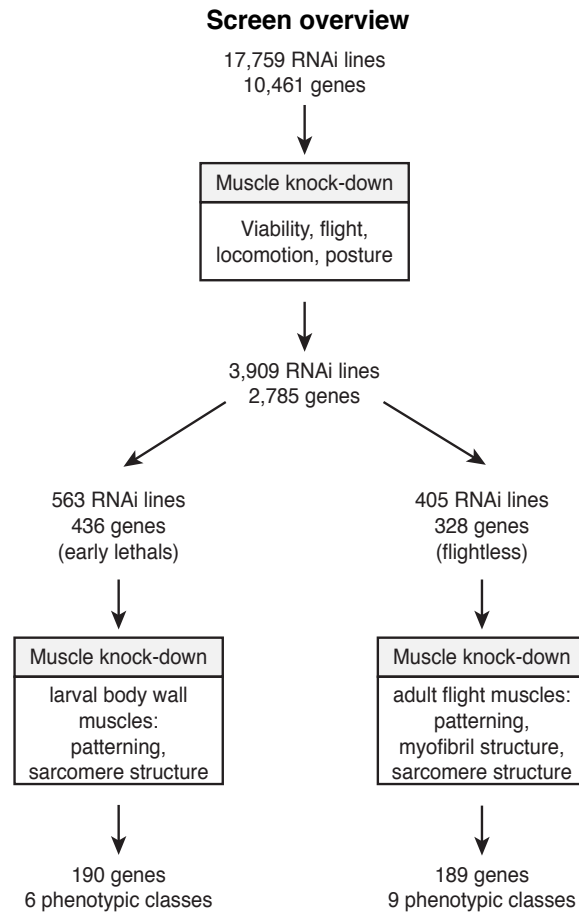
Microarrays. IFM from 50 flies were dissected with fine forceps in PBS and the RNA was isolated using TriPure (Roche). RNA was labelled and hybridized to Agilent chips according to the manufacturer (Agilent). Only transcripts expressed above log threshold 8 were analysed. All experiments were performed in biological duplicates.

Bioinformatics. Hypergeometric distribution was used to assess the probability for a particular term to be enriched or depleted from a gene set compared with the reference set of all screened genes. A heatmap representation of scores is shown. To evaluate if the evolutionary conservation within a gene set is higher or lower than expected, we score the incidence of finding predicted orthologs for Flybase genes in a wide taxonomic range of species (At- *Arabidopsis thaliana*, Sc- *Saccharomyces cerevisiae*, Mm- *Mus musculus*, Hs- *Homo sapiens*, Ce- *Caenorhabditis elegans*, Am- *Apis mellifera*, Ag- *Anopheles gambiae*). The ortholog resources used are Compara (v49), Inparanoid (v6.1), Orthomcl (v2), Homologene and eggNOG. For each gene

set potential functional conservation to human was evaluated using phenotype location data provided for disease-related OMIM records in their Clinical Synopsis (<http://www.ncbi.nlm.nih.gov/omim>). Orthology information as above was used to establish links between *Drosophila* genes and human disease genes. To define the muscle expression set of genes we searched the BDGP database with the terms 'larval muscle', 'body muscle' and 'visceral muscle'.

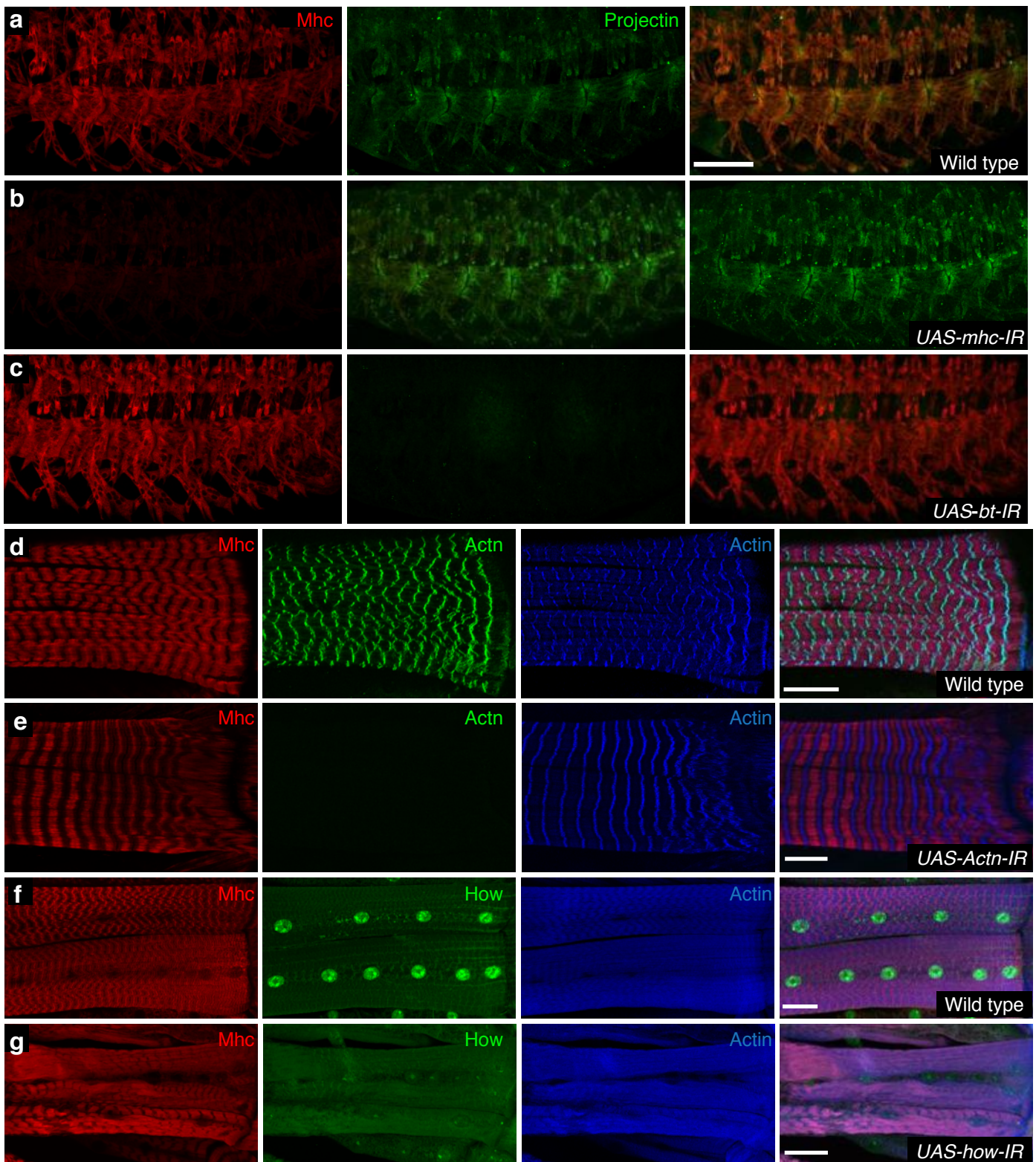
References.

28. Schnorrer, F., Kalchhauser, I. & Dickson, B.J. The transmembrane protein Kon-tiki couples to Dgrip to mediate myotube targeting in *Drosophila*. *Dev Cell* **12**, 751-766 (2007).
29. Saide, J.D. *et al.* Characterization of components of Z-bands in the fibrillar flight muscle of *Drosophila melanogaster*. *J Cell Biol* **109**, 2157-2167 (1989).
30. Schmid, A. & Sigrist, S.J. Analysis of neuromuscular junctions: histology and in vivo imaging. *Methods Mol Biol* **420**, 239-251 (2008).
31. Nabel-Rosen, H., Dorevitch, N., Reuveny, A. & Volk, T. The balance between two isoforms of the *Drosophila* RNA-binding protein how controls tendon cell differentiation. *Mol Cell* **4**, 573-584 (1999).
32. Lakey, A. *et al.* Identification and localization of high molecular weight proteins in insect flight and leg muscle. *EMBO J* **9**, 3459-3467 (1990).
33. Burkart, C. *et al.* Modular proteins from the *Drosophila* *sallimus* (*sls*) gene and their expression in muscles with different extensibility. *J Mol Biol* **367**, 953-969 (2007).
34. Dye, C.A. *et al.* The *Drosophila* *sanpodo* gene controls sibling cell fate and encodes a tropomodulin homolog, an actin/tropomyosin-associated protein. *Development* **125**, 1845-1856 (1998).



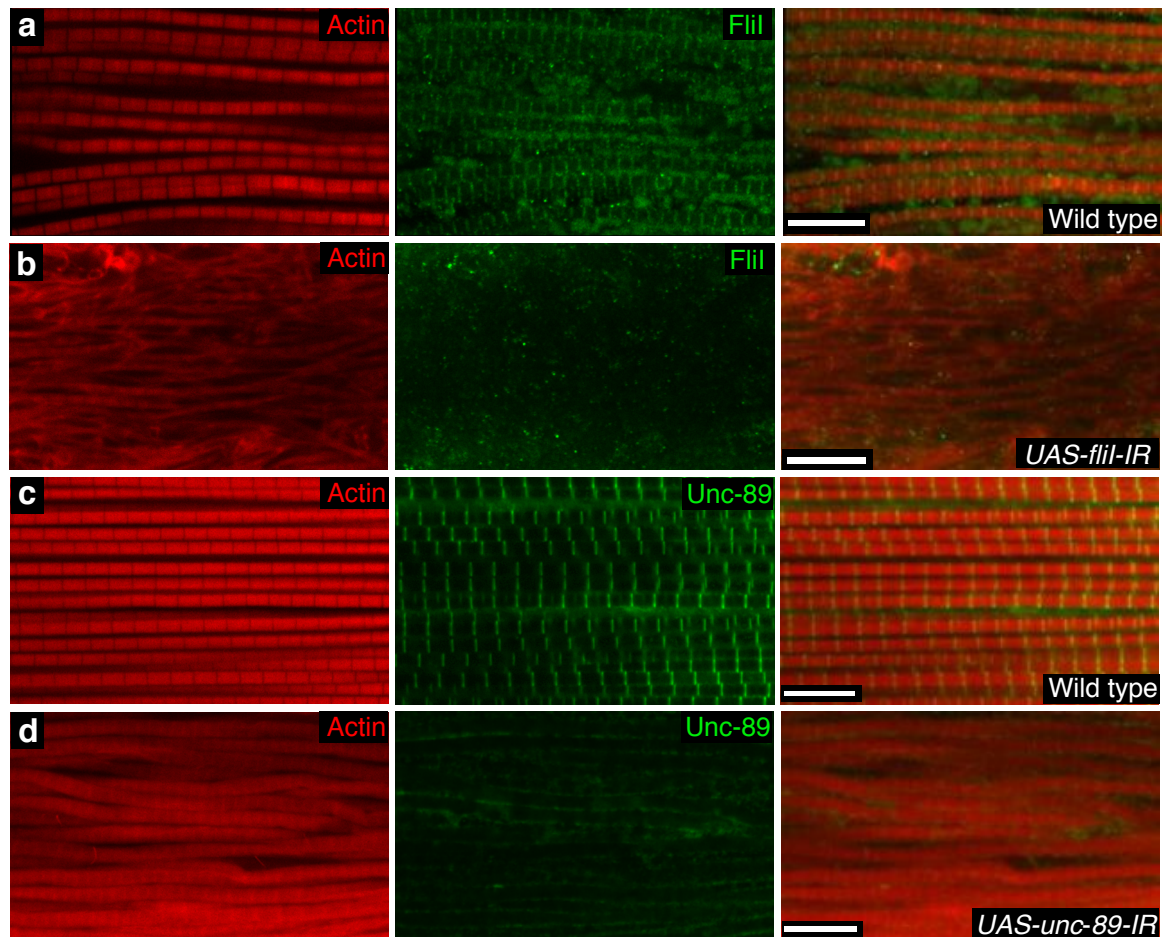
Supplementary Figure 1 | Screen overview

Overview of primary and secondary *Mef2-GAL4* screens. Genes identified in the primary screen were assigned to specific classes according to viability, flight, locomotion and wing posture, and selected genes assayed in secondary screens according to their phenotype.



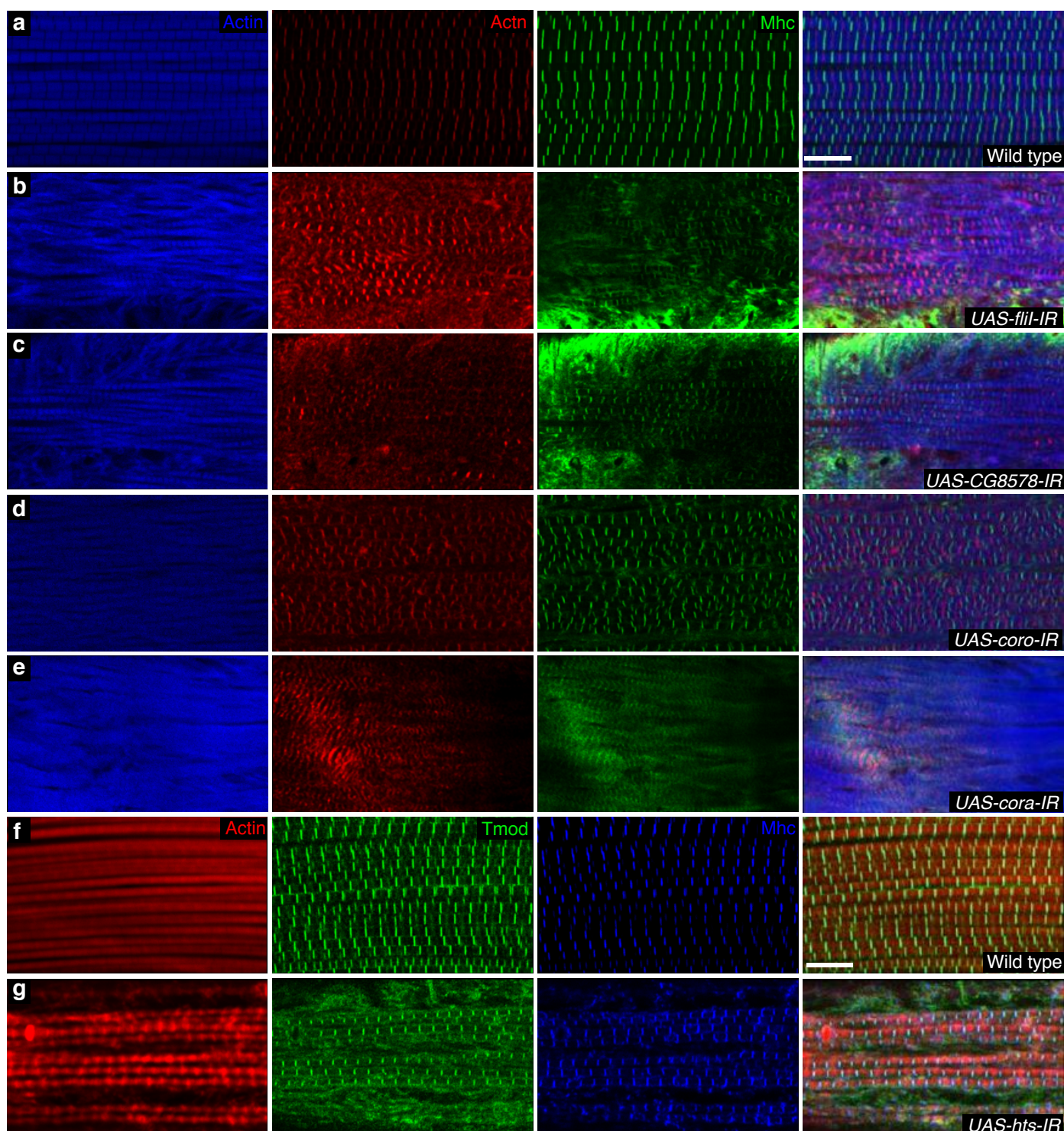
Supplementary Figure 2 | Larval muscle protein knock-down.

Body muscles of stage 17 embryos stained with anti-Mhc in red and anti-Projectin in green in wild type (a), *UAS-mhc-IR* (TF7164) (b), and *UAS-bt-IR* (TF46253) (c); scale bar, 50 μ m. Body muscles of L3 larvae stained with anti-Mhc in red and anti-Actinin (d, e) or anti-How (f, g) in green in wild type (d, f), *UAS-actn-IR* (TF7760) (e), and *UAS-how-IR* (TF13756) (g); larvae in (d) and (e) were fixed in methanol, scale bar, 25 μ m.



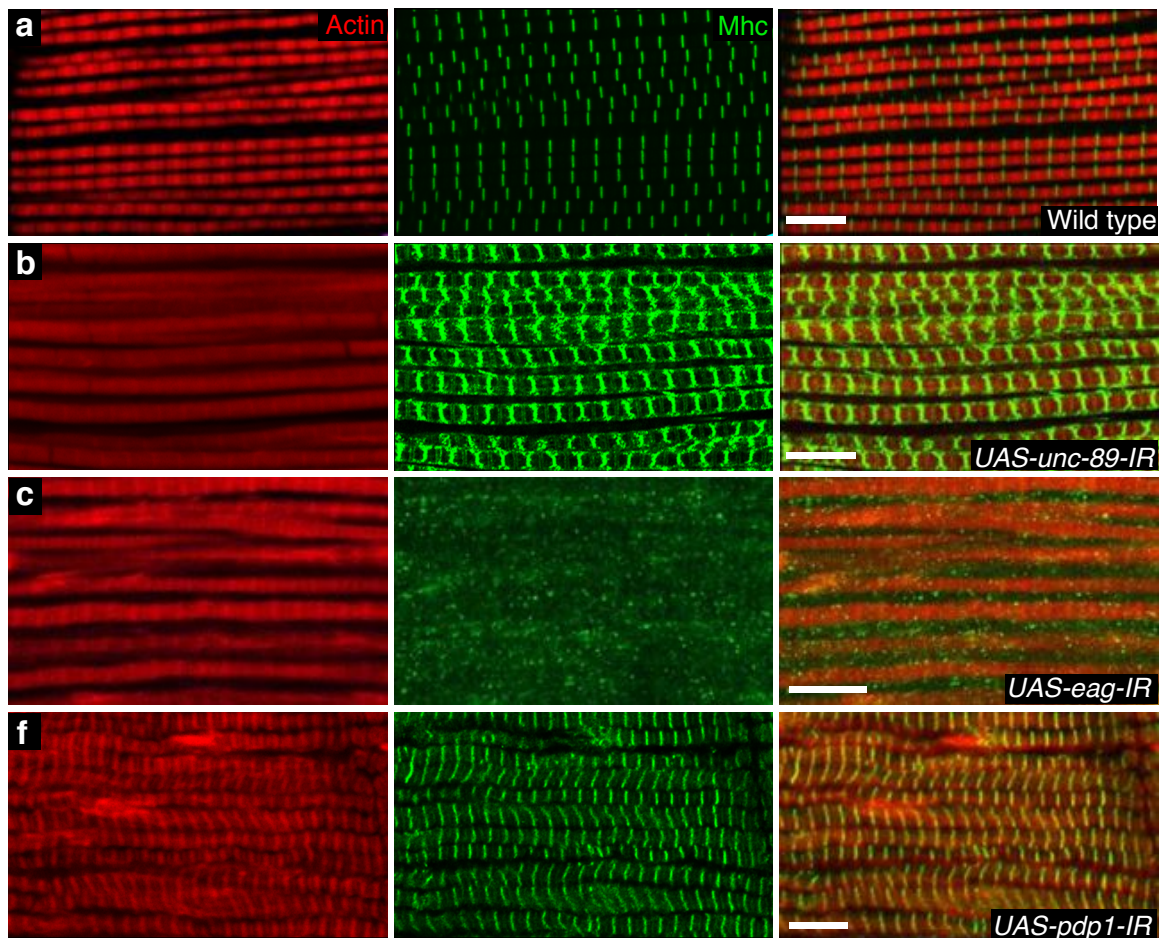
Supplementary Figure 3 | IFM protein knock-down.

Myofibrils from adult flight muscles stained in with phalloidin in red, anti- α -FliI (**a,b**) in red or anti-Unc-89 (**c,d**) in green in wild type (**a,c**), *UAS-fliI-IR* (TF39528) (**b**), *UAS-unc89-IR* (TF29412) (**d**). Scale bar, 10 μ m.



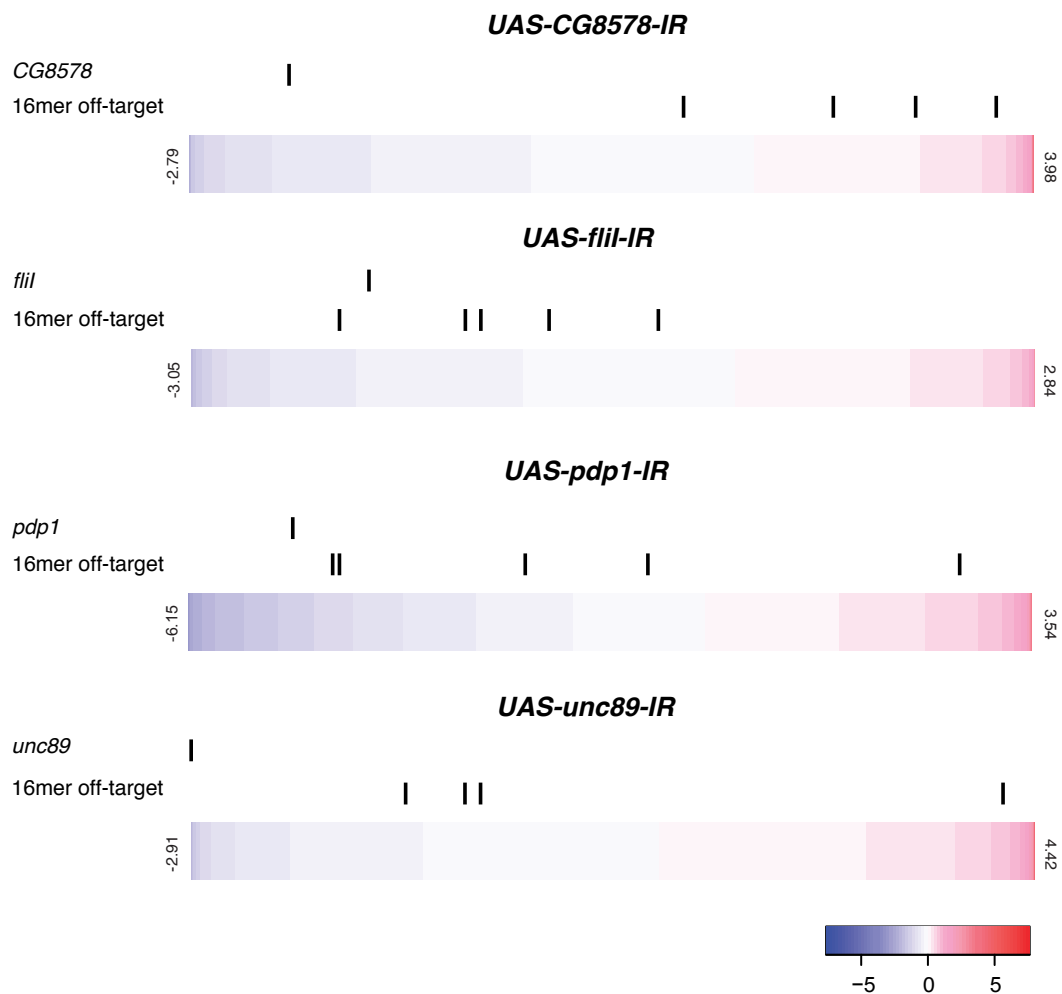
Supplementary Figure 4 | Myofibril morphology phenotypes.

(a-e) Myofibrils from adult flight muscles stained in with phalloidin in blue, anti- α -Actinin in red and anti-Mhc in green in wild type (a), *UAS-flii-IR* (TF39528) (b), *UAS-CG8578-IR* (TF35968) (c), *UAS-coro-IR* (TF44671) (d), and *UAS-cora-IR* (TF9787) (e). Myofibrils stained from wild type (f) and *UAS-hts-IR* (g) stained with phalloidin in red, anti-Tmod in green and anti-Mhc in blue. Scale bar, 10 μ m.



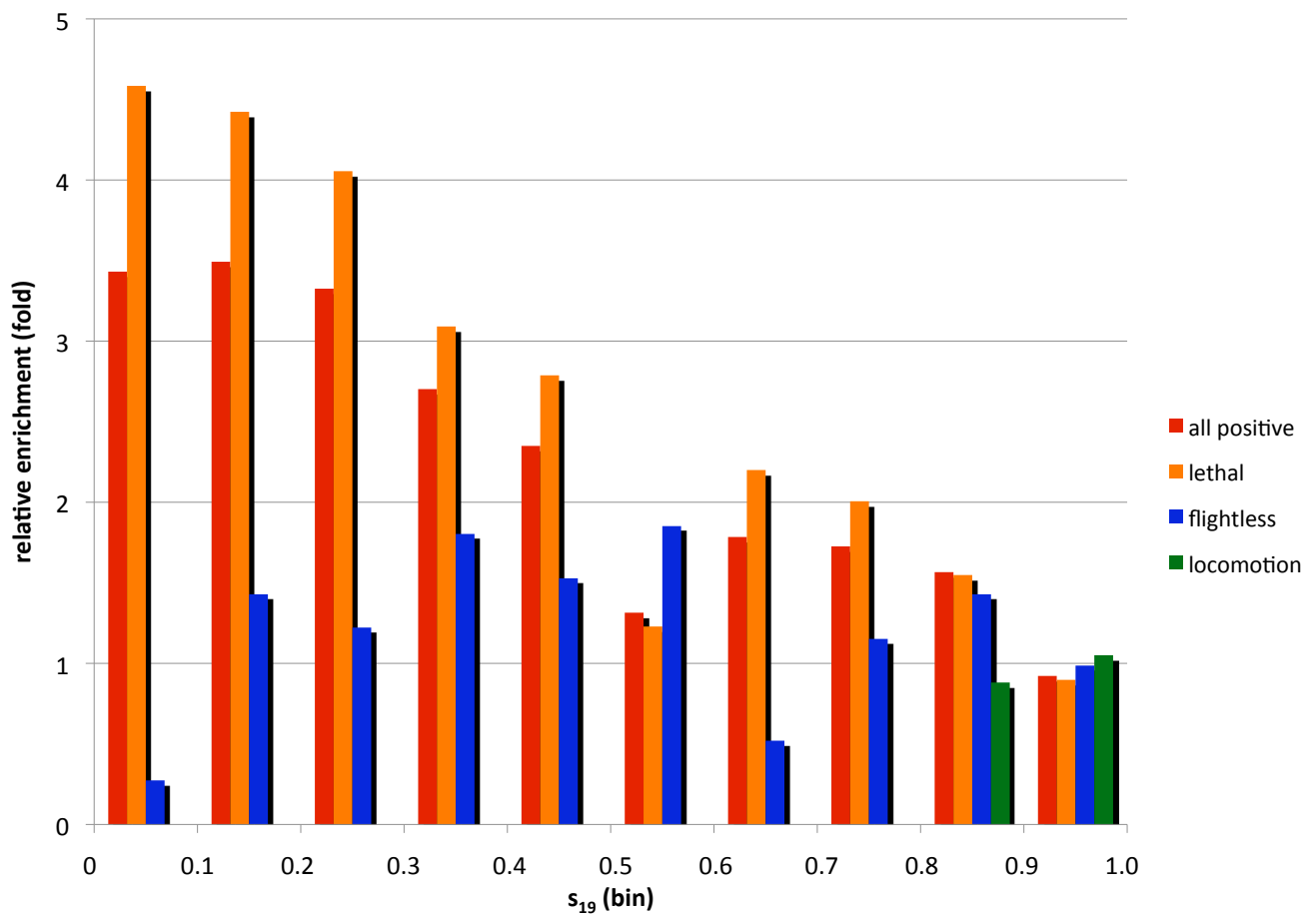
Supplementary Figure 5 | No distinct M phenotype.

Myofibrils from adult flight muscles stained with phalloidin in red and anti-Mhc in green in wild type (a), *UAS-unc89-IR* (TF29412) (b), *UAS-eag-IR* (TF9127) (c), and *UAS-pdp1-IR* (TF37769) (d). Scale bar, 10 μ m.



Supplementary Figure 6 | RNA levels in isolated IFMs.

Genome-wide expression profiles of dissected IFM fibers from wild-type adults compared to *CG578*, *flii*, *unc89* and *pdp1* knock-down. The log value of the fold change in mRNA levels compared to wild-type controls was determined for each gene expressed above a log threshold of 8. Genes were ranked according to the fold-change, and the rankings of the on-target gene and all predicted off-targets are shown. Off-targets were defined as having at least one exact 16mer match to the hairpin. Off-target genes show no enrichment for knock-down, whereas on-target mRNA levels are consistently reduced.



Supplementary Figure 7 | Choice of s_{19} cut off.

Number of RNAi lines scored positive in the *Mef2* screen, and in the library as a whole, binned according to s_{19} scores. Only lines with $s_{19} > 0.5$ were used in this study.

For Supplementary Tables 1-12, see separate Supplementary Information files.

Supplementary Table 1 | Phenotypic classes in primary screen.

Phenotypes in primary screen (Fig. 1b) listed by gene and transgenic RNAi line.

Supplementary Table 2 | Lethal stages in primary screen.

Lethality stages in primary screen (Fig. 1c) listed by gene and transgenic RNAi line.

Supplementary Table 3 | Positive controls.

Phenotypes of positive control genes in the primary *Mef2-GAL4* screen, listed by gene and RNAi line.

Supplementary Table 4 | Negative controls.

Phenotypes of negative control genes in the primary *Mef2-GAL4* screen.

Supplementary Table 5 | Gene validation.

List of genes tested with a second generation RNAi library.

Supplementary Table 6 | Muscle morphology phenotypes in larval screen.

Muscle morphology defects observed in the secondary screen of larval body wall muscles (Fig. 2a), as well as a list of all transformant lines tested.

Supplementary Table 7 | Sarcomere morphology phenotypes in larval screen.

Sarcomere morphology defects observed in the secondary screen of larval body wall muscles (Fig. 2b).

Supplementary Table 8 | Muscle morphology phenotypes in IFM screen.

Muscle morphology defects observed in the secondary screen of adult IFMs (Fig. 3a), as well as a list of all transformant lines tested.

Supplementary Table 9 | Myofibril morphology phenotypes in IFM screen.

Myofibril morphology defects observed in the secondary screen of adult IFMs (Fig. 3b), including a list of genes with actin blobs.

Supplementary Table 10 | Sarcomere morphology phenotypes in IFM screen.

Sarcomere morphology defects observed in the secondary screen of adult IFMs (Fig. 3c).

Supplementary Table 11 | Overlap of *Mef2* positives with *Mef2* targets and muscle expression.

List of genes that are predicted *Mef2* target genes, expressed in muscles and positive in the *Mef2* RNAi screen.

Supplementary Table 12 | Overlap of *Mef2* positives with late muscle cluster or genes expressed in adult muscle precursors.

List of genes positive in the *Mef2* RNAi screen and found in the late muscle cluster or to be expressed in adult muscle precursors in wing discs.

Publication IV

Spalt mediates an evolutionarily conserved switch to fibrillar muscle fate in insects

Cornelia Schönbauer¹, Jutta Distler², Nina Jährling^{3,4}, Martin Radolf⁵, Hans-Ulrich Dodt^{3,4}, Manfred Frasch² & Frank Schnorrer¹

Flying insects oscillate their wings at high frequencies of up to 1,000 Hz^{1,2} and produce large mechanical forces of 80 W per kilogram of muscle³. They utilize a pair of perpendicularly oriented indirect flight muscles that contain fibrillar, stretch-activated myofibres. In contrast, all other, more slowly contracting, insect body muscles have a tubular muscle morphology⁴. Here we identify the transcription factor Spalt major (*Salm*) as a master regulator of fibrillar flight muscle fate in *Drosophila*. *salm* is necessary and sufficient to induce fibrillar muscle fate. *salm* switches the entire transcriptional program from tubular to fibrillar fate by regulating the expression and splicing of key sarcomeric components specific to each muscle type. Spalt function is conserved in insects evolutionarily separated by 280 million years. We propose that Spalt proteins switch myofibres from tubular to fibrillar fate during development, a function potentially conserved in the vertebrate heart—a stretch-activated muscle sharing features with insect flight muscle.

To generate fast wing oscillations, both indirect flight muscle (IFM) units are attached to the thoracic exoskeleton. The contraction of one unit, the dorsal-longitudinal flight muscles (DLMs), deforms the thorax and moves the wings down; simultaneously it stretches and hence activates the second IFM unit, the dorsoventral flight muscles (DVMs), which moves the wings up again, generating an oscillatory movement of thorax and wings at high frequency^{2,5}. IFMs have a unique fibrillar organization to achieve these asynchronous, stretch-activated contractions.

We performed a genome-wide RNA interference (RNAi) screen for muscle morphogenesis in *Drosophila* and identified a function for *salm* in IFM development⁶. The conserved Spalt family of transcription factors has two members in *Drosophila*, *spalt major* (*salm*) and *spalt related* (*salr*)⁷. RNAi knockdown of *salm* in muscle leads to viable but flightless animals with a reduced number of DLMs (Fig. 1a, b). Detailed analysis of the actin cytoskeleton revealed a striking change in fibre organization in *salm* knockdown IFMs: instead of the fibrillar IFM morphology with distinct, unaligned myofibrils and nuclei located between the fibrils (Fig. 1c, g and Supplementary Fig. 1a), these muscles show a tubular morphology normally found in leg muscle, with aligned myofibrils and nuclei located in the tube centre (Fig. 1d, i and Supplementary Fig. 1b). Leg muscles are normal in *salm* knockdown flies (Fig. 1e, f, h, j). We confirmed the RNAi knockdown specificity with a second independent hairpin targeting a different region of *salm* that shows an identical phenotype (data not shown) and by a small deletion that removes *salm* and its neighbouring gene *salr* (Supplementary Fig. 1c, d).

Adult muscles develop in pupae by fusion of undifferentiated adult muscle progenitors (AMPs). DLMs form by fusion of AMPs with three larval templates, inducing their splitting into the six DLMs at 14 h after pupa formation (APF) (at 27 °C)⁸. This splitting is inhibited in *salm* knockdown pupae (Supplementary Movies 1 and 2). In wild-type DLMs, myofibrils start to assemble at 30 h APF with characteristically

spaced nuclei between the fibrils and distinct, unaligned fibrils visible by 45 h (Supplementary Fig. 2a–c, g–i). Leg myoblasts fuse and form tubular fibres with aligned filaments and nuclei located within the tube (Supplementary Fig. 2m–o). In *salm* knockdown IFMs, distinct fibrils never form; instead, a tubular organization similar to leg muscles develops (Supplementary Fig. 2d–f, j–l, p–r). Together, this evidence shows that *salm* is required to initiate IFM-specific muscle fate.

To investigate the mechanism of how *salm* determines IFM identity, we analysed *salm* expression. *Salm* is specifically expressed in adult IFMs, lost in *salm* knockdown and absent from leg muscles (Supplementary Fig. 3a–d). At 12 h APF *Salm* is present in the DLM templates to which the AMPs fuse. This expression increases after

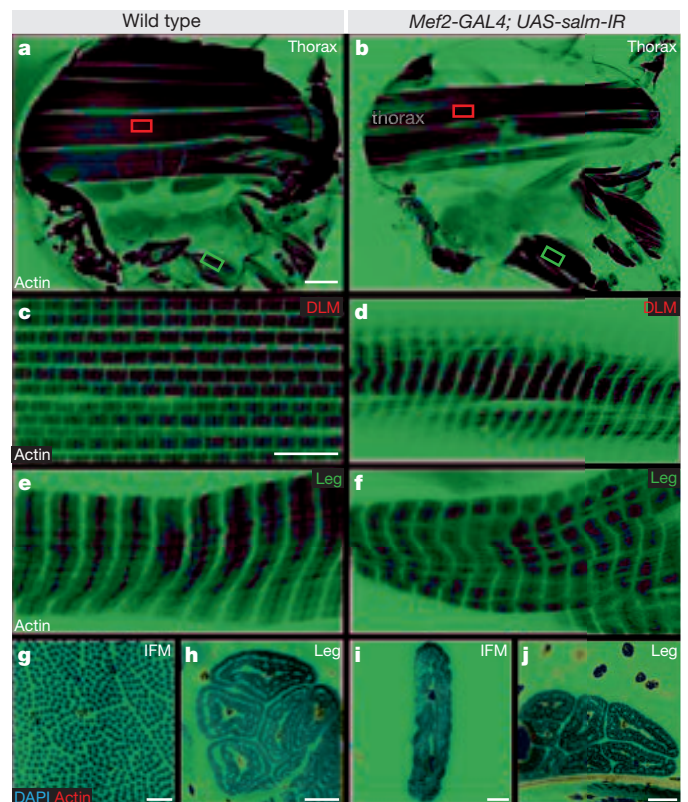


Figure 1 | *salm* specifies fibrillar flight muscle. **a, b**, *Drosophila* wild-type (**a**) and *Mef2-GAL4; UAS-salm-IR* (where IR is inverted repeat) (TF3029) (**b**) hemi-thorax stained with phalloidin. Boxes indicate the approximate views in **c–f**. **c, d**, Fibrillar IFMs (DLMs) in wild type (**c**) are transformed to tubular IFMs (DLMs) in *UAS-salm-IR* (**d**). **e, f**, Tubular leg muscles in wild type (**e**) and *UAS-salm-IR* (**f**). **g–j**, Cross-sections of wild-type IFMs (**g**) and leg muscles (**h**) compared to tubular IFMs (**i**) and leg muscles (**j**) in *Mef2-GAL4; UAS-salm-IR* stained with phalloidin and 4',6-diamidino-2-phenylindole (DAPI). Scale bars 100 μm in **a, b**, 10 μm in **c–j**.

¹Max-Planck-Institute of Biochemistry, Am Klopferspitz 18, 82152 Martinsried, Germany. ²Friedrich-Alexander-University Erlangen-Nuremberg, Biology Department, Developmental Biology Division, Staudtstr. 5, 91058 Erlangen, Germany. ³Vienna University of Technology, FKE, Dept. of Bioelectronics, Floragasse 7, 1040 Vienna, Austria. ⁴Medical University of Vienna, Center for Brain Research, Spitalgasse 4, 1090 Vienna, Austria. ⁵Institute of Molecular Pathology (IMP), Dr. Bohrgasse 7, 1030 Vienna, Austria.

template splitting at 24 h and is lost in *salm* knockdown IFMs (Fig. 2a, b, d, e and Supplementary Fig. 3e). Using a GAL4-reporter line we detect *salm* expression in the templates from 8 h APF onwards throughout IFM development (Supplementary Fig. 4 and Supplementary Movie 3). With the same line, we confirmed that *salm* is absent in developing leg muscles (Fig. 2c, f), consistent with the idea that *salm* selects fibrillar muscle fate.

If *salm* indeed specifies fibrillar muscles, overexpressing *salm* in tubular muscle should switch its sarcomere organization from tubular to fibrillar. We ectopically expressed *salm* using *Mef2-GAL4* in combination with *Tub-GAL80ts* and shifted the flies to restrictive temperature at 0 h APF, or using *1151-GAL4*, which is expressed in AMPs and developing muscles until about 40 h APF⁹. In both cases, ectopic *salm* expression induces a clear transformation of the tubular leg muscles into fibrillar IFM-like muscles (Fig. 2g–i, m, n). As a consequence, these transformed leg muscles do not function properly and flies die as pharate adults. We find a similar transformation in the abdominal muscles upon ectopic *salm* expression (Fig. 2j–l, o, p). This demonstrates that *salm* is sufficient to specify fibrillar muscle fate and to switch the developmental program from tubular to fibrillar fate. In trachea and eyes *salm* or both *salm* and *salr* are required for developmental fate decisions^{10,11}. However, the selection of fibrillar flight muscle fate is largely specific to *salm*, as knockdown of *salr* by RNAi does not cause a tubular transformation, and ectopic expression of *salr* in leg or abdominal muscle does not result in a fibrillar transformation (Supplementary Fig. 5a–g). Consistently, we detect a gain of the

IFM-specific protein Fln¹² and the IFM-specific isoform of Myofilin (Mf-IsoC)¹³, together with a repression of the body-muscle-specific Mf-IsoB/D, Mlp84B and Mlp60 (ref. 14), in *salm*- but not in *salr*-expressing leg muscle (Supplementary Fig. 5h). Thus, we conclude that *salm* is a master regulator of *Drosophila* indirect flight muscle development.

As *salm* acts as a developmental switch, its muscle expression is restricted to IFMs. It is unclear how this precise expression is regulated. *Salm* is not expressed in larval AMPs (Supplementary Fig. 6a); however, the larval AMPs that build the IFMs do express the transcription factor *vestigial* (*vg*)¹⁵ (Supplementary Fig. 6d). *vg*-null flies lack wings and halteres and have a defect in their IFMs¹⁵. We analysed the morphology of *vg* mutant IFMs in detail and notably found the same phenotype as in *salm* knockdown IFMs. *vg* mutant DLMs are reduced in number and show a tubular fibre phenotype (Fig. 3a, c, i). Their leg muscles are normal, which is as expected because these flies are viable and can walk (Fig. 3e). Importantly, *Salm* protein is lost in *vg* mutant IFMs (Fig. 3g). To investigate whether *vg* has an additional function downstream of *salm*, we expressed *salm* using *1151-GAL4* in *vg* mutants and found a complete rescue of the *vg* IFM phenotype (Fig. 3b, d, j). We did not observe a fibrillar transformation of leg muscles, possibly because *Salm* levels driven with *1151-GAL4* in *vg* mutant legs are too low to override the leg muscle fate (Fig. 3f, h). Interestingly, overexpression of *salr* also results in some rescue of *vg* mutant IFMs, probably mediated by regained *Salm* expression (Supplementary Fig. 6f, i, l, o). Together this demonstrates that *vg* is required upstream of *salm* for its IFM expression, and that *salm* does not require *vg* to implement the fibrillar flight muscle program.

Interestingly, *vg* with its cofactor *scalloped* (*sd*)¹⁶ is not sufficient to induce fibrillar fate. Misexpression of *vg* and *sd* neither results in a fibrillar transformation nor in *salm* expression in leg muscles or wing

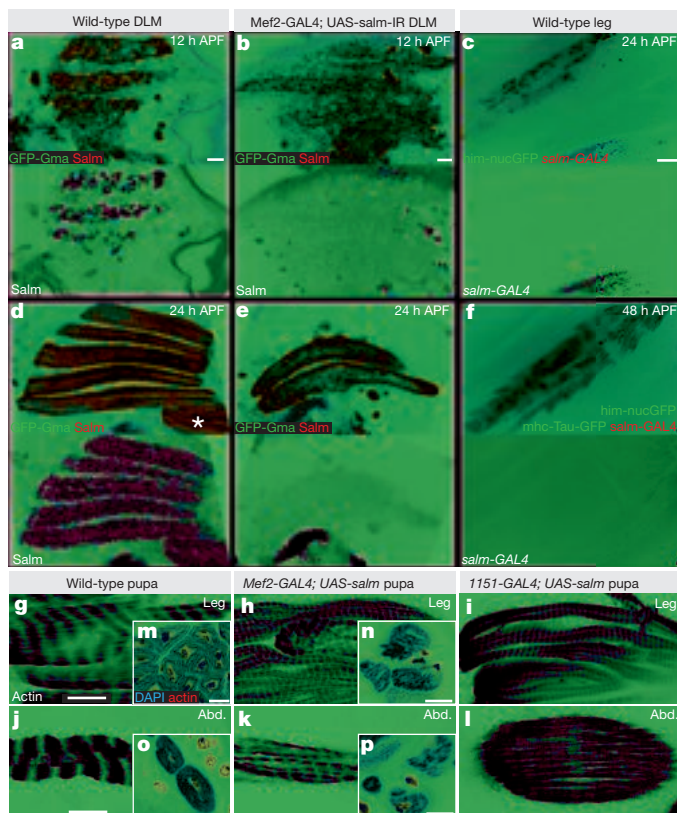


Figure 2 | *Salm* expression is sufficient to induce fibrillar muscle fate. a–f, Wild-type (a, d) or *salm* knockdown DLMs (b, e) expressing *Mef2-GAL4*, *UAS-GFP-gma* stained with anti-*Salm* at 12 h (a, b) and 24 h APF (d, e); asterisk indicates DVMs. c, f, Wild-type leg muscles labelled with *Him-nucGFP* at 24 h APF (c) or *Him-nucGFP* and *mhc-TauGFP* at 48 h APF (f). g–l, Phalloidin staining of late pupal leg muscles (90 h APF) (g–i) or abdominal muscles (j–l) of wild type (g, j), *Tub-GAL80ts; Mef2-GAL4; UAS-salm* shifted at 0 h APF from 18 °C to 30 °C (h, k) and *1151-GAL4; UAS-salm* (i, l). m–p, Cross-sections of leg and abdominal muscles of pupae with the indicated genotypes stained with phalloidin and DAPI. Scale bars, 10 μm.

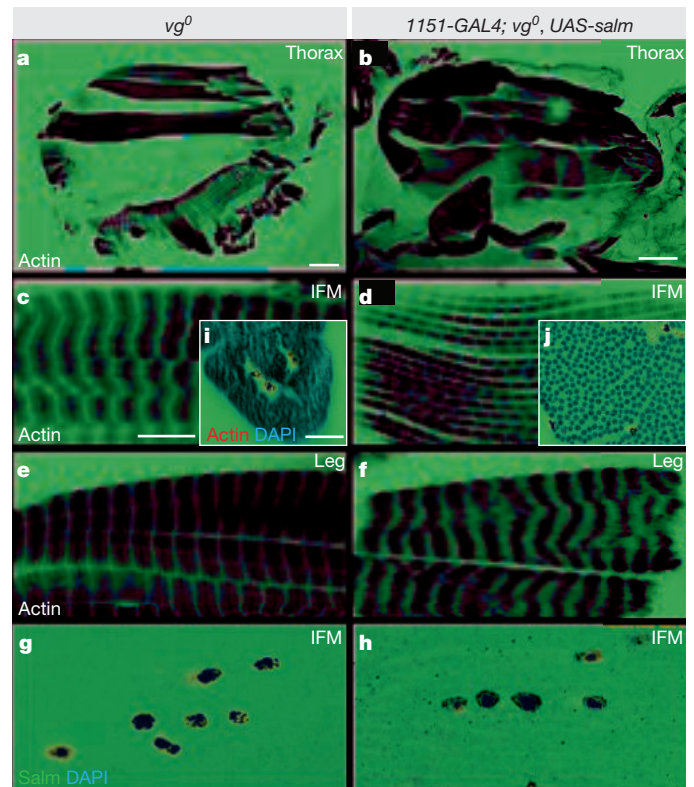


Figure 3 | *vg* functions upstream of *salm*. a, b, IFM phenotype of *vg*⁰ mutant hemi-thorax (a) is rescued by expression of *UAS-salm* with *1151-GAL4* (b). c–j, IFMs in *vg*⁰ are tubular (c; see i for cross-section), and are rescued by *1151-GAL4; UAS-salm* (d; see j for cross-section). Leg muscles are normal (e, f). *Salm* staining in *vg*⁰ IFMs (g), *1151-GAL4; vg*⁰, *UAS-salm* IFMs (h). Scale bars 100 μm in a, b, 10 μm in c–h.

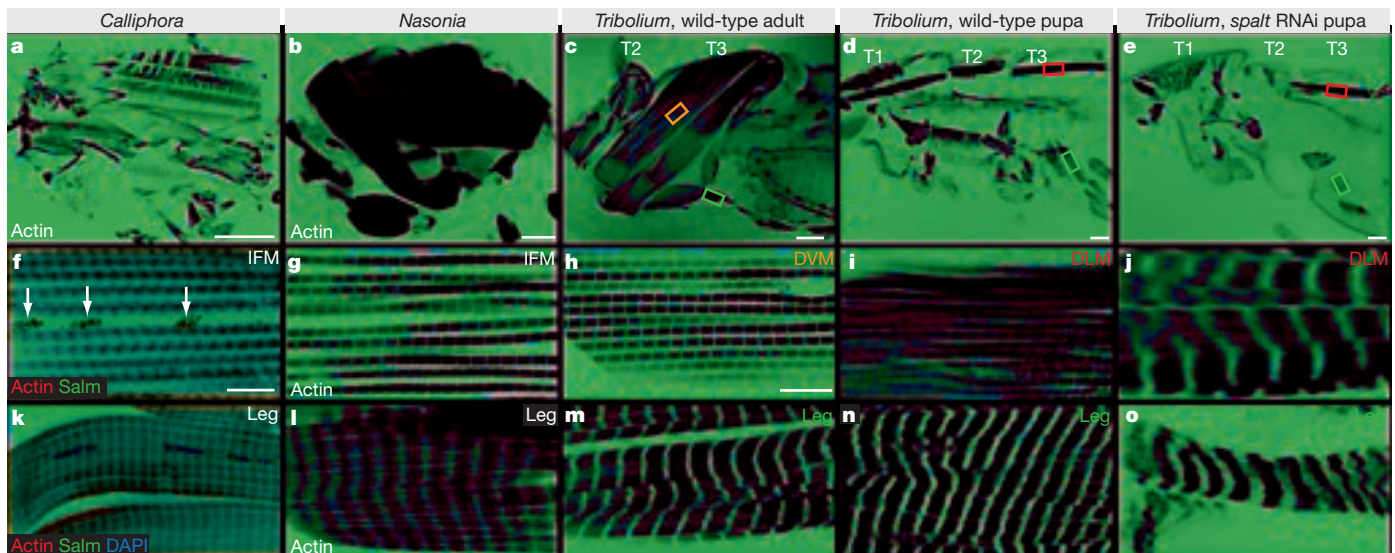


Figure 4 | Fibrillar insect flight muscle requires *spalt* function. **a, b,** Hemi-thorax of *Calliphora* (**a**) and *Nasonia* (**b**). **c–e,** Agarose sections of adult *Tribolium* (**c**), control wild-type (**d**) and *spalt* RNAi *Tribolium* pharate pupa (**e**); boxes indicate approximate areas in **h–j**, **m–o**. **f–o,** Indicated species or genotypes show fibrillar IFMs (**f–i**) and tubular leg muscles (**k–o**). *Calliphora*

disc AMPs (Supplementary Fig. 6a–c, g, j, m, p). In contrast to *vg*, the *Lbx1* homologue *ladybird early* (*lbe*) is specifically expressed in AMPs associated with the leg disc and can abrogate *vg* expression if mis-expressed in the wing disc¹⁷ (Supplementary Fig. 6d, e). Consistently, we found that *1151-GAL4*-driven *lbe* blocks *Salm* expression in the IFMs, leading to tubular IFM morphology (Supplementary Fig. 6h, k, n, q). In summary, *salm*, but not *vg*, is capable of overruling the leg muscle program and determining the fibrillar muscle fate if expressed in leg myoblasts. We propose that in the absence of *Salm* the tubular fate program is initiated by default and does not necessarily require *lbe*, which is absent from many tubular muscles such as the abdominal muscles.

To investigate further the mechanism by which *salm* induces and executes the fibrillar program, we performed microarray analysis of dissected wild-type IFMs and *salm* knockdown IFMs using two independent hairpin constructs, and of wild-type leg muscles. Notably, we found that most known IFM-specific proteins or protein isoforms are downregulated in *salm* knockdown IFMs, including the IFM-specific stretch-sensitive TpnC4 (ref. 18), Fln¹², Mf-IsoC¹³, Prm-IsoC/D¹⁹ and Strn-Mlck-IsoE²⁰ (Supplementary Tables 1, 2 and Supplementary Fig. 7a). Interestingly, we also identified *vg* as downregulated, suggesting that *salm* is required to maintain *vg* expression in IFMs and initiates a feed-forward loop by activating its own activator. Consistently, *salm* knockdown leads to a gain of body-muscle-specific proteins such as MP20 (ref. 21), and body-wall-muscle-specific actins, TpnC41, Mlp84B¹⁴, Mf-IsoB/D¹³, Prm-IsoA¹⁹ and Msp300-IsoE/G (Supplementary Table 1). The *salm*-induced switch is largely transcriptional, but also changes alternative splicing, as is the case for Mf or Strn-Mlck. We confirmed a number of these changes by western blot and antibody staining (Supplementary Fig. 7b–h). Again, *salr* expression is not changed in *salm* knockdown IFMs, arguing for a specific role of *salm* in IFM patterning. We also note that Act88F, which is enriched in IFMs as compared to leg muscles, is not changed in *salm* knockdown IFMs. However, Act88F is also expressed in a subset of tubular leg muscles, questioning its specific role in IFM development²². Together, these data indicate that *salm* initiates a network of gene expression by regulating transcription and alternative splicing that switches the molecular architecture of the muscle from tubular to fibrillar morphology.

Many winged insects use IFMs to move their wings at various frequencies^{1,2}. We wished to determine the IFM morphology in different insect orders across an evolutionary distance of 280 million years

(Supplementary Fig. 8)²³. We chose *Calliphora* as a second dipteran species, the wasp *Nasonia* as a hymenopteran and the beetle *Tribolium* as a coleopteran representative. All these species have a fibrillar organization of their IFMs and a tubular organization of their leg muscles (Fig. 4a–c, f–h, k–o). We found that *Salm* expression in *Calliphora* is IFM specific (Fig. 4f, k), indicating that the functional distinction of muscle types correlates with *salm* expression in dipteran species. To investigate functionally a potential role of *spalt*, we used systemic RNAi in *Tribolium*²⁴. Injection of *spalt* dsRNA into *Tribolium* larvae leads to pupae that are unable to complete metamorphosis and die as pharate adults. Histological analysis of the DLMs reveals a marked transformation to the tubular muscle morphology after *spalt* knockdown (Fig. 4e, j), as opposed to the fibrillar morphology in control injected animals (Fig. 4d, i). Hence, *spalt* is required in *Tribolium*, as it is in *Drosophila*, to specify fibrillar flight muscles, suggesting that *spalt* function as a regulator of fibrillar flight muscles is conserved in all insects harbouring stretch-activated indirect flight muscles.

Mice and humans possess four *spalt-like* (*SALL*) genes, none of which are expressed in differentiated striated body muscles^{25,26}. This is not surprising, as all vertebrate body muscles harbour aligned sarcomeres that resemble the tubular insect muscles. Interestingly, *SALL1* and *SALL3* are both expressed in mouse and human hearts^{25,26}, which contain distinct unaligned myofibrils in cardiomyocytes²⁷ and utilize the stretch-modulated Frank–Starling contraction mechanism²⁸. Mutations in human *SALL1* cause the heart abnormalities observed in Townes–Brocks syndrome²⁹, leading us to speculate that *spalt* function determines fibrillar stretch-activated muscle all the way up to vertebrates.

Mice and humans possess four *spalt-like* (*SALL*) genes, none of which are expressed in differentiated striated body muscles^{25,26}. This is not surprising, as all vertebrate body muscles harbour aligned sarcomeres that resemble the tubular insect muscles. Interestingly, *SALL1* and *SALL3* are both expressed in mouse and human hearts^{25,26}, which contain distinct unaligned myofibrils in cardiomyocytes²⁷ and utilize the stretch-modulated Frank–Starling contraction mechanism²⁸. Mutations in human *SALL1* cause the heart abnormalities observed in Townes–Brocks syndrome²⁹, leading us to speculate that *spalt* function determines fibrillar stretch-activated muscle all the way up to vertebrates.

METHODS SUMMARY

All RNAi crosses were performed at 27 °C. Adult or pupal flight or leg muscles were bisected and stained with phalloidin or antibodies. For early pupal stages muscles were dissected or pupae were embedded in agarose and sectioned. For time-lapse movies pupae were mounted in Voltalef oil and imaged using a spinning disc confocal.

Full Methods and any associated references are available in the online version of the paper at www.nature.com/nature.

Received 26 May; accepted 13 September 2011.

- Dudley, R. in *The Biomechanics of Insect Flight* (ed. Dudley, R.) 75–158 (Princeton Univ. Press, 2000).
- Dickinson, M. Insect flight. *Curr. Biol.* **16**, R309–R314 (2006).

3. Lehmann, F. O. & Dickinson, M. H. The changes in power requirements and muscle efficiency during elevated force production in the fruit fly *Drosophila melanogaster*. *J. Exp. Biol.* **200**, 1133–1143 (1997).
4. Bernstein, S. I., O'Donnell, P. T. & Cripps, R. M. Molecular genetic analysis of muscle development, structure, and function in *Drosophila*. *Int. Rev. Cytol.* **143**, 63–152 (1993).
5. Dudley, R. in *The Biomechanics of Insect Flight* (ed. Dudley, R.) 36–74 (Princeton Univ. Press, 2000).
6. Schnorrer, F. *et al.* Systematic genetic analysis of muscle morphogenesis and function in *Drosophila*. *Nature* **464**, 287–291 (2010).
7. de Celis, J. F. & Barrio, R. Regulation and function of Spalt proteins during animal development. *Int. J. Dev. Biol.* **53**, 1385–1398 (2009).
8. Dutta, D., Anant, S., Ruiz-Gomez, M., Bate, M. & VijayRaghavan, K. Founder myoblasts and fibre number during adult myogenesis in *Drosophila*. *Development* **131**, 3761–3772 (2004).
9. Anant, S., Roy, S. & VijayRaghavan, K. Twist and Notch negatively regulate adult muscle differentiation in *Drosophila*. *Development* **125**, 1361–1369 (1998).
10. Franch-Marro, X. & Casanova, J. *spalt*-induced specification of distinct dorsal and ventral domains is required for *Drosophila* tracheal patterning. *Dev. Biol.* **250**, 374–382 (2002).
11. Mollereau, B. *et al.* Two-step process for photoreceptor formation in *Drosophila*. *Nature* **412**, 911–913 (2001).
12. Reedy, M. C., Bullard, B. & Vigoreaux, J. O. Flightin is essential for thick filament assembly and sarcomere stability in *Drosophila* flight muscles. *J. Cell Biol.* **151**, 1483–1500 (2000).
13. Qiu, F. *et al.* Myofilin, a protein in the thick filaments of insect muscle. *J. Cell Sci.* **118**, 1527–1536 (2005).
14. Stronach, B. E., Siegrist, S. E. & Beckerle, M. C. Two muscle-specific LIM proteins in *Drosophila*. *J. Cell Biol.* **134**, 1179–1195 (1996).
15. Bernard, F. *et al.* Control of *apterous* by *vestigial* drives indirect flight muscle development in *Drosophila*. *Dev. Biol.* **260**, 391–403 (2003).
16. Halder, G. *et al.* The Vestigial and Scalloped proteins act together to directly regulate wing-specific gene expression in *Drosophila*. *Genes Dev.* **12**, 3900–3909 (1998).
17. Maqbool, T. *et al.* Shaping leg muscles in *Drosophila*: role of *ladybird*, a conserved regulator of appendicular myogenesis. *PLoS ONE* **1**, e122 (2006).
18. Agianian, B. *et al.* A troponin switch that regulates muscle contraction by stretch instead of calcium. *EMBO J.* **23**, 772–779 (2004).
19. Arredondo, J. J. *et al.* Control of *Drosophila* paramyosin/miniparamyosin gene expression. Differential regulatory mechanisms for muscle-specific transcription. *J. Biol. Chem.* **276**, 8278–8287 (2001).
20. Patel, S. R. & Saide, J. D. Stretchin-klp, a novel *Drosophila* indirect flight muscle protein, has both myosin dependent and independent isoforms. *J. Muscle Res. Cell Motil.* **26**, 213–224 (2005).
21. Ayme-Southgate, A., Lasko, P., French, C. & Pardue, M. L. Characterization of the gene for mp20: a *Drosophila* muscle protein that is not found in asynchronous oscillatory flight muscle. *J. Cell Biol.* **108**, 521–531 (1989).
22. Nongthomba, U., Pasalodos-Sanchez, S., Clark, S., Clayton, J. D. & Sparrow, J. C. Expression and function of the *Drosophila* ACT88F actin isoform is not restricted to the indirect flight muscles. *J. Muscle Res. Cell Motil.* **22**, 111–119 (2001).
23. Savard, J. *et al.* Phylogenomic analysis reveals bees and wasps (Hymenoptera) at the base of the radiation of holometabolous insects. *Genome Res.* **16**, 1334–1338 (2006).
24. Tomoyasu, Y. & Denell, R. E. Larval RNAi in *Tribolium* (Coleoptera) for analyzing adult development. *Dev. Genes Evol.* **214**, 575–578 (2004).
25. Parrish, M. *et al.* Loss of the *Sall3* gene leads to palate deficiency, abnormalities in cranial nerves, and perinatal lethality. *Mol. Cell Biol.* **24**, 7102–7112 (2004).
26. Nishinakamura, R. *et al.* Murine homolog of *SALL1* is essential for ureteric bud invasion in kidney development. *Development* **128**, 3105–3115 (2001).
27. Manisastry, S. M., Zaal, K. J. & Horowitz, R. Myofibril assembly visualized by imaging N-RAP, α -actinin, and actin in living cardiomyocytes. *Exp. Cell Res.* **315**, 2126–2139 (2009).
28. Shiels, H. A. & White, E. The Frank-Starling mechanism in vertebrate cardiac myocytes. *J. Exp. Biol.* **211**, 2005–2013 (2008).
29. Surka, W. S., Kohlhase, J., Neunert, C. E., Schneider, D. S. & Proud, V. K. Unique family with Townes-Brocks syndrome, *SALL1* mutation, and cardiac defects. *Am. J. Med. Genet.* **102**, 250–257 (2001).

Supplementary Information is linked to the online version of the paper at www.nature.com/nature.

Acknowledgements We thank M. Affolter, D. Bäumer, M. Beckerle, B. Bullard, E. Chen, K. Clark, C. Desplan, K. Jagla, A. Lalouette, J. Posakony, D. Reiff, J. Saide, S. Sprecher, R. Schuh, G. Tanentzapf, J. Vigoreaux, K. VijayRaghavan, the Bloomington and the VDRC stock centres for fly stocks, antibodies and insect species. We are grateful to B. Dickson, I. Hein, M. Klingler and M. Sixt for discussions, and to R. Fässler for support and discussions. We thank A. Kaya-Copur, H. Knaut, M. Spletter and N. Vogt for critical comments on the manuscript. This work was supported by the Max-Planck-Society, a Career Development Award by the Human Frontier Science Programme to F.S., a Doc-fforte predoctoral fellowship from the Austrian Academy of Sciences to C.S., and DFG grants to M.F.

Author Contributions C.S. performed most of the experiments, analysed the data and created most of the figures. F.S. acquired the time-lapse movies and performed western blots. J.D. and M.F. conducted the *Tribolium* RNAi experiments, M.R. performed the microarray analysis, and N.J. and H.-U.D. were involved in the initial characterisation of the *salm* mutant phenotype. F.S. conceived and supervised the project and wrote the manuscript with input from C.S. and M.F.

Author Information All raw data were submitted to the Gene Expression Omnibus under accession number GSE27502. Reprints and permissions information is available at www.nature.com/reprints. The authors declare no competing financial interests. Readers are welcome to comment on the online version of this article at www.nature.com/nature. Correspondence and requests for materials should be addressed to F.S. (schnorrer@biochem.mpg.de).

METHODS

Fly strains and genetics. All fly work, unless otherwise stated, was performed at 27 °C to enhance GAL4 activity. Two independent *UAS-salm-IR* lines (TF3029 and TF101052) were obtained from the VDRC stock centre. Sequences for all VDRC RNAi hairpins are deposited at <http://stockcenter.vdrc.at>; TRiP sequences can be found at <http://www.flyrnai.org>. *salm* hairpins were crossed to *Mef2-GAL4* (ref. 30). For knockdown of *salr*, we used TF28386 from the VDRC stock centre and the JF03226 TRiP line driven with *1151-GAL4* (ref. 9) or *Mef2-GAL4*, respectively. For ectopic expression of *salm*, *UAS-salm*³¹ was crossed to *Tub-GAL80ts*; *Mef2-GAL4* or *1151-GAL4* at 18 °C and shifted to 30 °C at 0 h APF to prevent early lethality. Similarly, crosses of *UAS-salm*, *vg*⁰ (ref. 15) with *1151-GAL4*; *vg*⁰/*CyO* were kept at 18 °C until 0 h APF and then shifted to 30 °C. Misexpression of *UAS-lbe* and *UAS-vg* was performed with *1151-GAL4* at 25 °C. For *salm* expression during pupal development, we used flies expressing *salm-GAL4/CyO* and *hmnuclear-GFP*, which marks undifferentiated myoblasts³², and with *mhc-TauGFP*³³ labelling all differentiated muscles. For the *salm* mutant mitotic clones, the FRT cell-lethal method was used³⁴. *hs-Flp*; *Df(2L)32FP-5*, *FRT40A/cl2L3*, *FRT40A* larvae were grown at 25 °C and heat-shocked twice for 60 min at 37 °C on two consecutive days. The IFM phenotype of flightless animals was analysed as described below. To construct *UAS-salr* the 8.0-kb *salr* genomic region was amplified with gene-specific primers (tgtagtcaagttcggtccagg and ttgtgtcagtgctagtaga) from genomic DNA and cloned into pUAST. Transgenic lines were generated using standard procedures.

Analysis of IFMs and leg muscles. Hemi-thoraces for imaging *Drosophila* adult and pharate pupal IFM and leg muscles were prepared and stained as described⁶. Actin was visualized with rhodamine phalloidin (Molecular Probes). Rabbit anti-Fln¹² and rabbit anti-Salm³⁵ were used at 1:50, and rabbit anti-Mlp84B was diluted 1:500¹⁴. Nuclei were visualized with DAPI or mouse anti-Lamin (Hybridoma Bank, clone ADL67.10) was used at 1:10. *Calliphora* IFM and leg muscle morphology was analysed by bisection of thoraces and staining with Salm antibody, phalloidin and DAPI. To examine the *salm* knockdown phenotype during late pupal development (30–60 h APF), wild-type *Mef2-GAL4*, *UAS-GFP-Gma* and *Mef2-GAL4*, *UAS-salm-IR*, *UAS-GFP-Gma* pupae of desired stages were fixed in 4% paraformaldehyde in PBST (with 0.5% Triton-X 100) overnight at 4 °C, washed twice for 10 min in PBST and then embedded in 7% agarose. Agarose blocks were cut in 90-µm sections with a vibratome. Sections were incubated with DAPI for 10 min, washed twice for 10 min in PBST and mounted in Vectashield. Similarly, *Tribolium*, and *Nasonia* IFMs, leg muscles, and all cross-sections were analysed by staining agarose sections with rhodamine phalloidin and DAPI. To analyse IFM morphology and *salm* expression in wild-type and *salm* knockdown flies during early pupal development, 12 h and 24 h APF pupae were dissected as described³⁶.

Immunolabelling of larval imaginal discs. Dissection and staining of 3rd larval instar wing and leg discs was performed as described³⁷. Wing and leg discs associated AMPs were labelled with *1151-GAL4*, *UAS-GFP-gma* and rabbit anti-Salm at 1:50 or anti-Vg at 1:200.

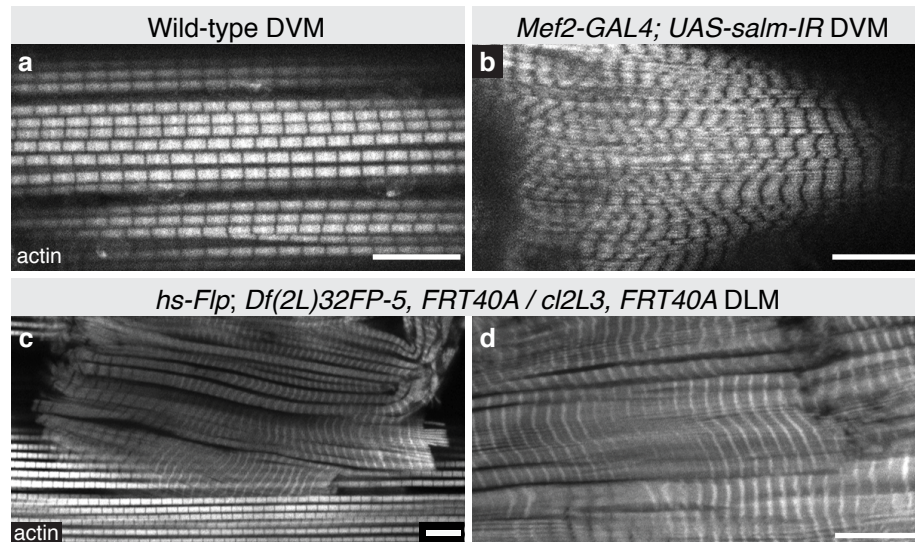
Time-lapse movies. Staged 8–10 h pupae were carefully cleaned with a wet brush and transferred into a custom-made slide with a slit fitting an entire pupa, dorsal side facing up. The pupa was slightly turned (10–20°) resulting in DLM templates facing up. A coverslip with a thin layer of 3S Voltaef oil facing the pupa was placed on top. Z-stack images were acquired every 5 min using a spinning disc confocal with a ×20 or ×40 objective (Zeiss, VisiTron).

RNAi in *Tribolium*. A 3,320-bp Tc'spalt (BeetleBase TC013501; GenBank CM000280.2) fragment was amplified from cDNA with gene-specific primers (Tc'sal P2 5'-CACCTCCAGCACCAACAAG-3', Tc'sal P7 5'-CCCCGTTGCTCCACATATGC-3') and cloned into pBluescript 2. PCR templates from this clone were generated with a T7 and a fused T7–T3 primer and used for *in vitro* dsRNA synthesis with the MEGascript T7 High Yield Transcription Kit (Ambion). dsRNA injections of 4th and 5th instar larvae (*Tribolium* wild-type strain San Bernardino) were performed as described²⁴. Larvae were anaesthetized on ice for 15 min and abdominally injected with *spalt* dsRNA (1 µg µl⁻¹) until the larvae had stretched visibly. After injection the beetles were kept on flour (5% yeast, 0.5% fumagillin) at 32 °C.

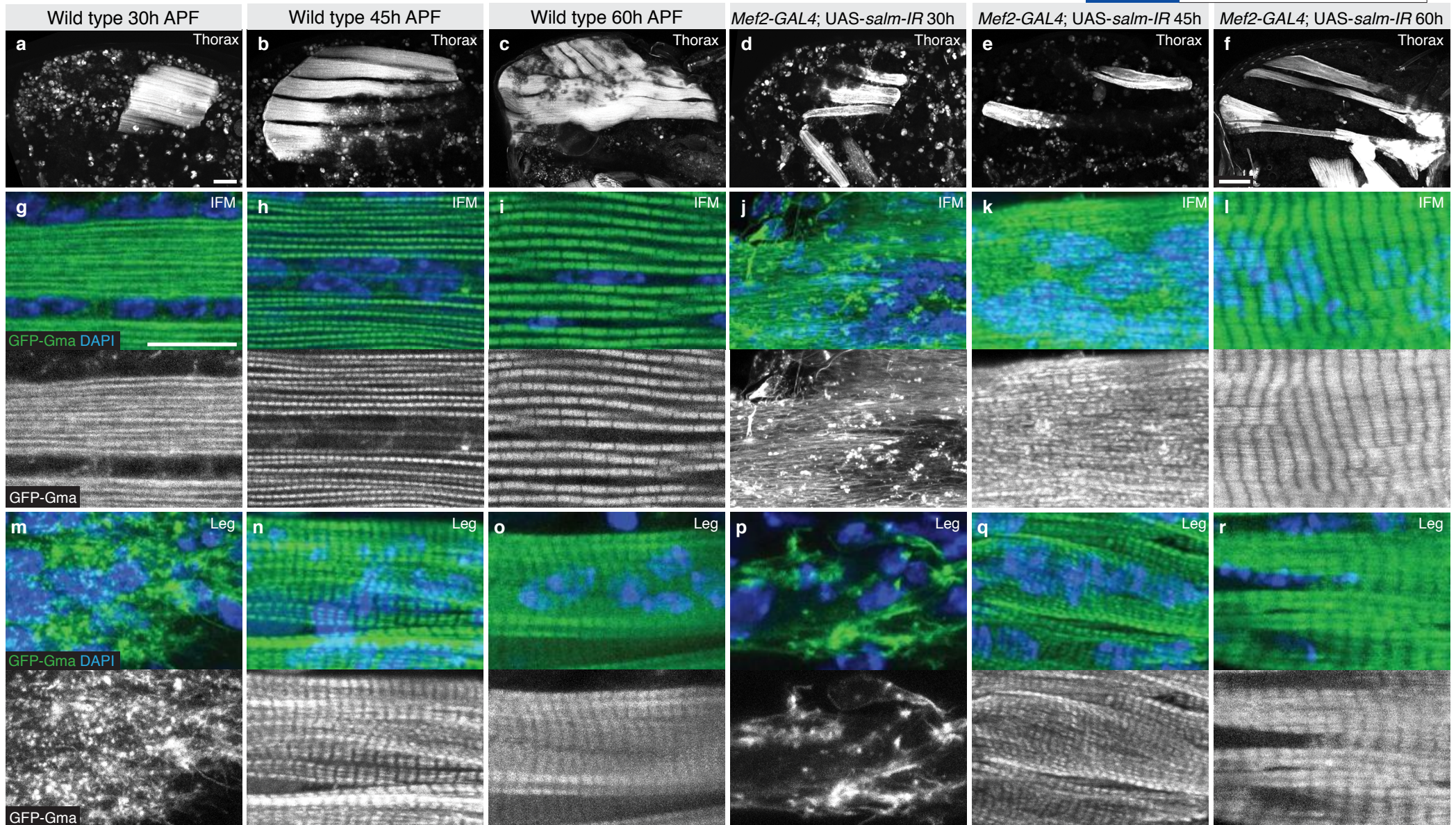
Microarray analysis. Wild-type IFMs, *salm* knockdown IFMs and leg muscles were dissected in PBS and homogenized in TriPure (Roche). RNA was extracted, labelled and hybridized to Agilent microarrays according to the manufacturer (Agilent). All experiments were performed in biological duplicates with one additional technical replicate. Log₂ fold change ratios of genes expressed above threshold 8.5 were averaged. All raw data were submitted to the Gene Expression Omnibus (GSE27502).

Western blot. Protein extracts from adult thoraces (without wings and legs), entire legs or dissected IFMs were blotted using standard procedures. Rabbit anti-Fln¹², rabbit anti-Mf³, and rabbit anti-Mlp60 (ref. 14) were used at 1:10,000, and rabbit anti-Mlp84B at 1:20,000 (ref. 14).

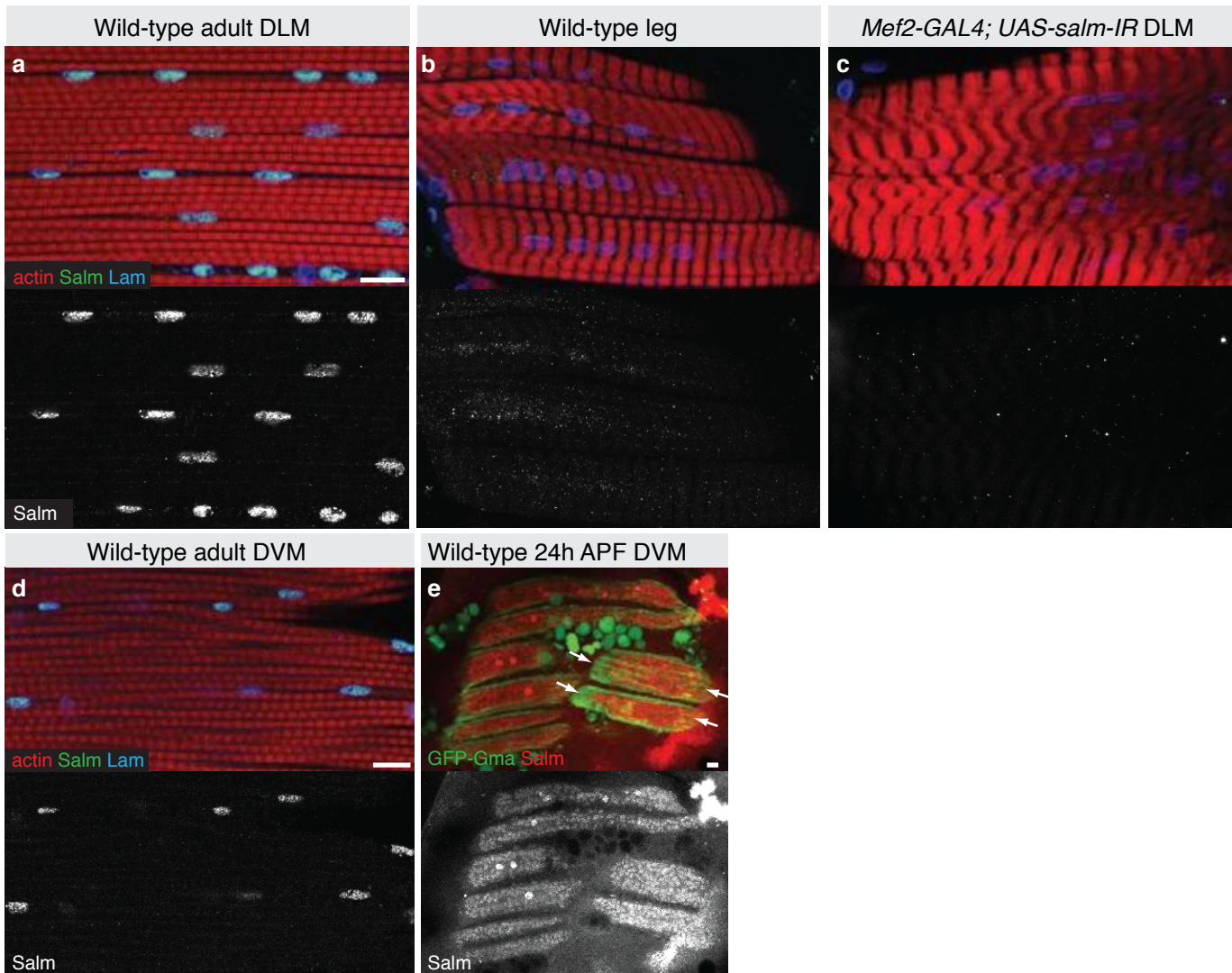
- Ranganayakulu, G., Schulz, R. A. & Olson, E. N. Wingless signaling induces *nautilus* expression in the ventral mesoderm of the *Drosophila* embryo. *Dev. Biol.* **176**, 143–148 (1996).
- Grieder, N. C., Morata, G., Affolter, M. & Gehring, W. J. *Spalt major* controls the development of the notum and of wing hinge primordia of the *Drosophila melanogaster* wing imaginal disc. *Dev. Biol.* **329**, 315–326 (2009).
- Rebeiz, M., Reeves, N. L. & Posakony, J. W. SCORE: a computational approach to the identification of *cis*-regulatory modules and target genes in whole-genome sequence data. Site clustering over random expectation. *Proc. Natl Acad. Sci. USA* **99**, 9888–9893 (2002).
- Chen, E. H. & Olson, E. N. Antisocial, an intracellular adaptor protein, is required for myoblast fusion in *Drosophila*. *Dev. Cell* **1**, 705–715 (2001).
- Newsome, T. P., Asling, B. & Dickson, B. J. Analysis of *Drosophila* photoreceptor axon guidance in eye-specific mosaics. *Development* **127**, 851–860 (2000).
- Kuhnlein, R. P. *et al.* *spalt* encodes an evolutionarily conserved zinc finger protein of novel structure which provides homeotic gene function in the head and tail region of the *Drosophila* embryo. *EMBO J.* **13**, 168–179 (1994).
- Fernandes, J. J., Celniker, S. E. & VijayRaghavan, K. Development of the indirect flight muscle attachment sites in *Drosophila*: role of the PS integrins and the stripe gene. *Dev. Biol.* **176**, 166–184 (1996).
- Klein, T. in *Drosophila: Methods and Protocols* (ed. Dahmann, C.) 253–264 (Humana Press, 2008).



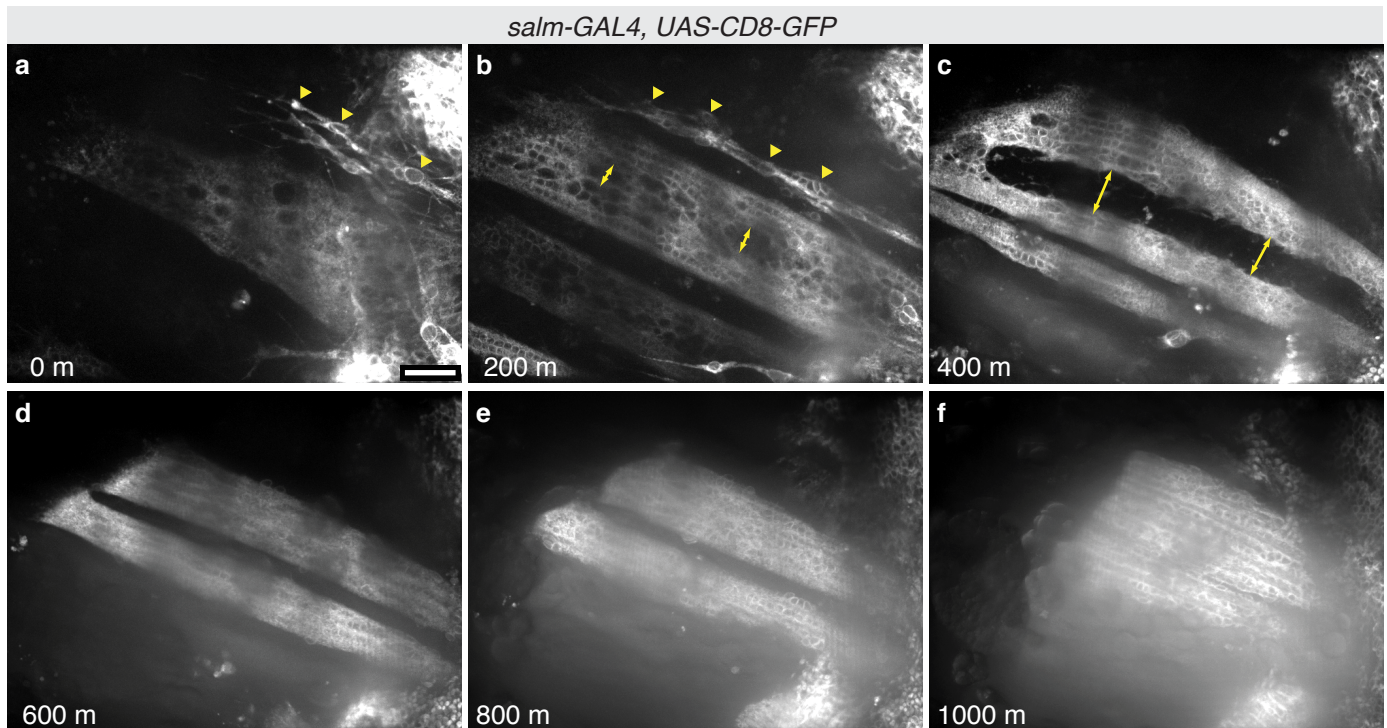
Supplementary Figure 1 | *salm* phenotype in DVMs and mutant clones. (a and b) Fibrillar DVMs in wild type (a) are transformed to tubular DVMs in *Mef2-GAL4, UAS-salm-IR* (b). (c and d) *salm, salr* double mutant clone in IFMs at low (c) and high magnification (d) reveals a tubular IFM phenotype. Scale bar 10 μ m.



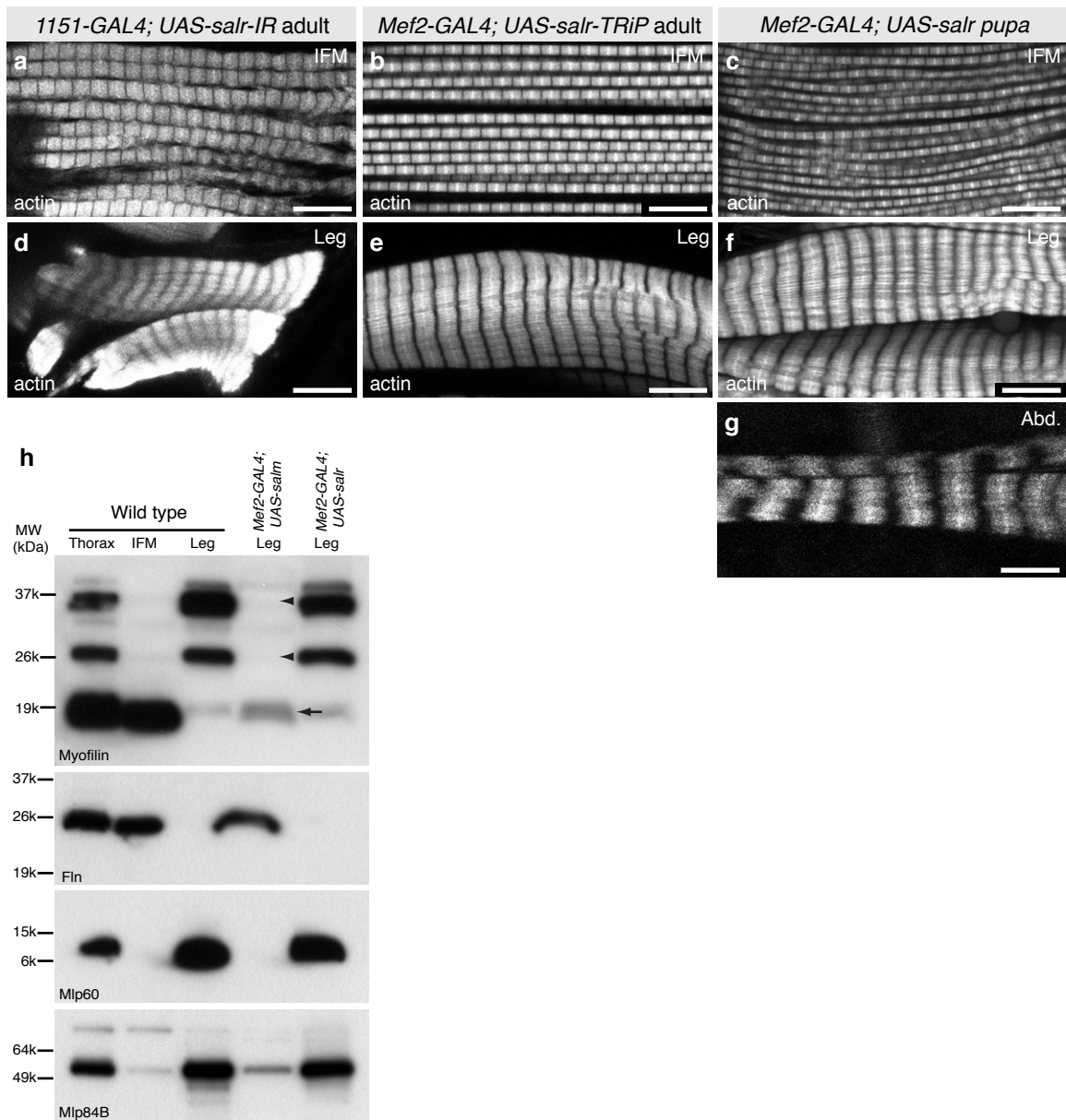
Supplementary Figure 2 | Late developmental IFM phenotype of *salm*. (a - f) Agarose sections of wild-type pupae (a - c) and *UAS-salm-IR* pupae (d - f) in which the forming DLMs were labelled with *Mef2-GAL4*, *UAS-GFP-gma* in green at 30h (a and d), 45h (b and e) and 60h (c and f). (small green cells are hemocytes containing the lysed remains of GFP expressing larval muscles). (g - l) Magnification of developing IFMs in wild-type (g - i) and *UAS-salm-IR* pupae (j - l) at the above time points; nuclei are stained with DAPI. Note the regularly arranged nuclei between the myofibrils in wild type and the centrally located nuclei in *UAS-salm-IR* tubular IFMs. (m - r) Forming leg muscles of wild type and *UAS-salm-IR* (p - r). Scale bar is 100 μm in a - f and 10 μm in g - r.



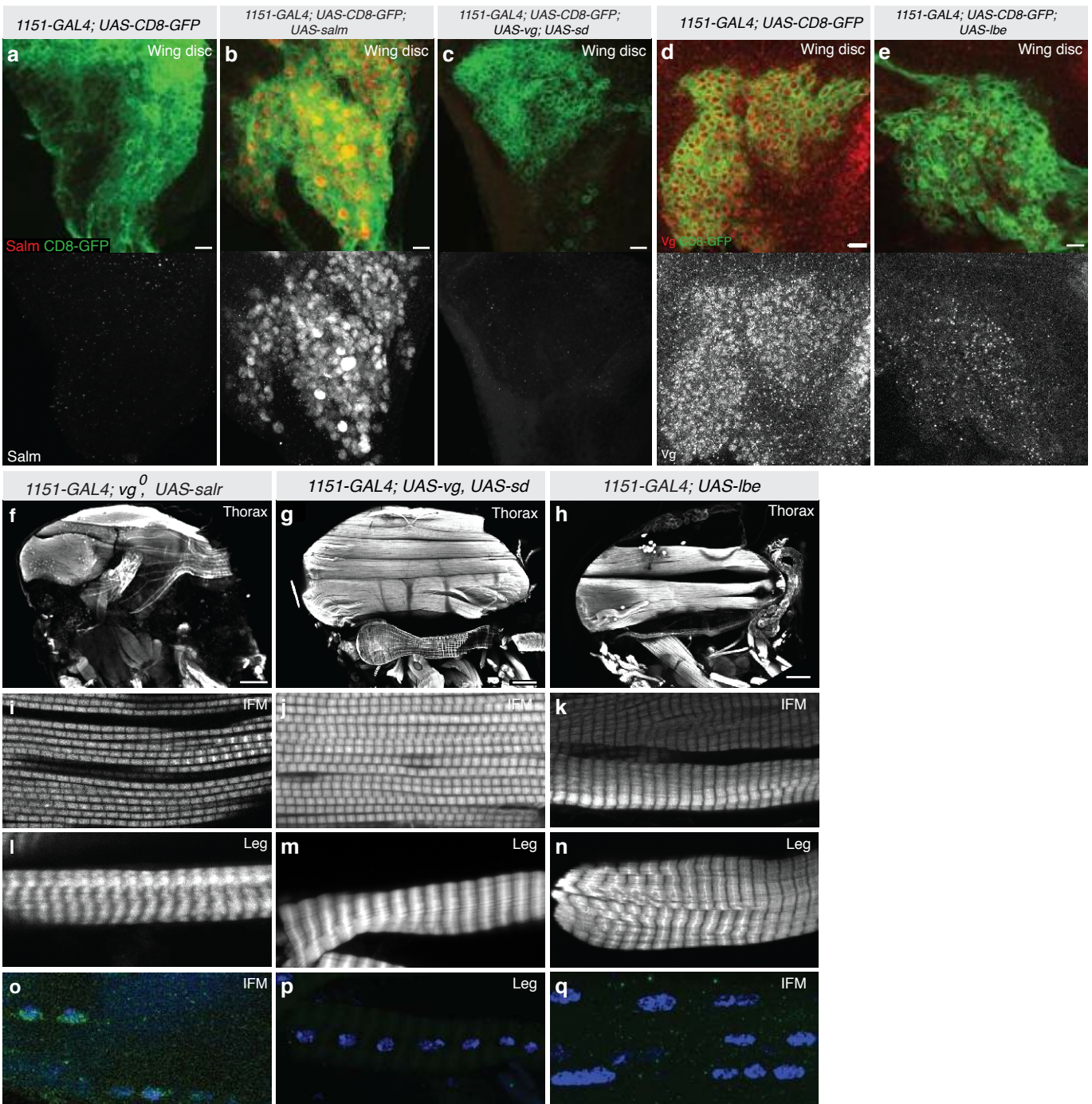
Supplementary Figure 3 | Salm expression in adult IFMs and pupal DVMs. (a - d) Wild-type DLMs (a), wild-type leg muscles (b), *Mef2-Gal4; UAS-salm-IR* DLMs (c) and wild-type DVMs (d) stained with anti-Salm, anti-Lamin and phalloidin. Note the specific expression of Salm in both types of IFMs but not leg muscles. (e) DVMs of 24h APF pupae expressing *Mef2-GAL4, UAS-GFP-gma* (e) stained with anti-Salm; arrows in (e) indicate the developing DVMs above the DLMs. Scale bar is 10 μ m.



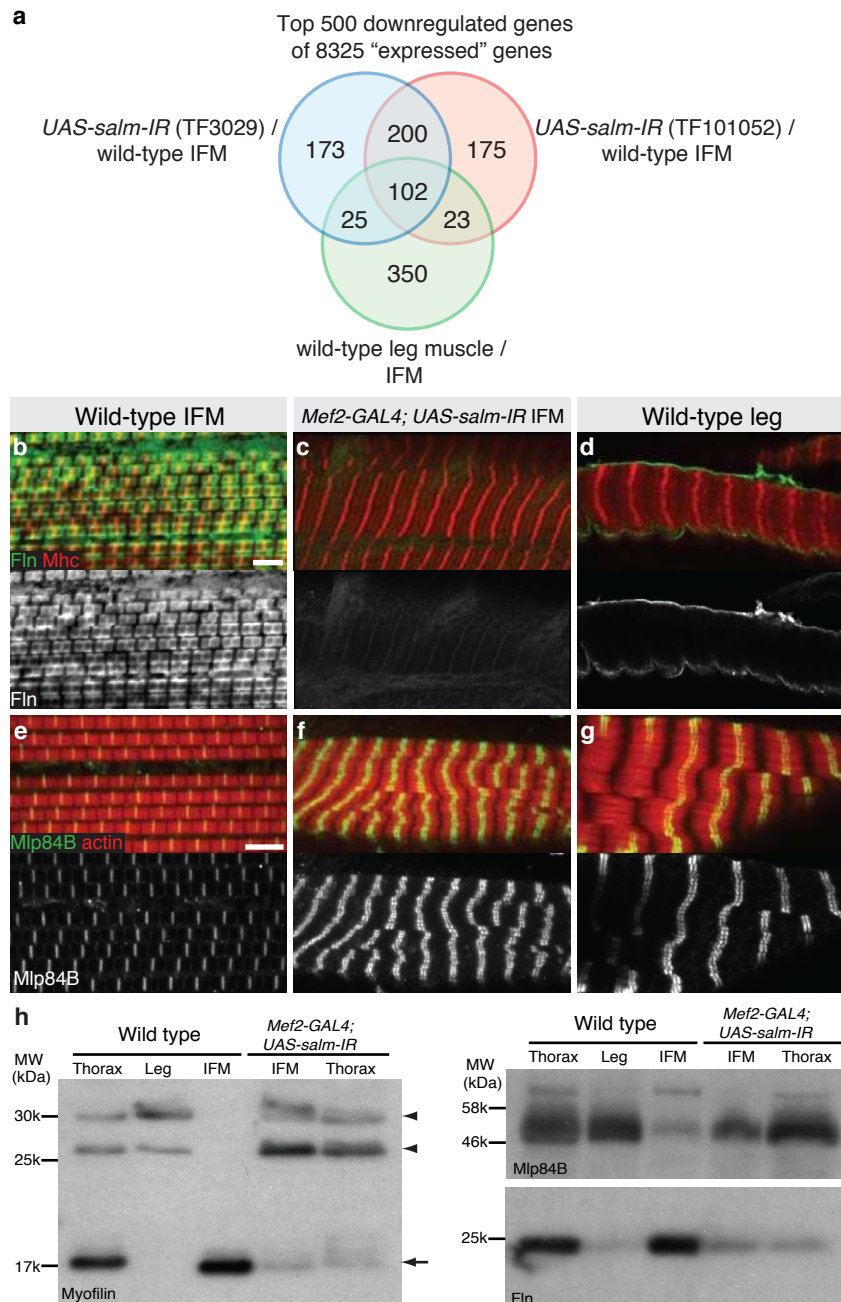
Supplementary Figure 4 | *salm* is expressed in developing IFMs. (a - f) *salm-GAL4, UAS-CD8-GFP* expression during pupal development in the forming DLMs at 10h APF before (a), during (b) and after template splitting (c). The region of DLM splitting is indicated by double-headed arrows in (b, c). Note *salm-GAL4* expression in a chain forming subclass of myoblasts before and during splitting (arrowheads in a, b). *salm-GAL4* expression persists in myofibers when myofibrils assemble (d - f). Images were taken from Supplementary movie 3. Time is indicated in minutes. Scale bar is 25 μ m.



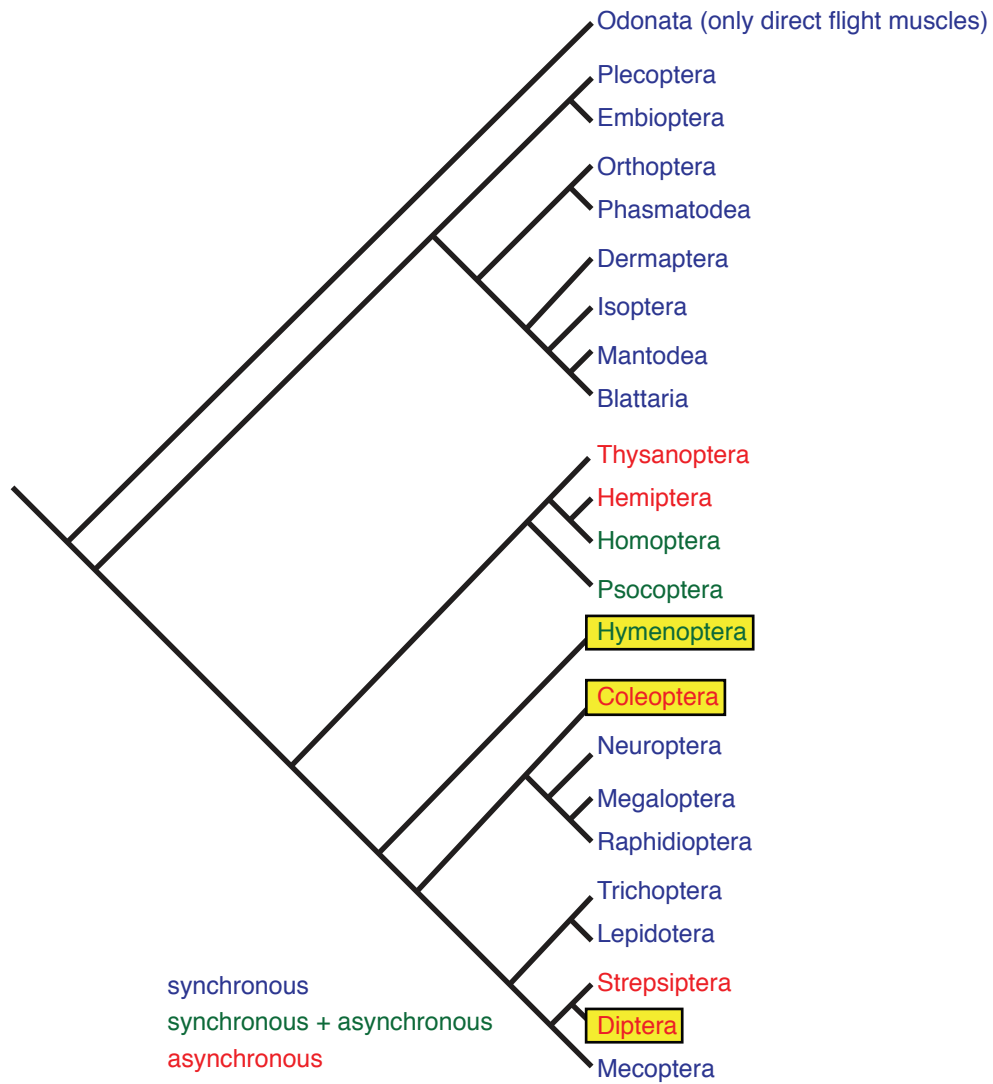
Supplementary Figure 5 | *salr* is not required for fibrillar muscle type specification. (a - c) IFMs from *1151-GAL4; UAS-salr-IR* VDRC RNAi line (a), *Mef2-GAL4; salr* TRiP RNAi line (b) and *Tub-GAL80ts; Mef2-GAL4; UAS-salr* shifted at 0h APF from 18°C to 30°C (c) were stained with phalloidin. Note that all IFMs remain fibrillar. (d - f) Leg muscles of the indicated genotypes. (g) Abdominal muscle of *Tub-GAL80ts; Mef2-GAL4; UAS-salr*. Note that *salr* in leg or abdominal muscles does not induce their fibrillar transformation (f, g). (h) Immunoblot of wild-type thoraces, IFMs and legs, compared to *Mef2-GAL4, UAS-salm* and *Mef2-GAL4, UAS-salr* legs, probed with anti-Myofilin, anti-Fln, anti-Mlp60, and anti-Mlp84B. Note the strong gain of Fln and some gain of the short Mf isoform (arrow), the repression of the long Mf isoforms (arrowheads) as well as of Mlp60 and Mlp84 in the *UAS-salm* but not the *UAS-salr* legs. Scale bar is 10 μ m.



Supplementary Figure 6 | *vg* is not sufficient to induce *Salm*. (a - c) 1151-GAL4, UAS-GFP-*gma* L3 wing discs with AMPs in green are stained with anti-*Salm* in red. Wild type (a), *UAS-salm* (b) and *UAS-vg, UAS-sd* (c). Note that *Salm* is not expressed wild-type wing discs and not gained in 1151-GAL4, *UAS-vg, UAS-sd* wing discs (c). (d and e) Vg antibody staining in red in 1151-GAL4, UAS-GFP-*gma* L3 wing discs (d) and 1151-GAL4, UAS-GFP-*gma, UAS-lbe* wing discs (e). Note the loss of Vg upon *lbe* expression in the AMPs. (f - h) IFM phenotype of *vg*⁰ mutant hemi-thorax is rescued by expression of *UAS-salm* with 1151-GAL4 (f), hemi-thorax expressing 1151-GAL4; *UAS-vg, UAS-sd* (g) and 1151-GAL4, *UAS-lbe* (h). (i - q) *vg*⁰ 1151-GAL4; *UAS-salm* IFMs (i) and 1151-GAL4, *UAS-vg, UAS-sd* IFMs (j) are fibrillar, 1151-GAL4, *UAS-lbe* IFMs are tubular (k) and leg muscles are normal (l - n). *Salm* is gained in 1151-GAL4; *UAS-salm* IFMs (o), absent from *UAS-vg, UAS-sd* leg muscles (p), and lost from 1151-GAL4, *UAS-lbe* IFMs (q). Scale bar is 10 μm in a - e, l - q and 100 μm in f - h.



Supplementary Figure 7 | Confirmation of microarray analysis. (a) Venn diagram displaying the overlap of the top 500 down regulated genes from *Mef2-GAL4, UAS-salm-IR* dissected IFMs (TF3029 or TF101052) and wild-type dissected leg muscles compared to wild-type IFMs. 102 down regulated genes are shared in all three cases. (b - d) Immunostainings of wild-type IFMs (b), *Mef2-GAL4, UAS-salm-IR* IFMs (c), and wild-type leg muscles (d) with anti-Fln. (e - g) Immunostainings of wild-type IFMs (e), *Mef2-GAL4, UAS-salm-IR* IFMs (f), and wild-type leg muscles (g) with anti-Mlp84B. Note the increased expression of Mlp84B in IFMs upon *salm* depletion (f). (h) Immunoblot of wild-type thoraces, IFMs and legs, compared to *Mef2-GAL4, UAS-salm-IR* IFMs and thoraces, probed with anti-Myofilin, anti-Mlp84B and anti-Fln. The 17 kDa Myofilin isoform (Mf-IsoC) is IFM specific and strongly reduced in *salm* knock-down IFMs (arrow) whereas the 30 and 25 kDa body-wall-muscle-specific isoforms are gained (arrowheads). Mlp84B is increased in *salm* knock-down IFMs, whereas Fln is strongly reduced in *salm* knock-down IFMs.



Supplementary Figure 8 | Flight muscle organisation in insects. Phylogenetic tree of winged insects adapted from [23, 38]. Orders with synchronous IFMs are depicted in blue, with asynchronous IFMs in red, and with both types in green. The orders investigated in this study are marked in yellow.

gene - isoform	logFC TF3029	logFC TF101052	logFC leg-IFM	Mef2-GAL4 RNAi phenotype	predicted function or domain
CG15434	-7.3	-4.0	-4.1	wild type	NADH ubiquinone oxidoreductase B8
Prm - IsoC/D	-4.8	-2.9	-3.8	n.a.	myofibril assembly
CG15617	-4.6	-3.7	-4.1	wild type	PDZ domain, unknown
CG33109	-4.6	-3.4	-1.7	n.a.	adult specific, unknown
Strn-Mlck - IsoE	-4.6	-2.0	-4.6	n.a.	myosin light chain kinase, isoform E adult specific
TpnC4	-4.4	-1.9	-4.7	flightless, fuzzy Z	flight muscle function, flight muscle specific troponin, stretch sensitive
CG2022	-4.1	-2.1	-1.6	wild type	peroxisomal membrane
CG34067	-4.0	-1.8	-2.8	n.a.	mitochondrial Cytochrome c oxidase subunit I mt:CoI
CG9619	-4.0	-1.9	-1.9	wild type	protein phosphatase type 1 regulator activity
mt:CoI	-4.0	-1.8	-2.8	n.a.	mitochondrial Cytochrome c oxidase subunit I mt:CoI
fln	-3.9	-1.6	-4.3	flightless, missing IFMs	muscle thick filament assembly
CG11617	-3.7	-2.3	-1.0	larval lethal, fading Z	homeobox transcription factor, muscle specific expression
CG13026	-3.7	-1.9	-2.3	wild type	unknown
CG34172	-3.6	-2.6	-2.1	n.a.	unknown
mt:ND5	-3.6	-2.1	-2.7	n.a.	mt:ND5 mitochondrial NADH-ubiquinone oxidoreductase chain 5
CG32230	-3.4	-2.3	-1.3	wild type	NADH dehydrogenase activity
CG12105	-3.3	-1.9	-2.6	wild type	unknown
mt:CoIII	-3.3	-1.7	-2.7	n.a.	mitochondrial Cytochrome c oxidase subunit III mt:CoIII
CG13144	-3.2	-2.4	-2.4	n.a.	unknown
CG9642	-3.1	-2.7	-3.7	wild type	set domain, transcription repressor? pupal specific expression
mt:ND1	-3.0	-1.6	-2.8	n.a.	mitochondrial NADH-ubiquinone oxidoreductase chain 1 mt:ND1
Mf - IsoC	-2.9	-2.7	-0.1	early pupal lethal	muscle thick filament assembly
CG11148	-2.9	-2.4	-2.1	wild type	1500aa, GYF domain, unknown
CG3964	-2.9	-1.4	-3.8	late pupal lethal	tubulin tyrosine ligase
mt:ND4	-2.9	-1.8	-2.6	n.a.	mitochondrial NADH-ubiquinone oxidoreductase chain 4 mt:ND4
trbd	-2.8	-1.8	-0.5	late pupal lethal	Zn finger, regulator of Wnt?
Neb-cGP	-2.8	-1.8	-1.8	flightless	unknown
CG9034	-2.8	-1.9	-1.6	adult lethal	unknown
CG30415	-2.7	-1.5	-1.4	larval lethal	unknown
slmo	-2.7	-1.7	-1.5	larval lethal	mitochondrial protein
salm	-2.6	-1.6	-2.4	flightless	Zn finger transcription factor, eye and trachea development
mt:CoII	-2.6	-1.7	-2.7	n.a.	mt:CoII mitochondrial Cytochrome c oxidase subunit II
Fhos	-2.5	-1.6	-1.0	flightless, irregular myofibrils	actin binding FH2
aret	-2.5	-0.9	-3.4	adult lethal / flightless	RNA binding, regulation of splicing
mt:ATPase6	-2.5	-1.6	-2.8	n.a.	mt:ATPase6 mitochondrial ATPase subunit 6
sesB	-2.4	-1.7	-1.3	larval lethal	mitochondrial carrier protein
cln3	-2.2	-1.1	-2.6	wild type	transporter
vq	-2.1	-1.1	-2.2	flightless	transcription factor, wing development
Obp51a	-2.1	-1.5	-3.6	wild type	unknown
CG6289	-2.0	-2.2	-2.7	wild type	unknown
Dup99B	-1.5	-1.8	-2.7	n.a.	regulation of oviposition
CG32154	-1.3	-1.2	-2.5	wild type	glutamine metabolism
Act88F	-0.3	0.8	-4.0	embryonic lethal	flight muscle function
salr	-0.2	0.5	-0.4	larval lethal	Zn finger transcription factor
CG5023	0.8	1.8	4.1	flightless	CH-domain, unknown
Msp-300 - IsoE/G	1.4	1.7	2.0	flightless	unknown
Mf - IsoB/D	1.5	1.2	4.4	early pupal	muscle thick filament assembly
zormin	1.5	1.6	3.2	lethal	titin related
chic	1.9	1.9	2.1	lethal	profilin
TpnC41C	2.1	1.9	4.3	n.a.	body muscle specific troponin
Act79B	2.2	2.3	4.7	pupal lethal	adult muscle specific actin
Mlp60A - IsoE	2.2	2.2	4.1	wild type	unknown
tsr	2.2	2.1	1.0	n.a.	cofilin
Mlp84B	2.3	2.6	5.4	wild type	body muscle function
Prm Iso A	2.3	2.1	2.9	n.a.	myofibril assembly
Tm1 - IsoB/C	2.4	1.9	4.2	pupal lethal	tropomyosin
Act57B	2.5	2.4	2.4	embryonic lethal, spotty Z	body wall muscle specific actin
Act87E	3.5	1.0	5.6	n.a.	body wall muscle specific actin
Mp20	3.6	3.0	4.6	wild type	body muscle specific
CG16885	4.3	2.0	3.2	pupal lethal	unknown

Supplementary Table 1

Supplementary Table 1 | Microarray results of IFM and leg muscle. Microarray analysis displaying log₂ ratios (FC = fold change) of *Mef2-GAL4*, *UAS-salm-IR* (TF3029 and TF101052) IFMs compared to wild-type IFMs, and leg muscles compared with wild-type IFMs. Selected genes or gene isoforms are listed. Green indicates significant down regulation in *salm* knock-down compared to wild-type IFMs, yellow indicates no change and orange marks up regulation of genes or gene isoforms. The phenotypic class of the *Mef2-GAL4* mediated RNAi knock-down for each gene from⁶ is shown. The predicted molecular function or structural domain for each gene is listed.

Supplementary Table 2 | Top 500 *salm* targets and IFM specific genes of microarray analysis List of the top 500 down regulated genes from *Mef2-GAL4*, *UAS-salm-IR* dissected IFMs (TF3029 or TF101052) and wild-type dissected leg muscles compared to wild-type IFMs. All 102 genes common are listed as well as the 302 genes commonly down regulated in the two *salm* hairpins and the 150 genes IFM specific genes down regulated in at least one *salm* hairpin. All 8325 "expressed" genes with an average expression above 8.5 on the microarray were scored and are listed. Sheet two displays all significantly enriched GO-terms in the common 102 *salm* targets and IFM enriched genes. Note the strong enrichment of mitochondrial GO-terms in addition to muscle specific GO-terms (see separate file for Supplementary Table 2).

Supplementary Movie 1 | Early IFM development in a wild-type pupa. An intact wild-type pupa labelled with *Mef2-GAL4*, *UAS-GFP-gma* was recorded from 10h APF every 5 min for about 14h. Note the splitting DLM muscles. Movie plays 5 frames per second.

Supplementary Movie 2 | Early IFM development in a *UAS-salm-IR* pupa. An intact *UAS-salm-IR* pupa labelled with *Mef2-GAL4*, *UAS-GFP-gma* was recorded from 10h APF every 5 min for about 15h. Note that splitting of the DLM muscles fails. Movie plays 5 frames per second.

Supplementary Movie 3 | *salm* expression in developing IFMs. Movie records the developing DVMs in a *salm-GAL4*, *UAS-CD8-GFP* expressing pupa from 10h APF. One frame was recorded every 5 min for about 20h. Movie plays 5 frames per second.

Tc'sal for RNAi injection 3320bp

CACCTCCAGCACCAACAAGTGTTGCAGTTACAACCTCATCAATCAGCTGCAACAGCAGTTGCAGATTGACAGATC
TAAAGCTGCAAGTCCCCTCTCGCCCCACCTTCCGAAAACGGGGAAAAATGCCCGGCTGAAGCTTCGCCACCCCC
ACAAAATTTGCCCGTTTCAAGGGAAACCAACCCCAACTCCCATAATACAGCCCCACAACCCATCGTACAAGAACC
ATCCGAGAACCAACGACTGAAATGAATGTTCTTGTCTCTACCTCTGCAGTCGCAGCACTGTTCCATATCATC
ATCACTAGCTTCAACTATAATCACTCACAATAACGAACCACCTTCATTAGACGAACCAAAATACGTTAGAGATGTT
GCAAAAGAGAGACTCAAGAGGCTTAGATAACGCCAGTCAGGGGTTATTGGCCACAAAATCTGGCCGACGAACCTGGC
CTTTAGGAGAAAACAAAGGCTCGTTATCGCCTTATGACTCCAAAGGGCGGAACGAACCGTTCTTCAAACACCGGTG
TCGGTACTGCGGAAAAGTCTTCGGCTCTGACTCGGCCCTGCAAAATACATATCCGTTCCCACACGGGAGAACGCC
CTACAAGTGCAATGTTTGTGGTAGTCGGTTTACCACGAAAAGTAACTTCAAAGTACATTTTCAAAGACATAGTGC
AAAGTTTCTCATATCAAAAATGAACCCGAATCCGGTCCCGGAACACCTAGACAAGTATCATCCACCGCTCTTAGC
TCAATTAGGACAACAGCCCTCGCTGTGCGCGGGCGTCCCCACCACATATGGGTTTTCCCGGAGGTCAACCCCTT
CCCACCCACCTCATTGCTCCTGTACCGACCCACGGCCCCCGCCGATTTGCTAAACAGTCGGCTGCAACCTTC
ACCGCACAGGCCTCAAGACCCGCCGCAAAGGCTCTTCCACCGCATCCCCTTTTTCATGAAGCGAGAGGAACAAGA
GGCTCCTGAGAATCTCACAAACCGGCAAGATCGCCAACCTCCCGTGCAGACACTCACTGCAAAATCGGAAATTTT
CGACGAAAAACGCGAATATGACGATGCACAATCCAATGTTCTCAGATAACACCAAAACAAGAACCAACGACGA
AGGCGAACACGAACCTGAGCGATACTCCTCTCCGGCGCCCTACGACGAATGCAGCATCGACAGCAAGTACAGCAA
CGAGGACACGCTGGGACGCGGAAGCCCGGGAGGAGACCATTTCGGAGAATATGCAAGATGAGCCTGAGAATCTCTC
GAATAAGAGCAATTCATAACAGTTCTTTGAGCATTTCCACGGTTCAGAGATTGCCGCAACTTTTCGTTCCGG
ACAAGTGAATTCGCCCGGAGTAGTACATCGTCGGGAAGCTTAGGCCAATTTCCAGCAACGCCAGTTCGATCC
AGCCAAAGACCCCGCTATCTACTCGAATTTATTGCCACGGCCAGGGAGCAACGACAATTCATGGGAGAGTTTGTAT
AGAAGTGACAAAAACGTCGGAAACAGCAAACTCCAACAGCTTGTGACAATATCGAACATAAACTTTTCCGATCC
GAATCAGTGTGTGATATGTCATCGAGTGTGTGTCGTCGAAGAGCGCCTTACAGATGCATTTATCGAATCACACCGG
CGAACGGCCGTTCAAATGTAAGATTTGTGGACGGCTTTCACCACCAAGGGCAATCTCAAGACACACATGGGGGT
GCACAGGGCCAAGCCCCCGATGCGGGTGTGTCACCAGTGCCTCGTCTGCCACAAAAGTTTACCAATGCGCTTGT
TCTGCAACAACATATCCGCTTTCACACGGGTGAACCCACTGATCTCCTCCGAGCAGATTCGAAGCGCTGAAGT
GAAAGACTTTCCGTCGCCGGGAGGATTCCCTTCGATTCATAATTCATTAATCCATTCCTTAGGGCAAGGGTTTGC
CGTTCCGGGGCTGTGCGCCTTAGGTACACACTCTCGATGAATCACAAAATATGAAAAATCGATAAAGAGGAACA
CGAATCGATGGACGACGATGATGACGACGACGATGACATGAGCAACTCCGAAAATCAAACCCGAGGTTTACTTC
CTCGCCAGATATGCAAGGAGTGCAGTACGATGGCTTCCAGTTGTCAATGAGTGGTTTTAAGTTGCTCTGCCGA
AGATTTATGTTCTACTAGGACTGCGGCTTCGGCTTCGCCGGTGCAAAATGGGGAGAAAATCGCCTTGCCAACTGGA
AATCACAAGTCCAGGCAGTTTCGGAGATTTCGAGCTTCGCCAAACCGGCTCACAAACGACACCCGTCAGGTTCCACG
TCCACCTTCTCTCAACATGCCGGCAGTCCGACTCCTTCCGAGTGCATTTCTTTGGGTGCTTTTAGACTTAACCCC
TCGAACTAACCAGCCTTTGATAACGAGTCCGGGTCCAGTCCCGGCCCGCCACCGGCTTTGTTTTCAACGTTCCG
ATTGATAACCACAGGTCAAGGTTCCACTCCTTTGATGTCATCGGCACCTTTCATCTTTGACGTCGCTGTTTTGAC
ATCCACTGCGTTAGTCCATTGCGTTTAGCCGTTGGACCAACAGGCCGTGGGAACACCACCTGTAACCTGTGTTTT
CAAGACGTTTCGTTGCAACTCTGCCTTGGAGATTCAATTACAGGAGTACACGAAAGAACGTCCTTTTAAATGCAG
TATCTGCGATAGAGGCTTCTCGACCAAGGACGGATGTGTATGCAGAGAGAGGCGTATCCAGGATGAAGCGGAGCC
TTGGAAGGCAAGCAAAAAGGAAAACCGGCTTCTCGCAAGTCAATACCATCGGTACTTCCGCTACCGATGAGCCCTGG
ATACGCCTCAAACCTGGATGCATATCGCGGGCAACATGAAGCAACACATGCTTACACATAAAAATAAGGGACATGCC
TCAACACATGTTTGAAGATAAAACCGCCGATAAGCGGAGATGAAAATCGCAACAATCCCAACAAAACCTTACCTCA
AAGGGAAGTTCAACCCAGCGAAAACGAACAACCCAACTCACACCTTCTATATCTGAGCAAAAACAAGA
GCAACTGGTTAAAAGGGAACCCACCGAGACGGAACCTACCTTGCCTAAACGTCATCCAGCTTACAGGCAAGTAA
GCACTTGTGCCACGATGCAATAAGAACTTCTCGTCCAGCTCGGCTTGCAGATACACATGCGTACGCACACCGG
CGATAAGCCGTTTCAGATGCACCGTGTGCCAGAAGCCTTACCACCAAGGGGAACCTCAAGGTACATATGGGAAC
GCATATGTGGAGCAACGGG

Supplementary Reference.

38. Dudley, R. Energetics and flight physiology, in *The biomechanics of insect flight*. (ed. R. Dudley) 159-202 (Princeton University Press, Princeton; 2000).